IEEE Access
Multidisciplinary | Rapid Review | Open Access Journal

Received October 7, 2020, accepted October 14, 2020, date of publication October 21, 2020, date of current version November 3, 2020.

Digital Object Identifier 10.1109/ACCESS.2020.3032826

A Comprehensive Survey on "Various Decoupling Mechanisms With Focus on Metamaterial and Metasurface Principles Applicable to SAR and MIMO Antenna Systems"

MOHAMMAD ALIBAKHSHIKENARI[1], (Member, IEEE), FATEMEH BABAEIAN[2], (Member, IEEE), BAL S. VIRDEE[3], (Senior Member, IEEE), SONIA AÏSSA[4], (Fellow, IEEE), LEYRE AZPILICUETA[5], (Senior Member, IEEE), CHAN HWANG SEE[6], (Senior Member, IEEE), AYMAN ABDULHADI ALTHUWAYB[7], (Member, IEEE), ISABELLE HUYNEN[8], (Senior Member, IEEE), RAED A. ABD-ALHAMEED[9], (Senior Member, IEEE), FRANCISCO FALCONE[10,11], (Senior Member, IEEE), AND ERNESTO LIMITI[1], (Senior Member, IEEE)

[1]Electronic Engineering Department, University of Rome "Tor Vergata," 00133 Rome, Italy
[2]Department of Electrical and Computer Systems Engineering, Monash University, Melbourne, VIC 3800, Australia
[3]Center for Communications Technology, London Metropolitan University, London N7 8DB, U.K.
[4]Institut National de la Recherche Scientifique (INRS), University of Quebec, Montreal, QC H5A 1K6, Canada
[5]School of Engineering and Sciences, Tecnologico de Monterrey, Monterrey 64849, Mexico
[6]School of Engineering and the Built Environment, Edinburgh Napier University, Edinburgh EH10 5DT, U.K.
[7]Electrical Engineering Department, Jouf University, Sakaka 72388, Saudi Arabia
[8]Institute of Information and Communication Technologies, Electronics, and Applied Mathematics, Université Catholique de Louvain, 1348 Louvain-la-Neuve, Belgium
[9]Faculty of Engineering and Informatics, University of Bradford, Bradford BD7 1DP, U.K.
[10]Electric, Electronic, and Communication Engineering Department, Public University of Navarre, 31006 Pamplona, Spain
[11]Institute of Smart Cities, Public University of Navarre, 31006 Pamplona, Spain

Corresponding author: Mohammad Alibakhshikenari (alibakhshikenari@ing.uniroma2.it)

This work was supported in part by the Ministerio de Ciencia, Innovación y Universidades, Gobierno de España (MCIU/AEI/FEDER,UE) under Grant RTI2018-095499-B-C31, in part by the Innovation Programme under Grant H2020-MSCA-ITN-2016 SECRET-722424, and in part by the U.K. Engineering and Physical Sciences Research Council (EPSRC) under Grant EP/E022936/1.

ABSTRACT Nowadays synthetic aperture radar (SAR) and multiple-input-multiple-output (MIMO) antenna systems with the capability to radiate waves in more than one pattern and polarization are playing a key role in modern telecommunication and radar systems. This is possible with the use of antenna arrays as they offer advantages of high gain and beamforming capability, which can be utilized for controlling radiation pattern for electromagnetic (EM) interference immunity in wireless systems. However, with the growing demand for compact array antennas, the physical footprint of the arrays needs to be smaller and the consequent of this is severe degradation in the performance of the array resulting from strong mutual-coupling and crosstalk effects between adjacent radiating elements. This review presents a detailed systematic and theoretical study of various mutual-coupling suppression (decoupling) techniques with a strong focus on metamaterial (MTM) and metasurface (MTS) approaches. While the performance of systems employing antenna arrays can be enhanced by calibrating out the interferences digitally, however it is more efficient to apply decoupling techniques at the antenna itself. Previously various simple and cost-effective approaches have been demonstrated to effectively suppress unwanted mutual-coupling in arrays. Such techniques include the use of defected ground structure (DGS), parasitic or slot element, dielectric resonator antenna (DRA), complementary split-ring resonators (CSRR), decoupling networks, P.I.N or varactor diodes, electromagnetic bandgap (EBG) structures, etc. In this review, it is shown that the mutual-coupling reduction methods inspired

The associate editor coordinating the review of this manuscript and approving it for publication was Lei Ge.

by MTM and MTS concepts can provide a higher level of isolation between neighbouring radiating elements using easily realizable and cost-effective decoupling configurations that have negligible consequence on the array's characteristics such as bandwidth, gain and radiation efficiency, and physical footprint.

INDEX TERMS Decoupling methods, metamaterial (MTM), metasurface (MTS), multiple-input-multiple-output (MIMO), synthetic aperture radar (SAR), isolation enhancement, array antennas.

I. INTRODUCTION

SAR and MIMO [1] are arguably the state-of-the-art methodologies for enhancing the capacity of radio links via multiple transmitting and receiving antennas to have multipath scattering. Conventionally, MIMO and SAR systems are defined as practical techniques for transmitting and receiving signals stemming from multiple independent channels concurrently. This is typically implemented over the same radio channel with the aid of multiple antenna configurations without additional losses in radiation power in rich scattering surroundings. SAR and MIMO are also categorized under next generation wireless communication technologies due to their marked potential to improve system credibility and channel capacity by means of multiple antennas [2]. MIMO was as a practical solution to the data rate restriction of single-input single-output (SISO) systems. MIMO and SAR are generally used on different networks, and they also improve the transmission velocity of data [3] by using the maximum content of wireless telecommunication devices.

In [4], [5], various etched portable MIMO and SAR antenna apparatus are discussed. They are broadly applied in applications of mobile devices because of their adaptation with the system, better completeness, low cost, and simplicity of construction. The simplicity and genericity of the multi-antenna topology [6] utilized in the transmitting side and receiving side in MIMO and SAR systems allow for a more convenient implementation compared to other antenna array topologies. Also, such configurations reduce channel errors in communication systems to have enhanced data rates [7]. However, this may lead to multipath scattering due to the inherent high cohesion factor in the multi-signal distribution [8]. Additionally, the decreased distance between the antennas in array systems can potentially reduce the decoupling factor, which degrades the angle of arrival [9] in the estimation of carrier frequency offset [10] and signal to interference noise ratio [11]. It is good to note that the isolation between adjacent antennas decreases either by a huge flow of surface current from the stimulated ports or space radiation and surface waves. Also, the contrary influence of interferences on reflection coefficients cannot be ignored [12]. Hence, the main challenge in the implementation of antennas for MIMO and SAR applications is limiting the interferences between more recent compact etched antennas and other antenna configurations [13], [14]. Comprehensive studies based on models specifically designed to increase the isolation have been presented in recent times [15]–[27]. The basic approaches for enhancing isolation in multi-antenna systems typically involve the utilize of decoupling networks [17], neutralization lines [18]–[20], engraved parasitic elements [21], CSRRs [22], EBG architectures [23], DGSs [24], [25], and metasurfaces (MTS) and metamaterials (MTM) [26], [27]. Besides the multi-antenna systems, the decoupling methods to increase the isolation in broadband base station arrays have been presented in [28], [29]. In [30], easy comparison of disparate decoupling approaches containing parasitic elements, utilize PIN and varactor diodes, and decoupling networks has provided. In addition, the efficacy of varying relative permittivity of layers on antenna parameters is presented and discussed. These methods allow for the manipulation of mutual coupling through weakening, resisting, or reducing the surface current flow. Antenna configurations such as reconfigurable, engraved, dielectric resonator, metasurface, and metamaterial are widely adopted to destroy the harmful outcome of the interferences [30]–[35].

In the following survey, a comparative review is given on diverse methodologies for suppressing mutual-coupling in antenna arrays for application in MIMO and SAR systems based on metasurface (MTS) and metamaterial (MTM) properties. In addition, different antenna models based on conventional decoupling techniques are examined. The antenna performance is characterised in terms of operating frequency range, degree of isolation between adjacent radiators, radiation gain and efficiency. In essence, this survey highlights the practicality and constraints of various mutual-coupling suppression techniques for antenna arrays that are available today to antenna designers. Though in [30], [36], [37] the theoretical aspects of SAR and MIMO antenna isolation are discussed, these articles do not discuss the diverse range of mutual-coupling isolation. Moreover, there is a dearth of literature on the current techniques and design principles for mitigating mutual coupling in antenna arrays based on the MTS and MTM properties. This survey provides the latest diverse decoupling techniques available to improve their radiation performance of high dense antenna arrays.

Rest of the paper has organized as follows. Section II is on mutual coupling definition. Section III is on the various decoupling methods. Sections IV and V present the main parts of this survey which focus on the diverse decoupling methods inspired metamaterials and metasurfaces for antenna array application in MIMO and SAR systems. Section V also provides a comprehensive comparison table which includes several research studies. Finally, this survey has concluded in Section VI.

II. MUTUAL COUPLING DEFINITION

In antenna array systems, the mutual coupling generally refers to the energy attracted through a nearby antenna when an antenna is operational. It changes the reflection coefficient(s), input impedance(s), and radiation pattern(s). To provide an analytical background for mutual coupling, some empirical models have been presented and discussed in [38], according to Equation (1) and Equation (2).

$$MC_{mn} = \exp\left(-\frac{2.d_{mn}}{\lambda}(\alpha + j\pi)\right), \quad m \neq n \tag{1}$$

$$MC_{mm} = 1 - \frac{1}{N}\sum_{m}\sum_{m\neq n} MC_{mn} \tag{2}$$

where MC_{mn} represents the mutual coupling and the space between the m^{th} and n^{th} antennas is defined by d_{mn}. The number of antennas and the parameter controlling the level of coupling are presented by N and α, respectively.

Practically, the isolation level pertains not only to the array topology but also on the stimulations of the array antennas and other factors. It is normally estimated applying the dB-valued S-parameter between the m^{th} and n^{th} antennas (i.e., $20\log 10(|S_{mn}|)$), and equivalently the isolation $-20\log 10(|S_{mn}|)$ between them.

A detailed understanding of the isolation mechanism will invariably relate to the transmitting/receiving mode. The isolation mechanisms are discussed below, considering the transmitting and receiving modes independently.

A. ISOLATION IN TRANSMITTING MODE

Fig.1 displays that the antennas "m'' and "n'' in a typical array are considered. A generator is considered to antenna "n'', the produced energy of the generator "1" radiates within area "2" and onto the m^{th} antenna "3". The portion of the energy arrived at the m^{th} antenna re-scatters within area "4" and the residual energy moves in the direction of the source "5". A deduction of the re-scattered energy "4" will be take-up by the n^{th} antenna "6". This mutual interplay

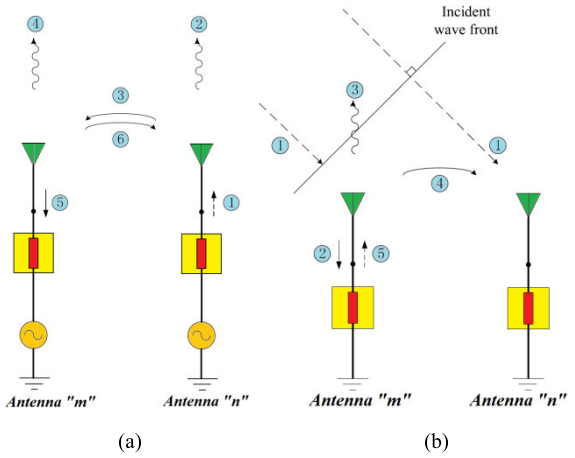

FIGURE 1. Investigation of mutual coupling architecture in (a) transmitting and (b) receiving modes [14].

is an ongoing procedure, and it is iterative. However, it is usually best to select the first few repetitions because the re-scattered energy reduces drastically after each repetition. The general far-field is derived from the vector summation of the re-scattered and radiated fields. Hence, the mutual coupling varies the pattern of the antenna. The wave "5" is added vectorially to the reflected wave and incident wave of the m^{th} antenna. This enhances the standing wave and changes the m^{th} antenna's input impedance. Mutual coupling varies both the self-impedance of the antenna and the mutual impedance.

B. ISOLATION IN RECEIVING MODE

Assuming the plane wave "1" exceed toward the array reaching the m^{th} antenna. It evolves a current in the m^{th} antenna. The portion of the incident wave travels within the receiver as "2" and the remaining segment is re-scattered within area "3". Some of the re-scattered wave is conducted onto the n^{th} antenna "4", where it adds (vectorially) to the incident plane wave "5". Thus, the received wave through an element is the vector summation of the direct waves and the coupled waves from other elements. To optimize the received energy (i.e., lowest re-scattered energy), the m^{th} antenna's terminating impedance has to be selected. Therefore, the re-scattered wave "3" is annulled via the reflected wave "5". In a receiving mode, the antenna's performance under consideration can be evaluated through stimulating the antenna with the other antenna interrupted with a 50-ohm load.

III. VARIOUS DECOUPLING TECHNIQUES

In literature, several isolation enhancement approaches are available such as decoupling networks, parasitic element approach, slot etching and ground plane structures, neutralization lines, PIN diode, varactor diode and feeding structures, frequency-selective surface (FSS), characteristic modes, and EBG structures [13]–[16], [30], [35]–[37]. These approaches have been briefly discussed in this section. Additionally, due to some disadvantages and restrictions of the abovementioned methods, which have been discussed in details in the next part, the metasurface and metamaterial decoupling methods have been proposed and investigated in deep, which enable the designers to model SAR and MIMO antenna systems with minimized mutual coupling in a compact footprint area for mass production.

A. DECOUPLING NETWORK APPROACH

Decoupling networks are applied to obtain enough isolation in MIMO and SAR antenna systems. They work on the methodology of the transformation of the cross-admittance term to purely imaginary amount via step up transmission lines or through discrete elements. Eigen mode disintegration [39], manmade structure [40], coupled resonator [41], and inserted elements [42] are some examples of the isolating layouts.

Modeling the decoupling scheme between the antenna arrays is easy to implement [35]–[52]. Specified decoupling

TABLE 1. Comparison on the performance parameters of decoupling networks based MIMO and SAR antennas.

Ref.	[56]	[57]	[58]	[59]
Dimensions / Substrate	72.4 × 20 × 0.8 mm^3 Rogers RO4350B	70 × 35 × 0.8 mm^3 FR-4	112 × 55 × 1.6 mm^3 FR-4	40 ×100 × 0.8 mm^3 FR-4
Isolation (dB)	≥ -27.6 dB @ 2.18 ~2.65 GHz	≥ -32 dB @ 3.45 ~3.55 GHz	≥ -15 dB @ 2.4 ~2.48 GHz ≥ -15 dB @ 5.15 ~5.35 GHz	≥ -15 dB @ 3.5 ~3.6 GHz
Applied Approach	Diamond-shaped pattern ground resonator	Reactive dummy loads	Coupled resonator decoupling method	Pattern diversity decoupling method
Efficiency / Gain	66~70.5 % / 1.39dBi	82 % / -	66~75 % / -	50% / -
No. of Ports / Applications	Dual Ports / IMS	Triple Ports / WiMAX	Dual Ports / ISM and WLAN	Eight Ports / WiMAX
Remarks	Complex layout and medium dimension	Easy configuration	Dual-band and Large dimension	Easy configuration and maximum ports

approaches provide mutual reduction at the cost of some ohmic losses. The isolating method annuls the original interference by producing a supplementary coupling route; therefore, the mutual coupling is reduced, and far-field properties become better.

Similarly, the SAR and MIMO decoupling performance can be boosted through implementing an indistinct line and lumped components [53]–[55]. It is placed between the SAR and MIMO antenna arrays to increase gain and reduce the mutual coupling. The shunt component based decoupling network is applied to increment the performances to have acceptable decoupling between the antennas.

Various types of the decoupling network approaches to increment the decoupling between the array antennas have been presented and explained in the literature such as diamond-shaped patterned ground resonator (DSPGR)-plane decoupling network [56], dummy load-based decoupling approaches [57], coupled resonator decoupling network (CRDN) [58], and multi-element pattern diversity based decoupling network [59]. Table 1 depicts a comparison of the characteristics of MIMO antennas using decoupling networks. In [59], the highest efficiency and the lowest mutual coupling of −32 dB are achieved utilizing the most straightforward configuration of dummy loads. The dual-band operations are exhibited in [58].

B. PARASITIC ELEMENT DECOUPLING APPROACH

Engraved slit or parasitic element antennas use two orthogonal modes to generate a broad frequency band via coupling in ground plane and/or in radiating patch [60]. In this method, the isolation between elements is optimized by producing an additional coupling route [61], [62]. One of the two coupling routes opposes the signal arriving from the other coupling road, which causes an improvement in isolation level. Indirectly linked decoupling components such as folded shorting strip, meandered slot, and vertical parasitic strip are recognized as a parasitic element [63]–[65]. Ease of implementation, size, and comfortable generation applying PCB technology and/or waveguides are the main benefits of the parasitic or slot antenna. The placement of parasitic elements has to be implemented meticulously, and it is not very straightforward. This procedure increases the performance parameters of the array antennas.

Various types of the parasitic element decoupling approaches based on the square ring slit [66], metal strip reflector [67], [68], stepped feed-line and open-ended ground slit [69], and single-shared-radiation component and meandered feeding lines [70] to obtain lowest interference between the array elements have been proposed and illustrated in the literature. Table 2 mentions the studied specifications of parasitic or slot antennas. The maximum amount of gain and bandwidth is achieved in [66]. The structure in [67] provides optimum efficiency with an easy layout. The antenna in [68] presents the highest isolation value of −22dB. A new shared radiation element antenna is investigated in [70].

C. DEFECTED GROUND STRUCTURE (DGS) DECOUPLING METHOD

DGS introduces the slits realized on the antenna's ground plane [71]. It is pursued as an appearing method for improving many parameters of MIMO and SAR antenna systems [72]. Also, it participates dramatically to increment the isolation. A general way is to create the slit in the ground plane. Howbeit, the slit can improve the isolation, it may also enhance the back radiation [73]–[75]. Various sorts of slits can be engraved on the ground (GND) as well as on the patch for decoupling improvement, shifting frequency, footprint area decrement, and multiband operation. The printed slit controls the flowing current flowing on the ground plane by repressing the interferences between the adjacent elements and behaves such a band-stop filter.

Various types of the DGS isolating mechanisms have been discussed in the literature. A few examples of the these isolating mechanisms are S-shaped DGS [76], square ring DGS [77], T-shaped metallic stub based DGS [78], electrically small meandered DGS [24], [79], ground plane loaded with complementary split ring resonator (CSRR) [22], concentric square ring patch with CSRR loaded GND [80], CSRR loaded GND [81], and slotted CSRR in GND [82]. Properties of several DGS antennas presented here are listed in Table 3. This table explains that antenna in [76] has

TABLE 2. Comparison on the performance parameters of slit or parasitic element based MIMO and SAR antennas.

Ref.	[66]	[67]	[69]	[70]
Dimensions / Material	66.25 × 66.25 ×1.6 mm^3 FR-4	25 × 30 × 1.6 mm^3 FR-4	42 × 25 × 1.6 mm^3 FR-4	22 × 24.3 × 1.52 mm^3 Rogers TMM4
Isolation Level (dB)	≥ -20 dB @3.0 ~12.0 GHz	≥ -20 dB @3.1 ~10.6 GHz	≥ -22 dB @3.2 ~12.0 GHz	≥ -15 dB @3.0 ~10.6 GHz
Applied Approach	Square ring slot and stepped feed line	Two coplanar stripline-feed staircase-shaped radiating elements	Open-ended ground slot and stepped-slot feed line	Meandered feed line and stub to ground linked through via
Efficiency / Gain	60% / 5~8 dBi	90% / 5.2dBi	≤80% / 4dBi	82% / 1.5~5.8 dBi
No. of Ports / Applications	Dual Ports / UWB	Dual Ports / UWB	Quad Ports / Portable UWB	Dual Ports / UWB portable devices
Remarks	Lowest ECC	Simple manufacture and small dimension	Low mutual coupling	Maximum gain and expensive substrate

TABLE 3. Comparison on the performance parameters of DGS MIMO and SAR antennas.

Ref.	[66]	[83]	[78]	[24]
Dimensions / substrate	100 × 72 × 3.81 mm^3 Rogers TMM6	60.2 × 60.2 × 1.6 mm^3 RF-4	22 × 26 × 0.8 mm^3 RF-4	50 × 160 × 0.8 mm^3 RF-4
Isolation Level (dB)	≥ -55 dB @ 2.57 GHz	≥ -25 dB @ 2.45 GHz	≥ -20 dB @ 3.1~11.8 GHz	≥ -20 dB @ 0.7~1.0 GHz
Applied Approach	S-formed periodic DGS	Square ring DGS	Trident-shaped Strip and Ground plane open ended slit	Open ended DGS-slit
Efficiency / Gain	93~96% / -1.79~3.75dBi	81% / 2.1dBi	85% / 3.6~6dBi	80% / 2dBi
No. of Ports/ Applications	Quad Ports/ WLAN	Quad Ports/ WLAN	Dual Ports/ UWB, WLAN, X-band notched	Quad Ports/ LTE
Remarks	Large thickness and high efficiency	Miniature structure and simple construction	Miniature structure and large bandwidth and filter	Complex structure and controllable isolation

TABLE 4. Comparison on the performance parameters of CSRR MIMO and SAR antenna.

Ref.	[22]	[80]	[81]	[82]
Dimensions / substrate	23 × 29 × 1.524 mm^3 Rogers TMM4	60 × 60 × 1.6 mm^3 FR-4	100 × 50 × 0.8 mm^3 FR-4	70 × 100 × 1.6 mm^3 Rogers4003
Isolation Level (dB)	≥ -15 dB @ 3 ~12 GHz	≥ -22 dB @ 2.2 ~2.7 GHz	≥ -18 dB @ 2.4~2.5 GHz	≥ -20 dB @2.45 GHz & ≥ -33 dB @5 GHz
Applied Approach	Stub and GND SCRR and	GND CSRR and concentric square ring patch and	GND and bottom plane CSRR	Slotted CSRR in GND
Efficiency / Gain	82% / 5.9dBi	72.57% / 4dBi	29% / -0.8dBi	86.64% / 4.025dBi
No. of Ports/ Applications	Dual Ports/ UWB	Quad Ports/ ISM	Quad Ports/ ISM	Dual Ports/ WLAN
Remarks	Large bandwidth and small structure	Horizontal and vertical polarized, easy layout	Large size and thinner thickness	Lowest mutual coupling, dual-band, and easy layout

the largest size and thickness. The antenna in [76] also achieves the highest efficiency and isolation of −55 dB. Even though the antenna in [24] presents the largest bandwidth accompanying band notch property and small size, it depicts considerably higher isolation performance than [66].

Table 4 shows the characteristics of the CSRR loaded ground plane antennas. For the antenna in [82], the highest efficiency at 86.62% and the most straightforward configuration with dual band properties is obtained. The antenna in [82] has higher isolation of −33 dB. Hence, it is more appropriate in comparison to other CSRRs.

D. NEUTRALIZATION LINE DECOUPLING APPROACH

Neutralization lines [84] are utilized to transit electromagnetic waves from one antenna to another via a metallic slot or lumped component. They create a contrary coupling which lowers the interferences at given frequencies between the elements. Neutralization lines have considered as particular isolation approaches, which annul the interferences via presenting a second road with an inverse phase and equal amplitude. Consequently, the utmost of neutralization lines accessible in literature are narrowband [85], [86]. The neutralization line is more appropriate for the SAR and MIMO systems with a low number of antenna arrays. In MIMO and SAR

TABLE 5. Comparison on the performance parameters of neutralization lines MIMO and SAR antennas.

Ref.	[87]	[88]	[18]	[89]
Dimensions / Material	36 × 65 × 1 mm^3 FR-4	135 × 80 × 0.8 mm^3 FR-4	50 × 40 × 1.6 mm^3 FR-4	4 cm × 4 cm × 1.6 mm FR-4
Isolation Level (dB)	≥ -15 dB @ 2.4 ~2.5 GHz	≥ -23 dB @ 750, 850, 2000, 2500 MHz	≥ -20 dB @ 2.45 and 5.8 GHz	≥ -21 dB @ 3.1 ~11 GHz
Applied Approach	Neutralization line	Crossed neutralization line with integrated inductors	Neutralization line with couple of inductor and capacitor	Stepped neutralization line
Efficiency / Gain	81% / 2.1dBi	31.86~61.73% / -1.79~3.75 dBi	78~85% / -	- / 3.28~4dBi
No. of Ports / Applications	Dual Ports / WLAL USB-Dongle	Dual Ports / LTE, GSM, WLAN	Dual Ports / WLAN	Quad Ports / UWB
Remarks	Small structure and easy configuration	Complex layout and minimum isolation	high efficiency and easy layout	Large dimension, largest bandwidth, and simple configuration

TABLE 6. Comparison on the performance parameters of frequency reconfigurable based MIMO and SAR antennas.

Ref.	[93]	[94]	[96]	[97]
Dimensions / Material	46 × 20 × 1.6 mm^3 FR-4	120 × 60 × 1.5 mm^3 RO-4350	90 × 50 × 0.8 mm^3 FR-4	150 × 150 × 0.8 mm^3 FR-4
Isolation Level (dB)	≥ -18 dB @2.39 ~2.48 GHz and 5.15 ~6.4 GHz (Off state)	≥ -12 dB @1.77 ~2.51 GHz ≥ -25 dB @0.75 ~7.65 GHz	≥ -47 dB @2.3 ~2.4 GHz (for D1 and D2 On-state), ≥ -30.8 dB @3.4 ~3.6 GHz (for D3 On-state), ≥ -43 dB @2.5 ~2.7 GHz (for D1 and d4 On-state)	≥ -20 dB @1.6 ~1.9 GHz (Off state) ≥ -20 dB @2.2 ~2.96 GHz (On state)
Applied Approach	RF MEMS Switches	Biasing network and varactor diodes per component	DC biasing network and pin diodes and	Biasing network and pin diodes switches
Efficiency / Gain	83% / 2.9dBi	65~81 % / 0.5~3.2 dBi	48.43~73.1% / 1.99~2.78dBi	55~83 % (Lower band) 75~92 % (Upper band) / 3~5dBi
No. of Ports / Applications	Quad Ports / WLAN	Five Ports / UWB and cognitive radio (CR)	Quad Ports / WiMAX	Triple Ports / LTE and portable wireless DTV media players
Remarks	Complex layout	Expensive substrate Complex layout	Highest isolation	Optimum efficiency and gain

antenna models, the difficulty of matching is quite evident. A neutralization line is a metallic structure with a thin thickness that dissolves the obstacle of matching and suppresses the coupling between antennas. The form, dimensions, and orientation of the neutralization line are related to the antenna components. However, finding the neutralization path is not very straightforward.

Various implementations of the neutralization line decoupling approach to reduce the array antenna's mutual coupling such as thin printed neutralization lines [87], pair of crossed neutralization lines [88], neutralization lines together with LC matching network [18], and neutralization lines between ground planes [89] have been presented and investigated in the literature. Table 5 describes the neutralization-based MIMO and SAR antenna properties. A couple of crossed neutralization lines is investigated in [88] with the thinnest substrate thickness and proper gain amounts. However, the antenna's layout is not simple. The antenna operates on multiple frequency bands and presents a minimum mutual coupling amount of −23 dB.

E. PIN DIODE, VARACTOR DIODE, AND FEEDING STRUCTURE DECOUPLING APPROACH

PIN diode, varactor diode, and feeding structures are also applied to suppress the mutual coupling effects [90]. PIN diode in antenna models generates dynamic radiation patterns. The implementation of PIN diode in MIMO and SAR antenna arrays results to enlarge the link capacity controls the antenna's length, and also increments decoupling. This attribute ensures the reconfigurability of the antenna's radiation [91].

Several switching-based decoupling methods where MEMS switches, *p-i-n* and varactor diodes are applied to expand the working frequency band and degrade the coupling have been proposed in the literature [92]. Some of them are based on back-to-back MEMS switches [93], slot-based P-I-N diodes [94], [95], planar inverted-F P-I-N diodes [96], and microstrip loop and slit frequency reconfigurable [97]. Table 6 lists the characteristics of the mentioned approaches. The antenna illustrated in [96] is not simple because of the presence of a shorting plate and a vertical corrected feed line. It has the maximum amount of

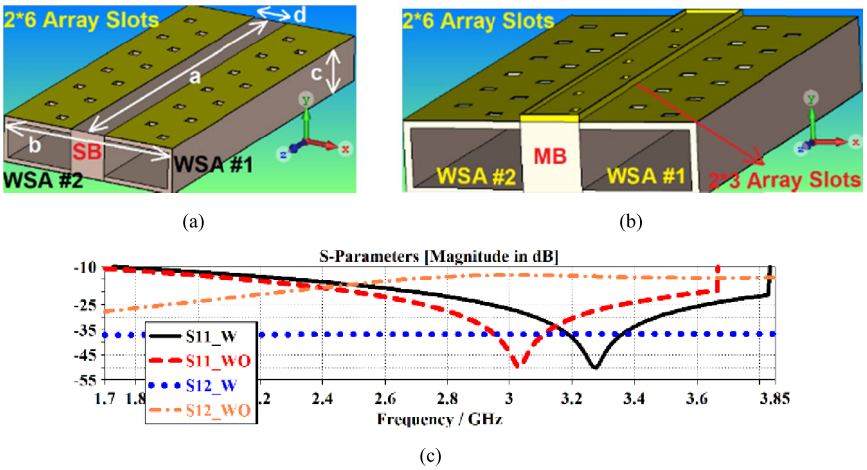

FIGURE 2. (a) Reference structure, (b) WSA antennas with MTS bulkhead, (c) reflection and transmission coefficients. WO and W represent without and with MTS bulkhead, respectively [112].

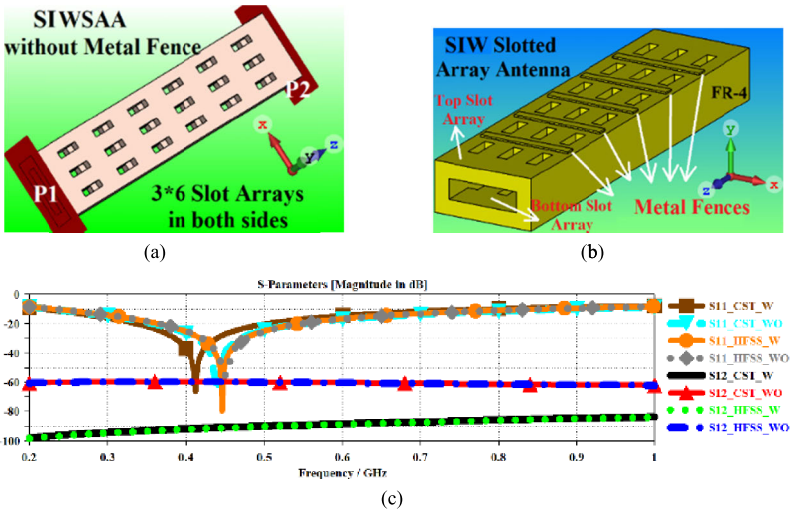

FIGURE 3. (a) Reference structure (WO), (b) proposed structure with metal fences (W), and (c) S-parameter performances [113].

gain. Also, it has the highest isolation amount of −47 dB. However, the antenna structure in [97] shows the optimum efficiency and gain of 92% and 5 dBi, respectively.

F. FREQUENCY-SELECTIVE SURFACE (FSS) DECOUPLING METHOD

FSS approaches can efficiently improve the isolation. However, they are discordant with low-profile structures, and they affect the radiation pattern [31]. This technique can be applied between the dielectric resonator antennas (DRA). This is obtained by accommodating an FSS between the DRAs that have been placed in the H-plane. The FSS contains an array of SRR cells that are embedded onto the E-plane. The SRR formation is modeled to achieve band-stop functionality inside the antenna frequency band.

G. ELECTROMAGNETIC BANDGAP (EBG) DECOUPLING STRUCTURE

An EBG structure blocks electromagnetic waves of a certain frequency or plays as a region to pass electromagnetic waves [98]. Various stop-band, pass-band, and band-gap frequencies can be recognized [99]. The EBG is a periodic adjustment of dielectric or metallic materials. Structure's periodicity and singular resonance of the elements can produce many bandgaps [100]. EBG presents parasitic inductance and capacitance. Thus, the phase constant of an electromagnetic wave distributing under the patch will be much greater than the transverse electromagnetic mode. As a result, the EBG element operates in a slow-wave medium with a wavelength shorter than the transverse electromagnetic mode. Conventionally, the EBG structure is located between the antenna arrays. While, for

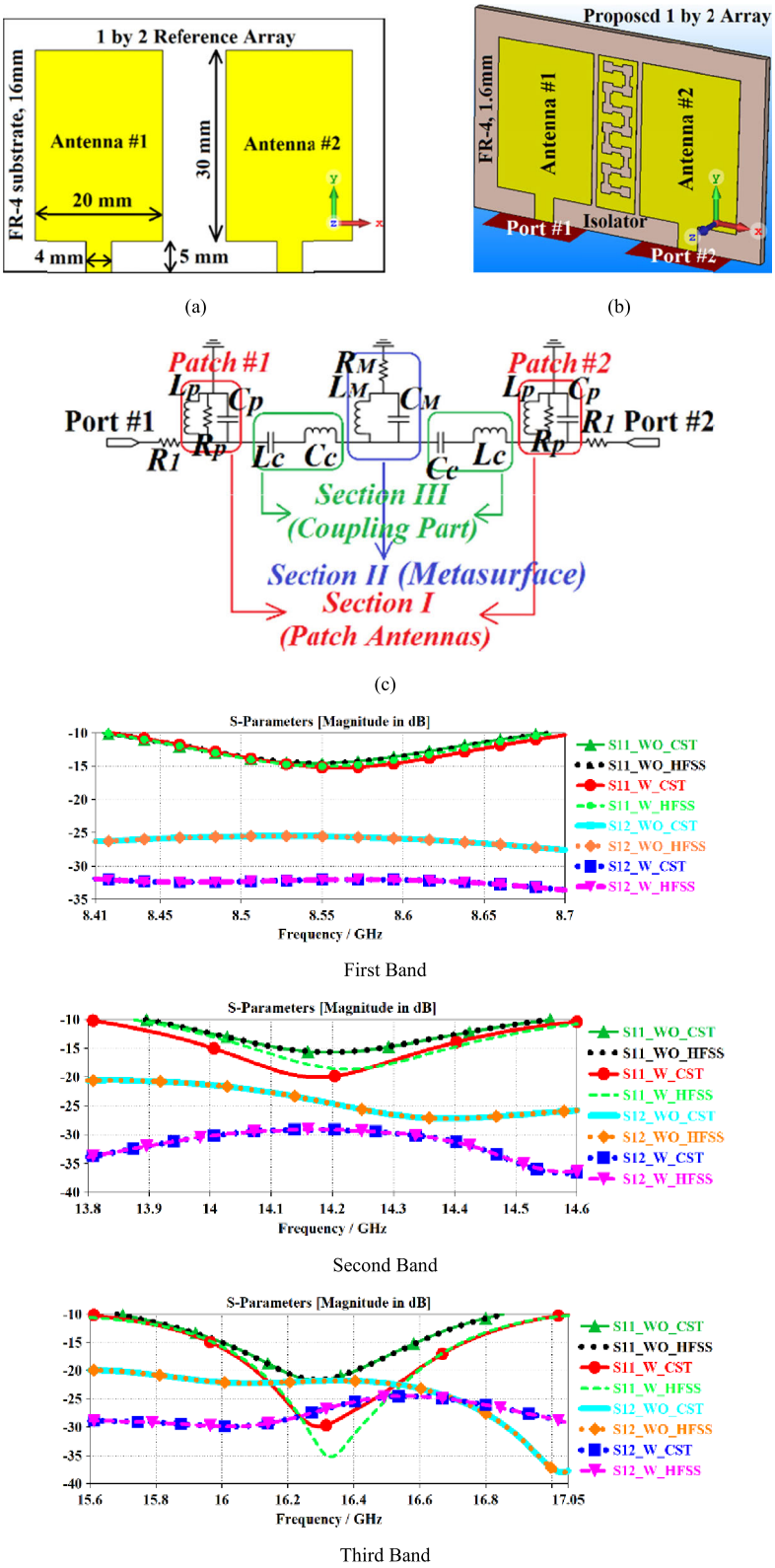

FIGURE 4. Configuration of (a) reference array antennas (WO), (b) proposed structure applying the MTS isolating sheet (W), (c) circuit diagram, (d) S-parameters, and (e) surface current distributions at 19.5 GHz (when one port is stimulated, the other one is matched to a 50-ohm load) [114].

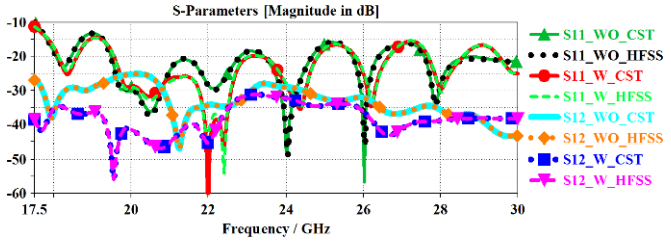

Fourth Band

(d)

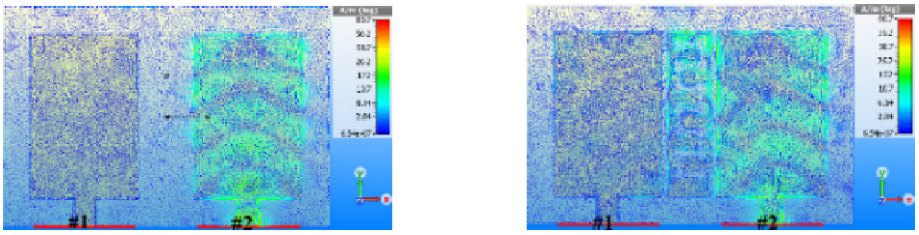

Without MTS isolating sheet

With MTS isolating sheet

(e)

FIGURE 4. ***(Continued.)*** **Configuration of (a) reference array antennas (WO), (b) proposed structure applying the MTS isolating sheet (W), (c) circuit diagram, (d) S-parameters, and (e) surface current distributions at 19.5 GHz (when one port is stimulated, the other one is matched to a 50-ohm load) [114].**

TABLE 7. **Comparison on the performance parameters of electromagnetic bandgap based MIMO and SAR antennas.**

Ref.	[101]	[102]	[103]	[104]
Dimensions / Substrate	95 × 95 × 2.284 mm^3 Rogers RO4350B	35 × 40 × 1.6 mm^3 FR-4	90 × 45 × 1.6 mm^3 FR-4	60 × 57 × 1.2 mm^3 FR-4
Isolation Level (dB)	≥ -25 dB @ 2.395 ~2.42 GHz	≥ -28 dB @ 2.45 ~2.55 GHz	≥ -30.35 dB @ 5.59 GHz	≥ -53.7 dB @ 2.43 ~2.54 GHz
Applied Approach	Vias and S-EBG	Dual layer mushroom EBG	8 Z-formed EBG	SRR and EBG
Efficiency / Gain	56.57% / 5.12dBi	64.42~66.94 % 4.55~4.92 dBi	NG / 2.42dBi	82% / NG
No. of Ports / Applications	Quad Ports / IMS	Dual Ports / IMS	Dual Ports / WLAN	Dual Ports / ISM
Remarks	Complex layout	Sorely complex layout and compact dimension	Simple layout and large dimension	High efficiency and simple layout

isolation improvement, the antenna array is enclosed via the EBG.

In the literature, several types of the EBG decoupling structures have been presented and discussed recently to improve decoupling between the array antennas in MIMO and SAR systems such as the mushroom type EBG [101], dual-layer multi-element EBG [102], periodic *Z*-formed EBG [103], and 1-D and SRR EBG [104]. Table 7 provides an overview of the presented EM band-gap technique-based MIMO and SAR antennas. Simplest structure with easy manufacture providing the highest isolation in order of −53.7 dB has been presented in [103]. The maximum efficiency of applying SRR and EBG has been presented in [104].

All the approaches discussed above are summarized in Table 8. From this table, most of them present isolation in order of 15dB, whereas the neutralization line method has the lowest isolation of 12dB. The benefits and drawbacks of several methods are listed in Table 9. The isolation value corresponds to the sort of antennas and the adopted ground plane.

IV. HIGH EFFICIENT DECOUPLING TECHNIQUES BASED ON THE METASURFACE (MTS) AND METAMATERIAL (MTM) PROPERTIES APPLICABLE IN SAR AND MIMO ANTENNA SYSTEMS WITH WIDE RANGE OF DESIGN POSSIBILITIES

The results presented in Section II and listed in Tables 1 - 9 show that the abovementioned decoupling approaches are just presented for a limited number of the array elements. In addition, the design process of some of them is complex and far way to practical realizations. Most of them are working at a specific range of frequency with low gain and efficiency, and they have affected the total physical size of the array antennas. In addition, they are not applicable for a wide range of design possibilities, and they have an asymmetric configuration which enables them for mass production.

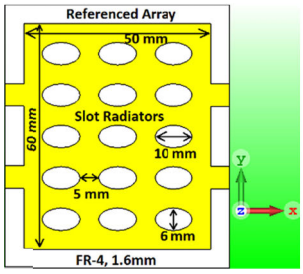

(a)

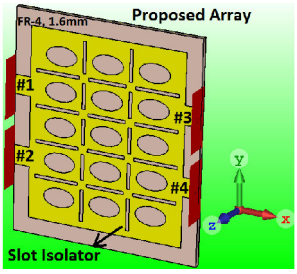

(b)

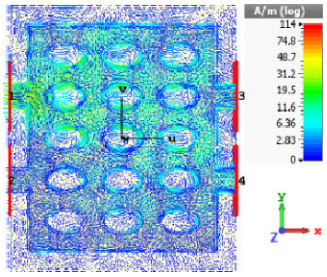

without linear slot isolators

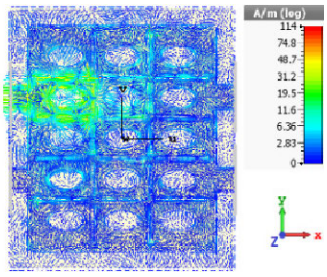

with linear slot isolators

(c)

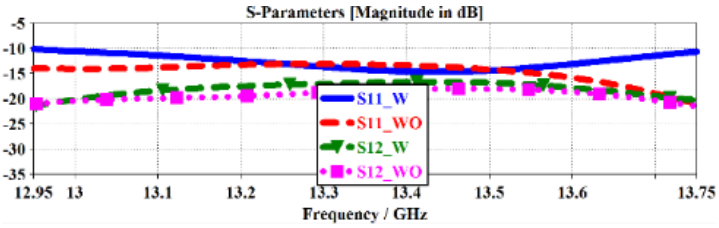

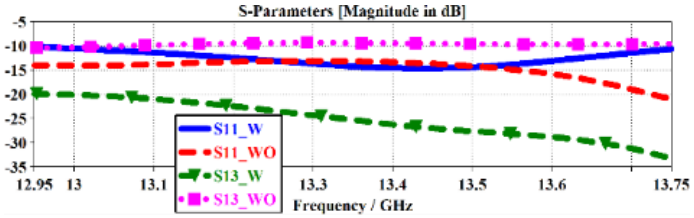

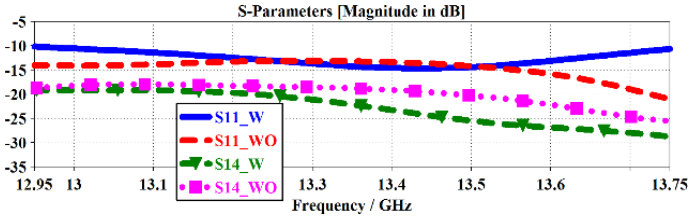

First band, 12.95 - 13.75 GHz (Ku-band)

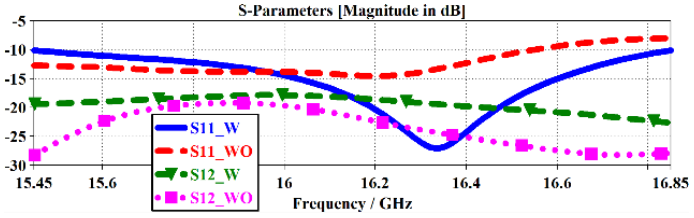

FIGURE 5. (a) Reference structure (WO), (b) proposed structure with (W) linear slot isolators, (c) surface current distributions at 22.5 GHz (when one port is stimulated, the others are matched to a 50-ohm load), and (d) S-parameters [115].

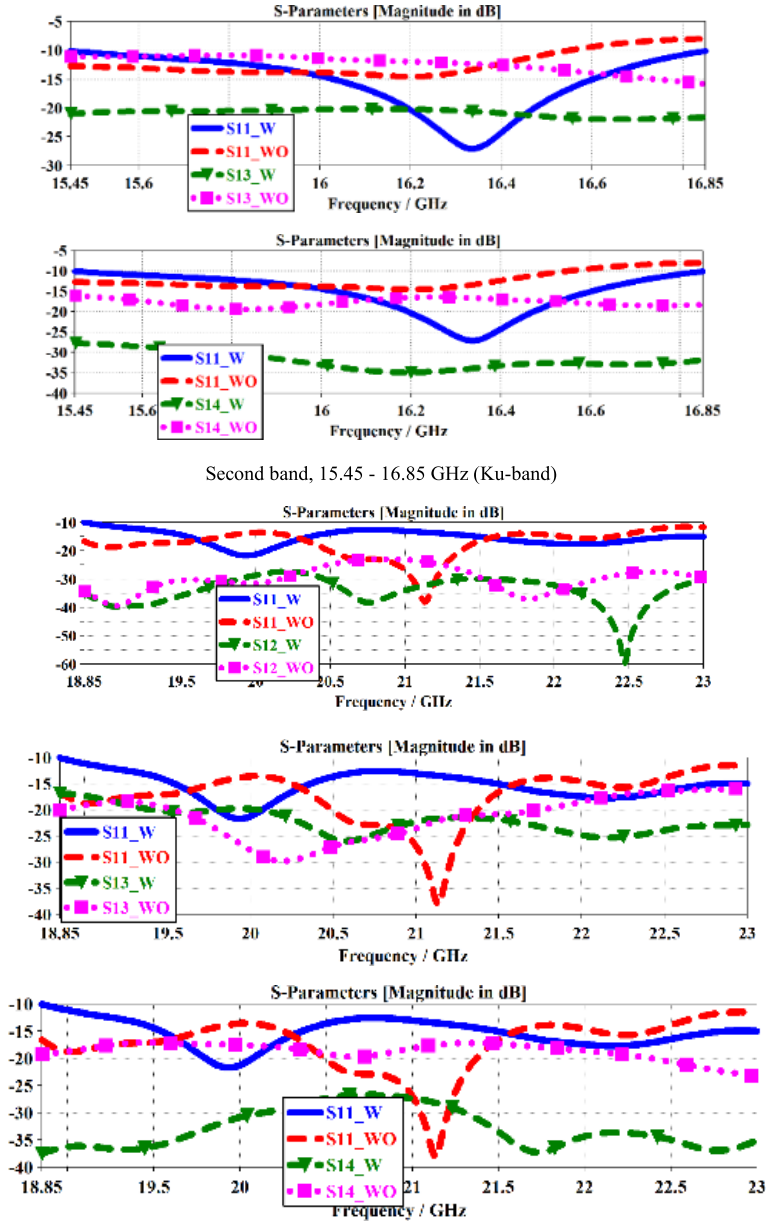

(d)

FIGURE 5. ***(Continued.)*** **(a) Reference structure (WO), (b) proposed structure with (W) linear slot isolators, (c) surface current distributions at 22.5 GHz (when one port is stimulated, the others are matched to a 50-ohm load), and (d) S-parameters [115].**

Waveguide slot array (WSA) antennas propose favorable properties that contain moderate cost, low-loss, and high power-handling ability [110]. While the major disadvantage of the WSA is the interferences between the slit antennas that reduce the bandwidth, gain, and recurves the radiation pattern. To employ WSA antennas in next generation SAR and MIMO systems, a low degree of coupling is required [111]. Several methods have been implemented to increase isolation [112]–[127]. Some commonly used methods include coplanar strip walls between the antennas [128], [129] and frequency selective surfaces [34]. However, these methods diminish the radiation pattern. This happens because a coplanar strip wall or an FSS wall does not have a good matching condition. Consequently, the radiation pattern is degraded because of reflected waves from the integrated wall between the antennas.

Therefore, in this part of the review study the new approaches are introduced to increment isolation between

TABLE 8. Compsrison among various decoupling mechanism with performance parameters.

Ref.	Isolation technique	Isolation shape	Frequency	Isolation	Gain	Size
[77]	Decoupling network	Two section transmission line	746–787 MHz	23 dB	3 dBi	55×110 mm^2
[48]	Decoupling network	T-shaped strip	1.65-1.9 GHz and 2.68-6.25 GHz	10 and 15 dB	1.35 and 4.22 dBi	55×110 mm^2
[49]	Decoupling network	Tunable and coupling network	2.4 GHz	20 dB	-	90 × 72 mm^2
[52]	Decoupling network	Tunable and coupling network	2.2-2.7 and 4.9-5.9 GHz	15 dB	2.9-4.5 dBi	40 × 40 mm^2
[53]	Decoupling network	Structure with lumped element	770 MHz	16 dB	-3.8 dBi	120×50 mm^2
[55]	Parasitic elements	Structure between antenna	2.4-2.485 GHz 3.2–3.5 GHz 5.15-5.85 GHz	16 dB	-	100×60 mm^2
[102]	Parasitic elements	Branch element/resonator	3–8.5 GHz	15 dB	5.75 dBi	26×40.5 mm^2
[106]	Parasitic elements	Branch element/resonator	800–2700 MHz	36 dB	3.2 dBi	-
[107]	DGS	Slotting	2.4-2.484 GHz	17.8 dB	3 dB	39.5×20 mm^2
[108]	DGS	Defected ground plane/partial ground	2.0–7.31 GHz	17 dB	3.67 dBi	54.82 × 96.9 mm^2
[85]	Neutralization lines	Simple line	2.4 GHz	19 dB	2.1 dBi	30 × 65 mm^2
[109]	Neutralization lines	Branch line/suspended line	760 MHz	12 dB	0.9 dBi	46 × 85 mm^2

TABLE 9. Benefits and drawbacks of isolation techniques.

Ref.	Techniques	Benefit	Drawback
[39] – [59]	Decoupling network	- Easy decoupling structure - Enhance far-field properties	- Sometimes additional space is needed - Generate ohmic losses
[60] – [70]	Parasitic elements	- Control the isolation - Suitable DG	- Shift in frequency due to parasitic elements
[71] – [82]	Defected ground structure (DGS)	- Small antenna dimension - Proper diversity	- usually not suited for mobile applications - Low gain
[84] – [89]	Neutralization lines	- Acceptable impedance matching - Proper diversity with DG	- Lower frequency band - Shorter bandwidth when compared with upper frequency band
[90] – [97]	PIN diode, Varactor diode and feeding arrangement	- Appropriate isolation - High gain	- Losses due to component - Short frequency band - Complex configuration
[98] – [104]	Electromagnetic Bandgap (EBG)	- Easy layout - Acceptable isolation	- Short bandwidth - Low gain

WSA antennas. These primarily involve placing an MTS between the waveguide slit antennas. Proposed techniques are exhibited to significantly repress the mutual coupling and increase the gain and working frequency band. They are effective and simple to implement.

Besides the metasurface- and metamaterial-inspired decoupling methods applied to WSA antennas, other efficient decoupling approaches based on the same concepts have been presented in bellow with providing an efficient number of examples and various type of designs for SAR and MIMO applications. The main advantages of the following designs are their simple prototypes with ease of manufacture process, low cost, high isolation level between the array elements, as well as, not being limited to small number of array elements, being applicable for a wide range of frequency band, having very negligible effects on the performance parameters with keeping constant the physical dimensions, and having symmetrical layouts which enable them for cost effective mass production.

A. MUTUAL-COUPLING REDUCTION BETWEEN WSA ANTENNAS INSPIRED MTS BULKHEAD FOR MIMO SYSTEMS

In [112], a novel mechanism has been presented to suppress the interferences between WSA antennas based on the MTS concept. This is obtained by locating an MTS bulkhead between the antennas, as depicted in Fig.2. The antenna's performance is displayed to improve when compared to the same reference structure with no MTS. The implemented antennas have a physical dimension of 40 mm × 20 mm × 5 mm and

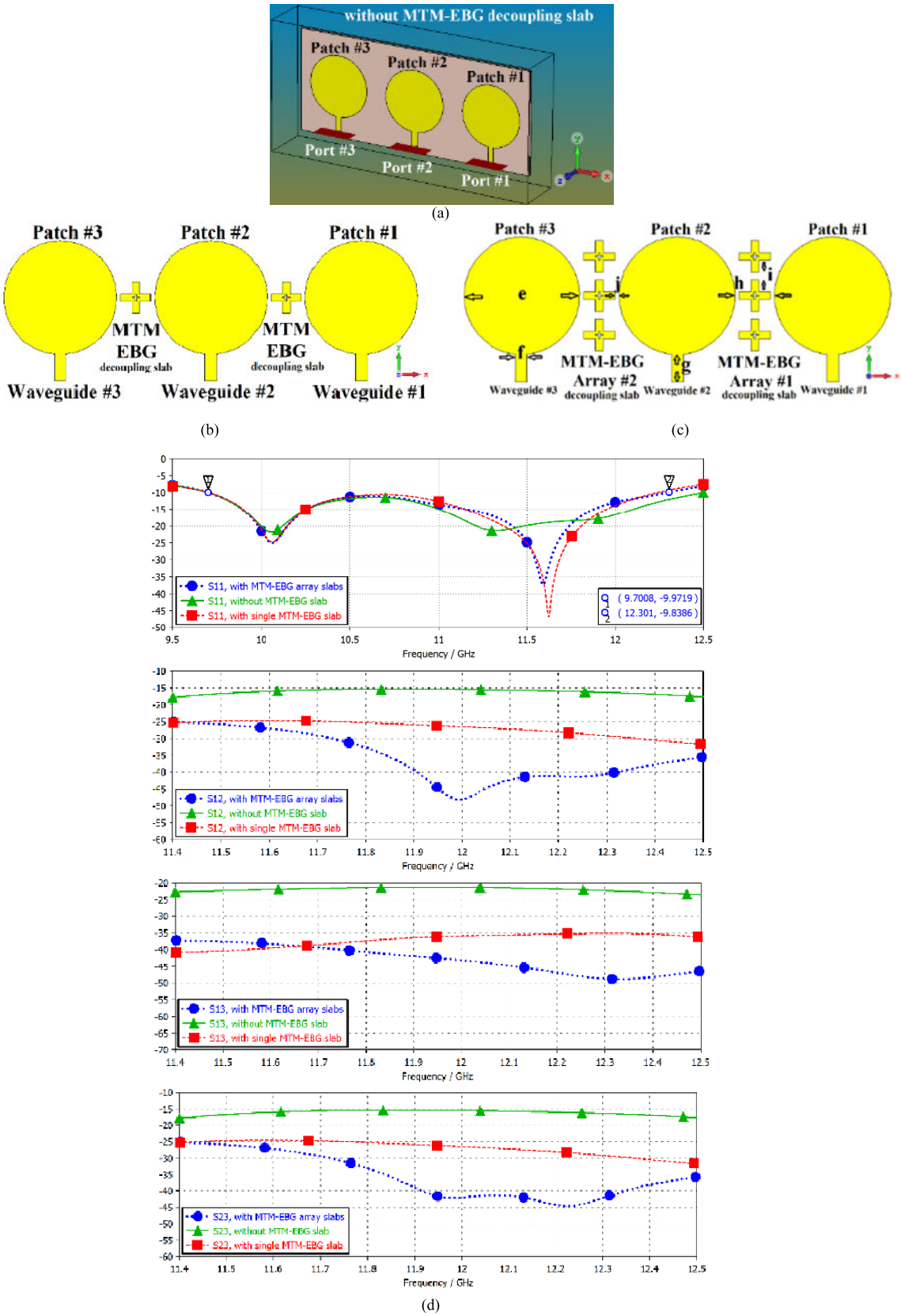

FIGURE 6. (a) Reference antenna array, (b) antenna array with single MTM-EBG decoupling slabs, (c) proposed antenna array with array of MTM-EBG decoupling slabs, (d) S-parameters performances, (e) distributed surface currents at resonance frequency of 10 GHz [116].

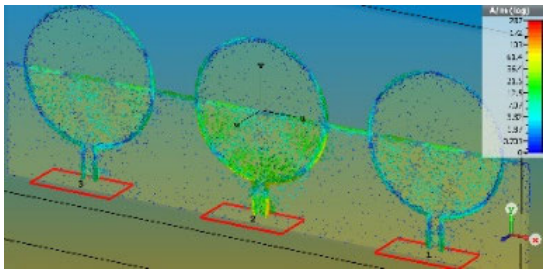
without MTM-EBG decoupling slab

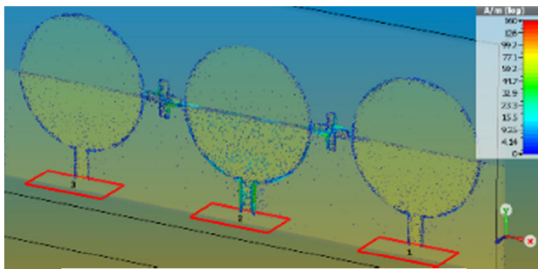
with single MTM-EBG decoupling slabs

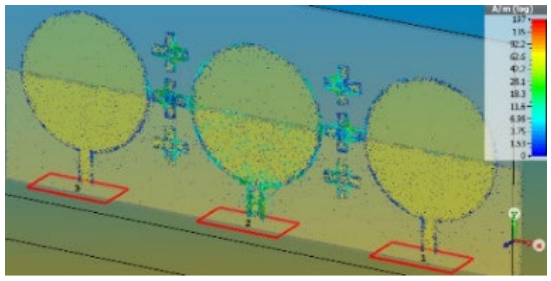
with array of MTM-EBG decoupling slabs

(e)

FIGURE 6. *(Continued.)* **(a) Reference antenna array, (b) antenna array with single MTM-EBG decoupling slabs, (c) proposed antenna array with array of MTM-EBG decoupling slabs, (d) S-parameters performances, (e) distributed surface currents at resonance frequency of 10 GHz [116].**

operate over a bandwidth of 1.7 GHz to 3.66 GHz, which relates to a practical bandwidth of 73.13%. The reference WSA antennas present an average isolation of -20 dB, while, with an MTS bulkhead, the decoupling is depicted to enhance to -36.5 dB. Furthermore, the bandwidth expands by ∼10%, and the gain increases by 14.66%. This mechanism will be very suitable for SAR and MIMO antenna systems where low coupling between adjacent radiation elements is necessary to improve the specifications of the structure and minimize array phase errors, as a necessity to increment the performance of the system.

B. REDUCTION IN INTERACTION BETWEEN LONGITUDINAL-SLOTTED ARRAY BASED ON SIW ANTENNA LOADED WITH METAL-FENCES OPERATING ACROSS VHF/UHF FREQUENCY-BANDS

In [113], it is investigated that substrate integrated waveguide longitudinal slotted array antenna (SIWLSAA) that is loaded with metal fences shows low mutual coupling throughout VHF/UHF bands. A reference SIWLSAA implemented for comparison aim includes 3 × 6 slotted arrays designed on the top-side, and the bottom-side of the FR-4 layer has the lowest mutual coupling of −63 dB between its slits. Suppression in mutual coupling is discussed by applying an easy, innovative way based on locating a metal fence between each row of the slit arrays. The mutual coupling is exhibited to better than -83 dB entire 0.2-1.0 GHz with a gain more than 1.5dBi, and a side-lobe level less than -40 dB. The presented SIWLSAA shown in Fig.3 is compact and has a physical dimension of 40 mm × 10 mm × 5 mm ($0.026\lambda_0 \times 0.006\lambda_0 \times 0.002\lambda_0$, where λ_0 is defined at 200 MHz). The proposed SIWLSAA will be very suitable for MIMO and radar system applications.

C. ANTENNA ISOLATION ENHANCEMENT APPLYING INTEGRATED MTS ISOLATOR FOR SAR AND MIMO APPLICATIONS

In [114], a decoupling structure based on MTS that is constructed of a square-wave slot pattern with overstated corners realized on a rectangular microstrip presents low mutual coupling between neighbor antennas for array systems. The 1 × 2 symmetric antenna array embedded with the proposed decoupling structure, which is exhibited in Fig.4, is modeled to work at ISM bands of X, Ku, K, and Ka. As demonstrated in Fig.4, the surface current distributions indicate that the isolation structure compounded of the square-wave slit soaks up the surface waves that would otherwise couple with the adjoining radiating parts. With this mutual coupling suppression technique, the following are observed: (i) the average isolations in the respective ISM bands mentioned above are 7, 10, 5, and 10 dB; and (ii) the center-to-center distance between the neighbor parts is decreased to 10mm (0.28λ). The average gain increment with the MTS decoupling is 2 dBi.

D. WIDEBAND HIGH ISOLATED WSA ANTENNA WORKING OVER KU- AND K- BANDS FOR RADAR AND MIMO SYSTEMS

An innovative approach to increase the isolation between the radiating parts of a waveguide slot array antenna has been proposed and elaborated in [115]. It has obtained by realizing slits between the waveguide oval-formed slits, as shown in Fig.5. The reference array has been implemented with an organization of 3 × 5 oval-formed slots. With embedding linear slits between the radiating oval-formed slots in both vertical and horizontal directions, major increment in isolation has obtained to have values of 24, 20, and 32 dB over the bands of 12.95 to 13.75 GHz (Ku-band), 15.45 to 16.85 GHz (Ku-band), and 18.85 to 23.0 GHz (K-band), respectively. The study on the surface current distributions displays that the slits act as an isolating architecture that soaks up the surface waves, which would be coupled with the adjacent elements. The center-to-center gap between the slits is 0.2λ that is at least two times less than the traditional array structures. Using the slit decouplings, the lowest and highest gains increase by 53.5% and 25.5%. Furthermore, the radiation patterns

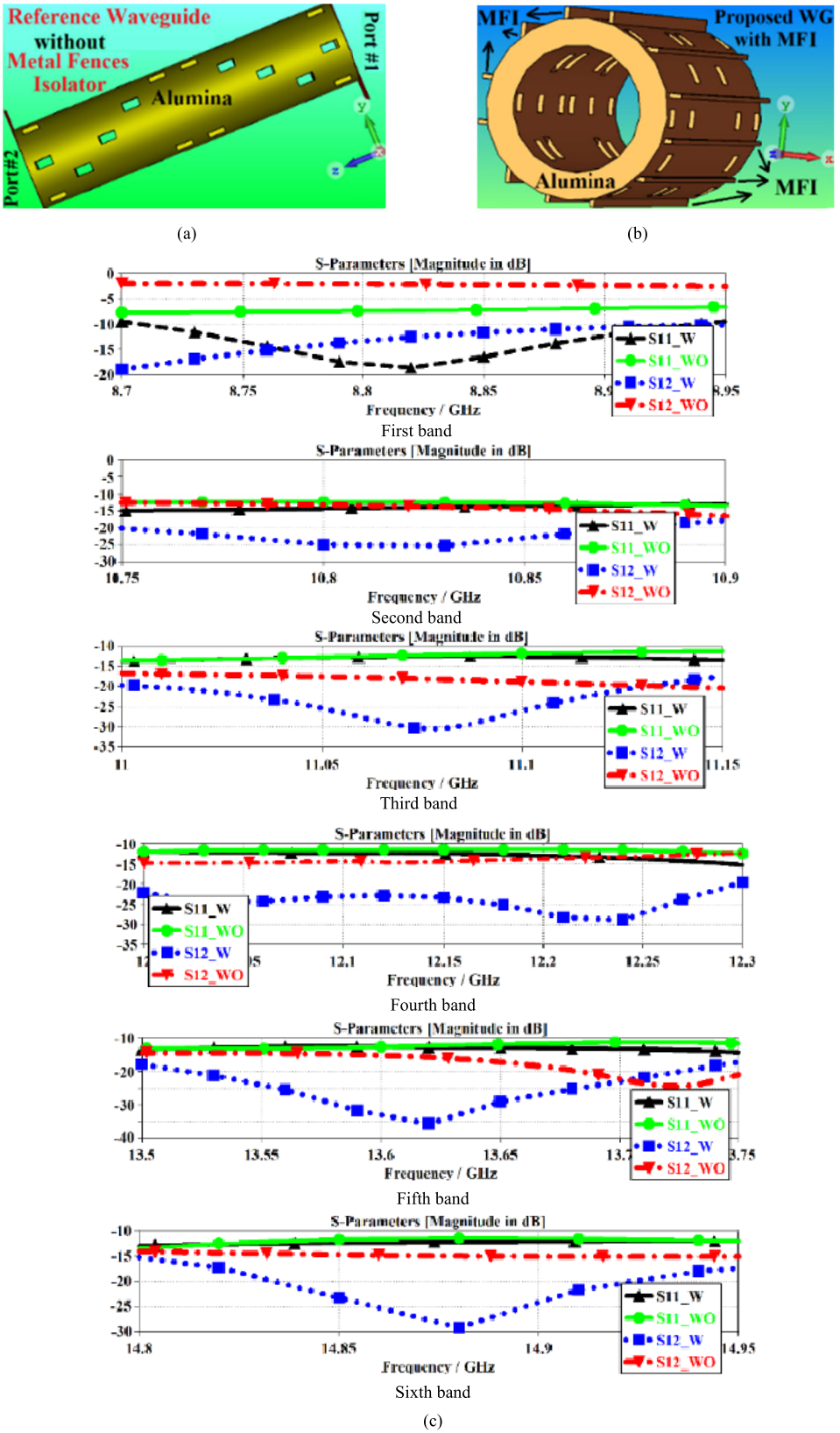

FIGURE 7. Geometries of (a) the reference structure (WO) and (b) the proposed structure with MFIs (W), and (c) S-parameter responses [117].

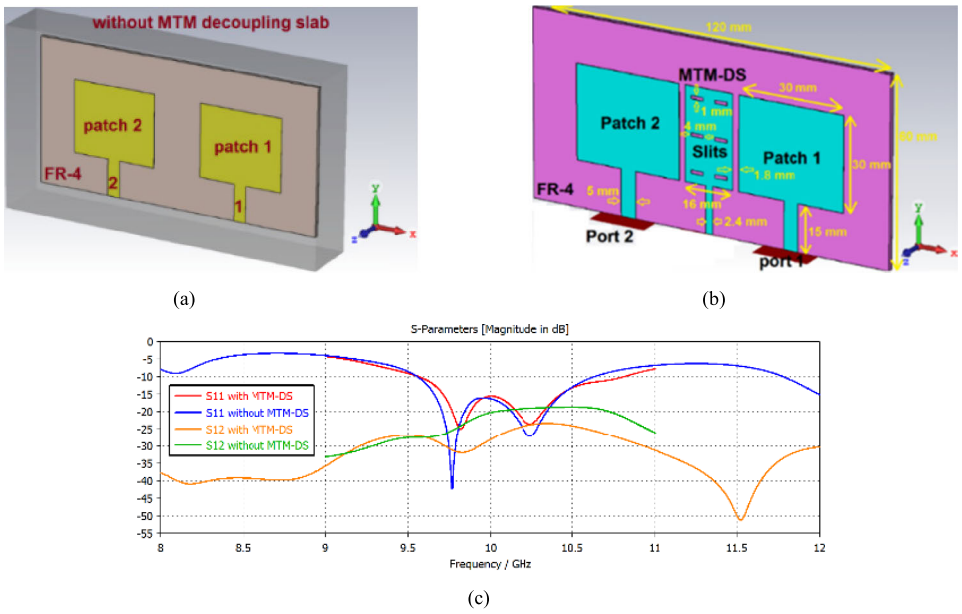

FIGURE 8. Layout of the antenna (a) without and (b) with MTM decoupling super substrate, and (c) S-parameters [118].

are unchanged. This technique is easy for employment and inexpensive for mass production.

E. EM DECOUPLING INSPIRED MTM CONTENT IN ANTENNA ARRAY SYSTEM TO SUPPORT FULL-DUPLEX APPLICATION

An electromagnetic technique to suppress the coupling between array antennas applying MTM EBG is presented and discussed in [116]. Fig.6 shows that the proposed configuration can be considered for a full-duplex array antenna system with short distances between the array elements ($0.33\lambda_0$) without any decay in the radiation pattern. By implementing this way, the decoupling is exhibited to increment by $>$30 dB in the array structure containing three patches modeled to work over 9.7 - 12.3 GHz. To more in-depth discernment, the E-field magnitude profiles without and with the MTM-EBG isolating structure are displayed in Fig.6. Obviously, the distributing E-field is not permitted to be coupled to the neighbor elements that affirms the efficiency of the presented method in decreasing surface waves. A parametric evaluation was utilized to maximize the isolation performances. The array structure has the physical and electrical sizes of 65 mm $\times$ 22.5 mm $\times$1.6 mm and $2.16\lambda_0 \times 0.75\lambda_0 \times 0.053\lambda_0$, respectively, where λ_0 is defined at the mid-band of 10 GHz.

F. ISOLATION ENHANCEMENT IN MTM SIW SLOTTED ANTENNA ARRAYS EMPLOYING METAL-FENCE DECOUPLING SLABS FOR SAR AND MIMO APPLICATIONS

A novel sort of decoupling approach is realized to an MTM substrate integrated waveguide (SIW) slotted antenna array in [117]. Fig.7 shows that the circular formed reference SIW antenna array is built from an Alumina layer with a physical size of 40 mm $\times$ 5 mm $\times$ 1.5 mm. Integrated into the reference structure are 38 slits with the same size, i.e., 2 mm $\times$ 1 mm $\times$ 1.5 mm. This structure workes across X-band to Ku-band, providing an average mutual coupling of about $-$10dB. The mutual coupling was suppressed through embedding metal fence decouplings between the radiation slits, which degraded the interferences by an average of 13dB. Furthermore, the impedance matching bandwidth is improved without decay in the radiation patterns. By utilizing the metal fence decouplings, the optimum obtained gain enhances by $\sim$10%. The proposed approach is easy to realize, and it has been presented for SAR and MIMO systems.

G. SUPPRESSION IN MUTUAL COUPLING APPLYING MTM SUPERSUBSTRATE FOR HIGH PERFORMANCE & DENSELY PACKED PLANAR PHASED ARRAYS

In [118], an efficient decoupling method is illustrated for a phased array. It is obtained via placing a MTM superstrate patch between the radiation parts of the phased array, as shown in Fig.8. The patch is implemented through integrating slits within the patch, where the slits are organized in a 2 $\times$ 3 array. This technique is applied to an FR-4 layer. An average isolation improvement of 5dB is obtained throughout its working bandwidth. This approach is: (i) easy to realize; (ii) suitable for planar antenna designs; (iii) simply applicable in practice; (iv) resilient and dominates the deficiencies of poor front-to-back ratio already presented in literature; and (v) appropriate for densely packed microstrip. Additionally, the presented method is exceptionally versatile for many applications having precise performance necessities.

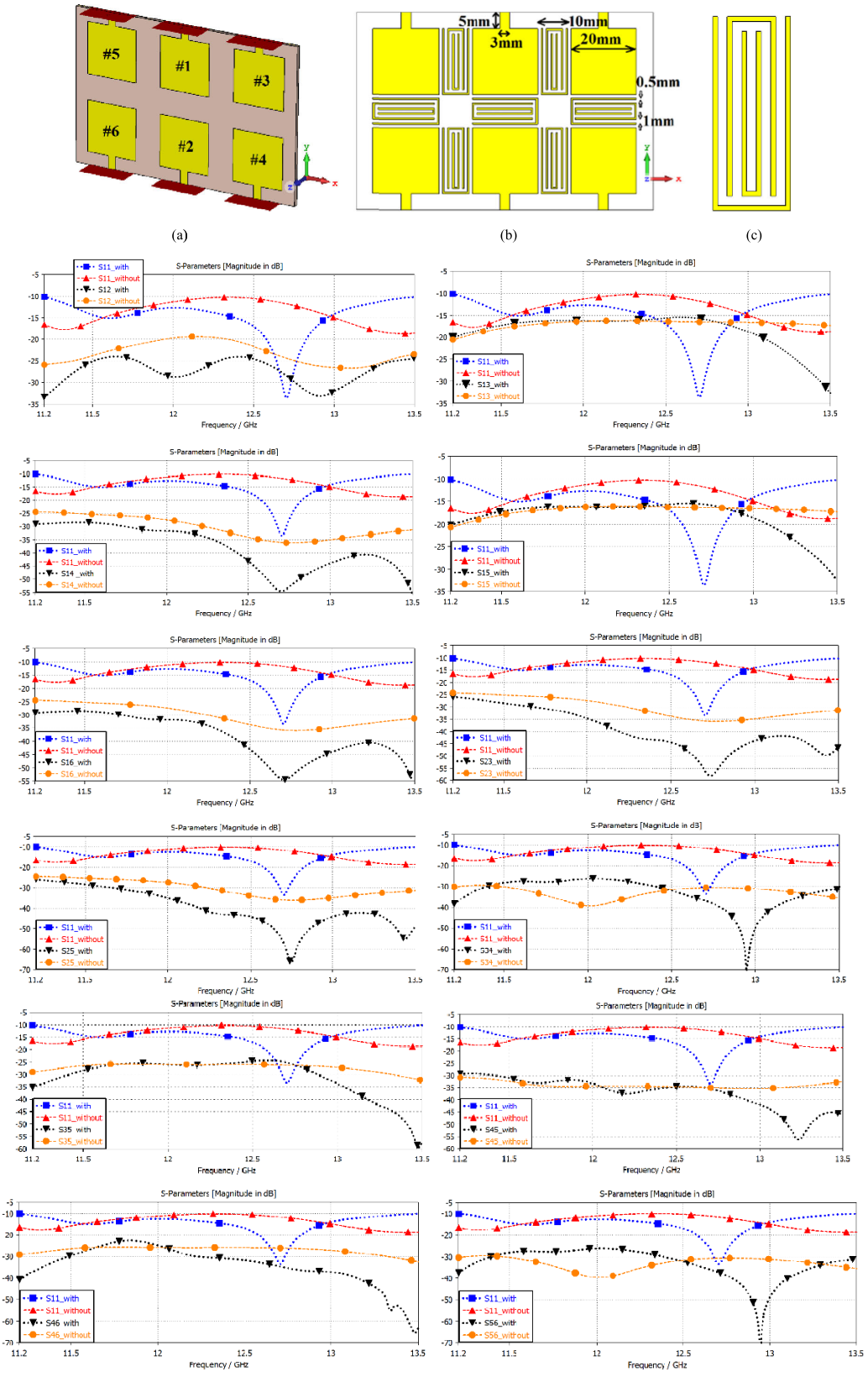

FIGURE 9. (a) Reference array antennas without isolation wall, (b) proposed array antennas with isolator wall, (c) isolator wall, (d) S-parameters [119].

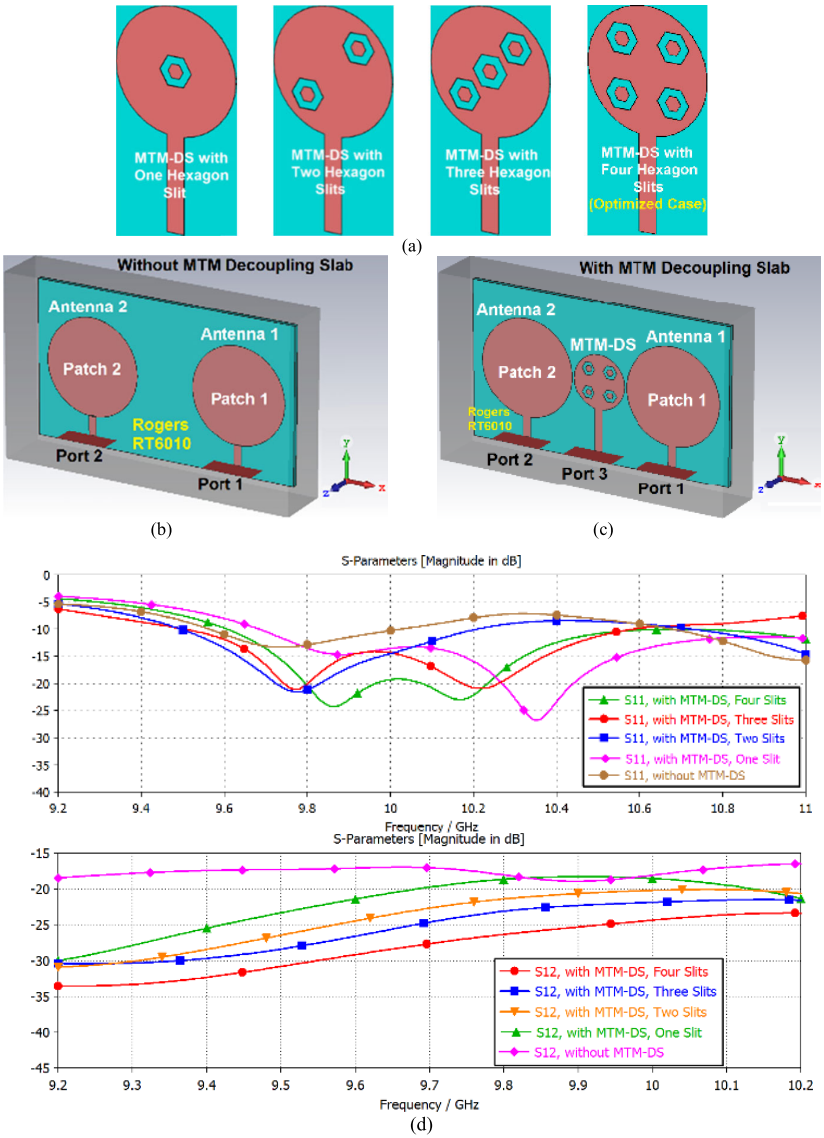

FIGURE 10. (a) MTM isolation sheets, (b) structure without MTM isolation sheet, (c) with multiple MTM isolation sheet, and (d) S-parameters [120].

H. HIGH ISOLATED ARRAY ANTENNAS FOR SAR APPLICATIONS OVER X- AND KU- BANDS

Modern MIMO and SAR need a frequency band which is larger than 1 GHz. Waveguide slot antennas are popularly utilized in MIMO and SAR systems because of their intrinsic benefits, namely power handling ability and high efficiency. However, these antennas have a confined frequency band. While the frequency band of slot antennas can be expanded through applying ridge waveguides, this way presents fabricating intricacy and is not cost-effective. An innovative solution has been proposed in [119] to implement a wide frequency band via applying a 2×3 array structure with the isolation between the antenna incremented by embedding a decoupling wall between the radiating antennas, as shown in Fig.9. The decoupling wall contains three intercoupled U-shaped microstrip transmission lines. By this method, the frequency band is wider than 2 GHz within the X-band and Ku-band.

I. DECOUPLING APPROACH INSPIRED MTM SUPERSUBSTRATE UTILIZED IN DENSELY PACKED ANTENNA ARRAYS

An easy and feasible mechanism for increasing the isolation between neighbor antennas is proposed and applied in [120]. Fig.10 shows that this is achieved by placing a smaller patch with MTM isolating structure between the antennas. The antenna structures are circular patches and the MTM decoupling structure is designed from a hexagonal slot resonator. The direct effect of realizing the MTM decoupling structure is 60% improvement in isolation between the closely spaced elements, 200% enhancement in impedance match, and 369% enhancement in the practical bandwidth. Because GND is

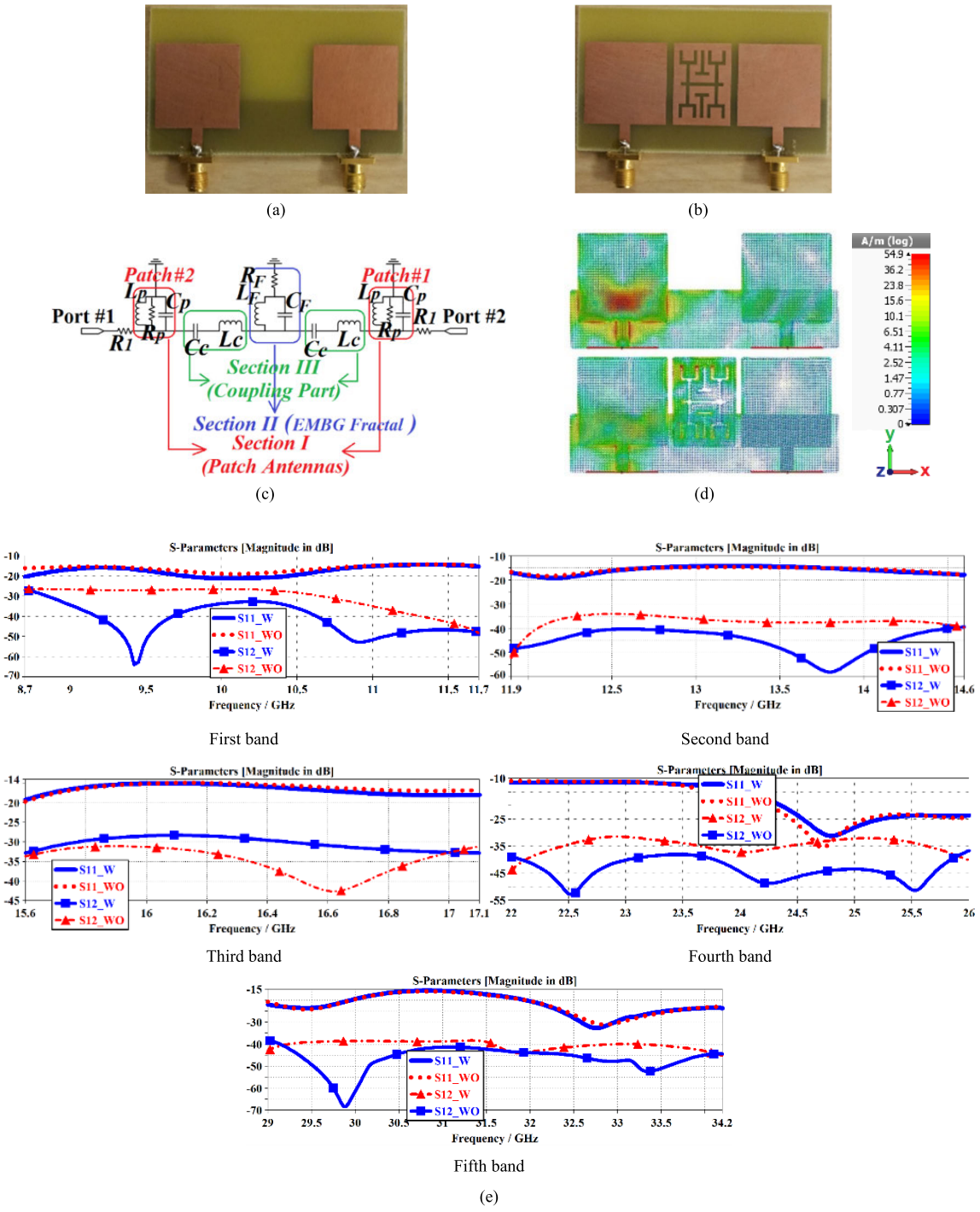

FIGURE 11. (a) Reference array (WO), (b) proposed array with EBG fractal decoupling sheet (W), (c) equivalent circuit diagram, (d) surface current distribution at 29.9 GHz, and (e) measured S-parameters [121].

unchanged, the front-to-back ratio is unaltered as well. The method is simply feasible and is efficiently applicable in beam scanning systems.

V. COMBINED ISOLATION TECHNIQUES

In this section, to achieve high and stable isolation between the radiation elements throughout the operating frequency band without affecting other performance parameters such as array's dimensions, bandwidth, and radiation properties, new array antennas based on combined isolation techniques are proposed, designed and manufactured. In other words, the proposed decoupling slabs located between the radiation elements for these new array antennas are realized based on the combination of the metasurface and metamaterial and electromagnetic bandgap concepts. As a result, high and stable isolations over entire

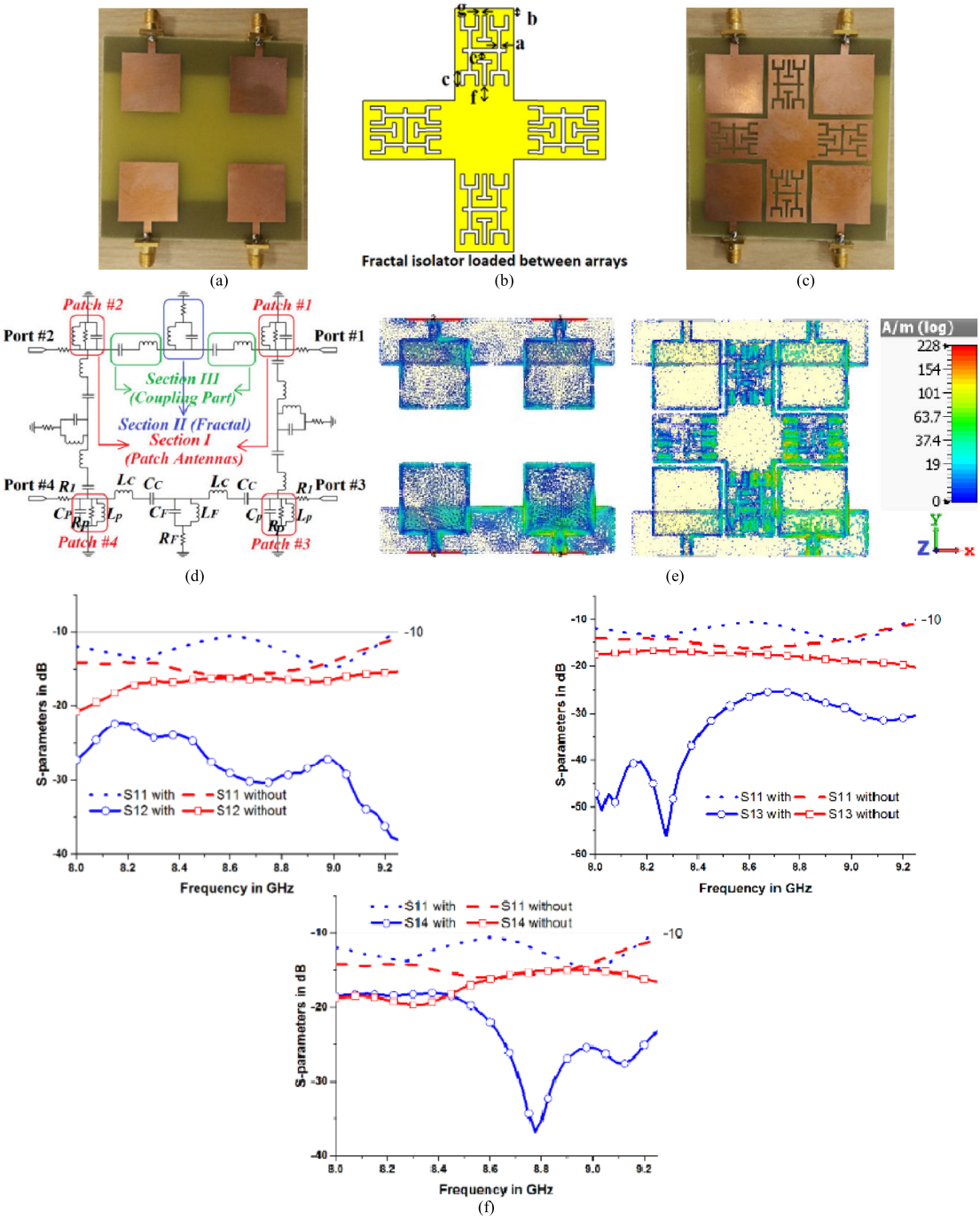

FIGURE 12. (a) Reference 2 × 2 antenna array, (b) crossed-shaped fractal decoupling structure, (c) proposed 2 × 2 array antennas with fractal isolator loading, (d) equivalent circuit diagram, (e) surface current density distributions without and with fractal isolator loading at 8.85 GHz, and (f) empirical S-parameters, [122].

bandwidths are achieved. The proposed works are discussed as follows.

A. INTERFERENCE REDUCTION BETWEEN CLOSELY PLACED ANTENNAS APPLYING EBG MTM FRACTAL LOADING

In [121], an efficient method is investigated to increase the isolation between the closely spaced antennas. It has been obtained by incorporating a fractal decoupling slab between the radiating patches, as displayed in Fig.11. The fractal isolating sheet is an EBG frame based on MTM. By adopting this way, the space between the patches has decreased to 0.65λ for isolation improvement at amounts up to 37, 21, 20, and 31dB at the X-, Ku-, K-, and Ka-bands, respectively, without decay in the radiation patterns. Two-element antennas are exhibited to work across a large frequency band, i.e., 8.7 to 11.7 GHz, 11.9 to 14.6 GHz, 15.6 to 17.1 GHz, 22 to 26 GHz, and 29 to 34.2 GHz. An optimum gain increment in order of 71% has

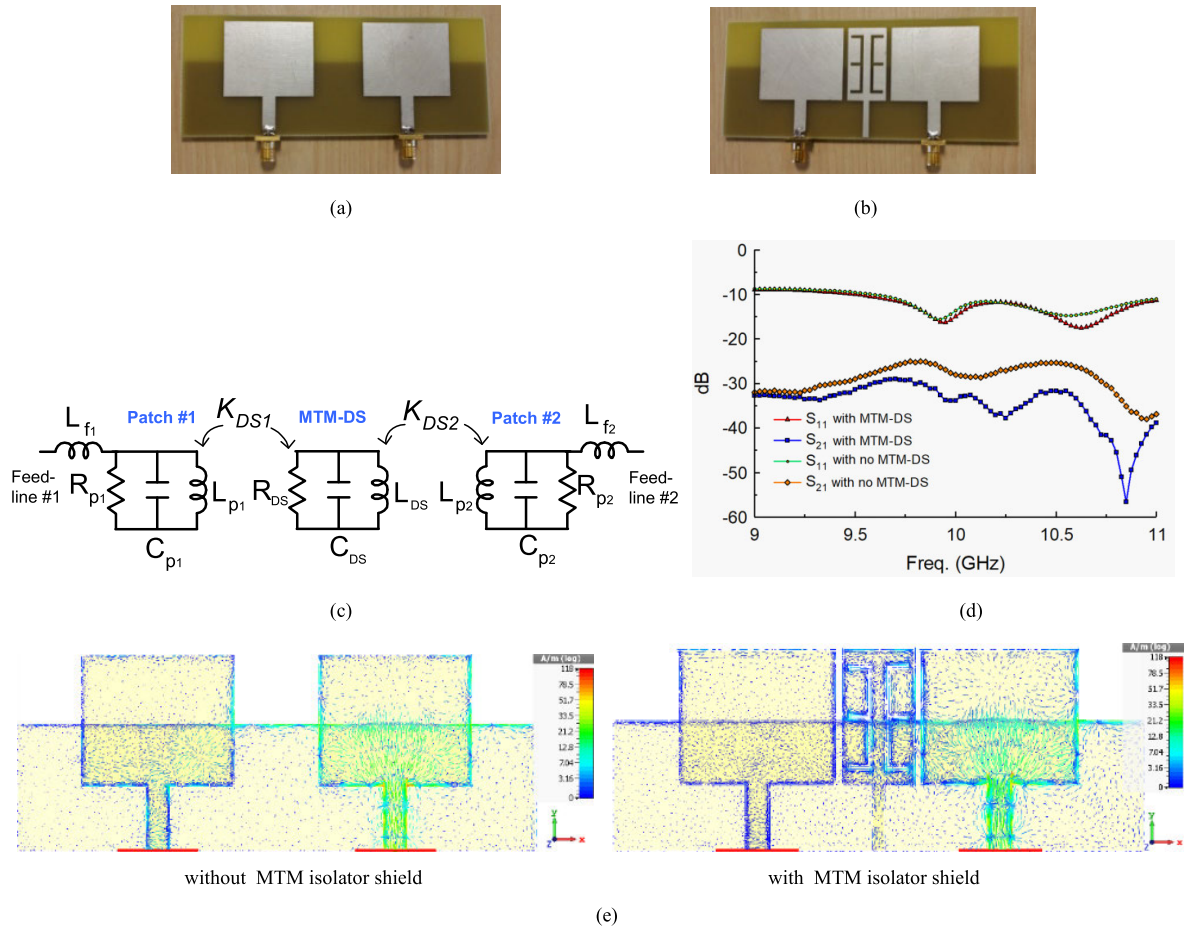

FIGURE 13. Antenna array (a) before apply MTM isolator shield and (b) after apply MTM isolator shield, (c) circuit of two patches with MTM-DS, (d) S-parameter responses, (e) surface current densities before and after apply MTM isolator shield at 10.65 GHz [123].

been achieved. The current density distributions demonstrate that the surface currents are decreased by presenting the fractal load between the adjacent elements. This affirms the realized decoupling structure behaves as an efficient isolation frame. The specifications of the antenna have been validated by experimental results. This approach can be used in several of the previously mentioned applications, and it is also suitable for adjacent antennas in arrays found in Radar, MIMO, and RFID systems.

B. STUDY ON MUTUAL COUPLING REDUCTION BETWEEN ADJACENT ARRAY ANTENNAS WITH REALIZATION OF FRACTAL MTM EBG ARCHITECTURE

The abovementioned technique presented in [121] was further developed and extended to a 2 × 2 antenna array with radiation elements in [122]. In [122], a decoupling MTM geometry based on fractal EBG frame, as displayed in Fig.12, considerably suppresses the coupling between the antennas. The assemblage of the MTM-EBG layout is cross-formed with fractal-formed slits engraved in each arm of the cross. The fractals are compounded of four interjoined 'Y-formed slits, which have separated with an inverted 'T-formed slit. The MTM-EMBG frame is located between the singular elements in a 2 × 2 array antennas. The experimental data illustrate the average isolation improvement across the operating bandwidth is 17, 37, and 17 dB between the antennas 1 and 2, 1 and 3, and 1 and 4, respectively. For this mechanism, metallic-via-holes are not required. The antenna array supports the bandwidth of 8 - 9.25 GHz for X-band operations, which relates to a practical bandwidth of 14.5%. The center-to-center distance between the neighbour antennas has decreased to $0.5\lambda_0$ without decay in the radiation patterns. The empirical gain changes between 4 and 7 dBi, and the radiation efficiency alters from 74.22% to 88.71%. This technique is feasible in the realization of neighbour antenna arrays applied in MIMO and SAR devices.

C. INTERACTION BETWEEN CLOSELY PACKED ARRAY ANTENNAS APPLYING MTS FOR MIMO AND SAR SYSTEMS

An efficient method to repress the interference between adjacent patches that is usual in densely packed antenna arrays has been proposed and demonstrated in [123]. These antennas provide frequency beam-steering ability required in MIMO and SAR systems. Fig.13 shows that the proposed technique applies an MTM decoupling slab that is incorporated between the radiating patches to increase the decoupling

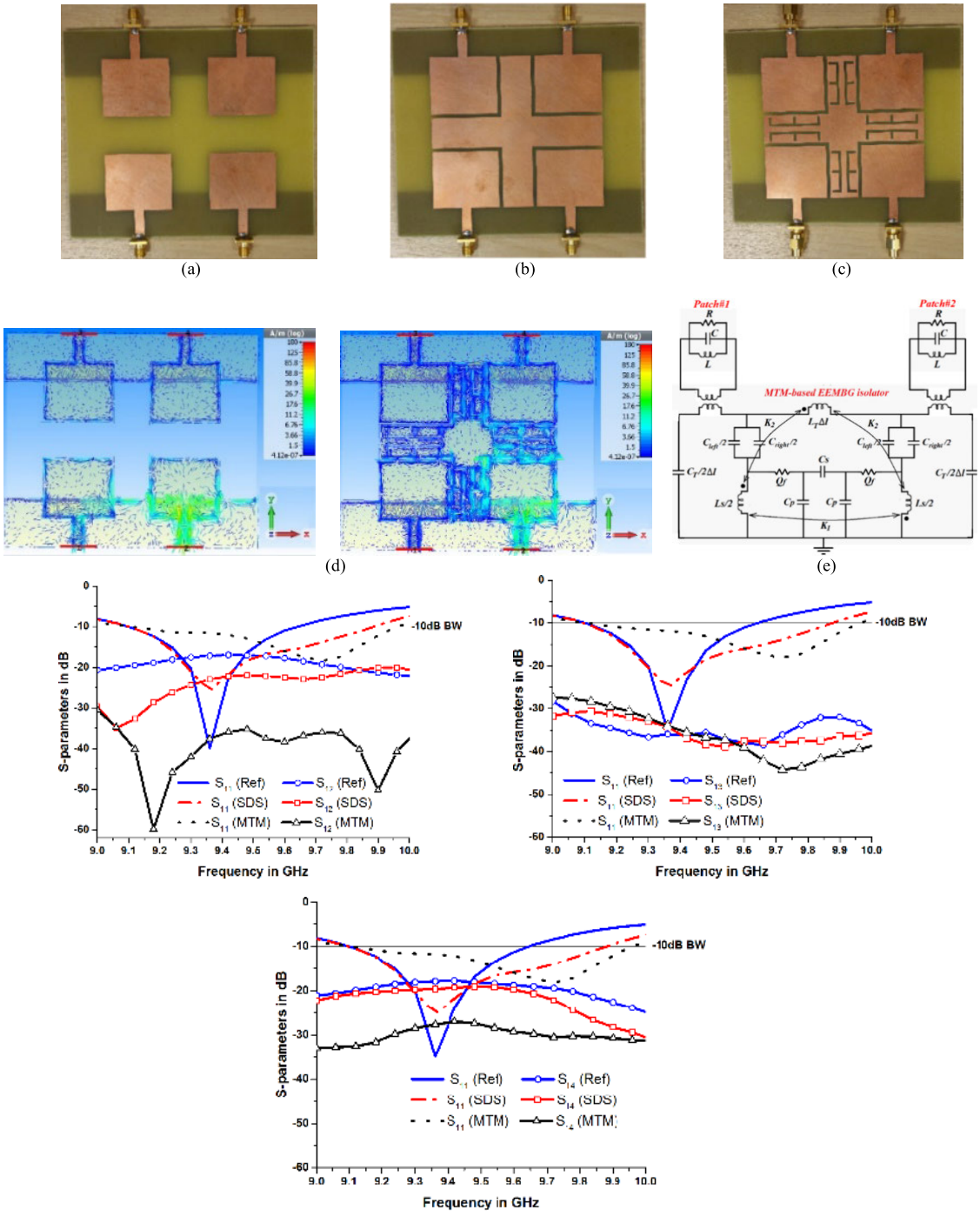

FIGURE 14. (a) Reference array antenna, (b) array structure with embedded simple isolator sheet, (c) array structure with embedded MTM based EBG isolator sheet, (d) current densities without and with the embedded MTM based EBG isolator sheet at 9.6 GHz, (e) circuit model, and (f) measured S-parameter responses [124].

between the antennas that would otherwise reduce the performance parameters. The MTM decoupling slab composed of mirror imaged E-formed slots etched on a patch with an inductive stub. Experimental data affirms that the average mutual coupling (S_{12}) is −27dB over 9 - 11 GHz without MTM decoupling slab. However, with the adoption of the MTM decoupling slab, the average mutual coupling decreases to −38dB. The distance between the antenna has decreased to $0.66\lambda_0$, where λ_0 is defined at 10GHz. Additionally, the employment of this method provides a 15% extension in the working frequency band. Furthermore, the decoupling influences are remarked through imagining the

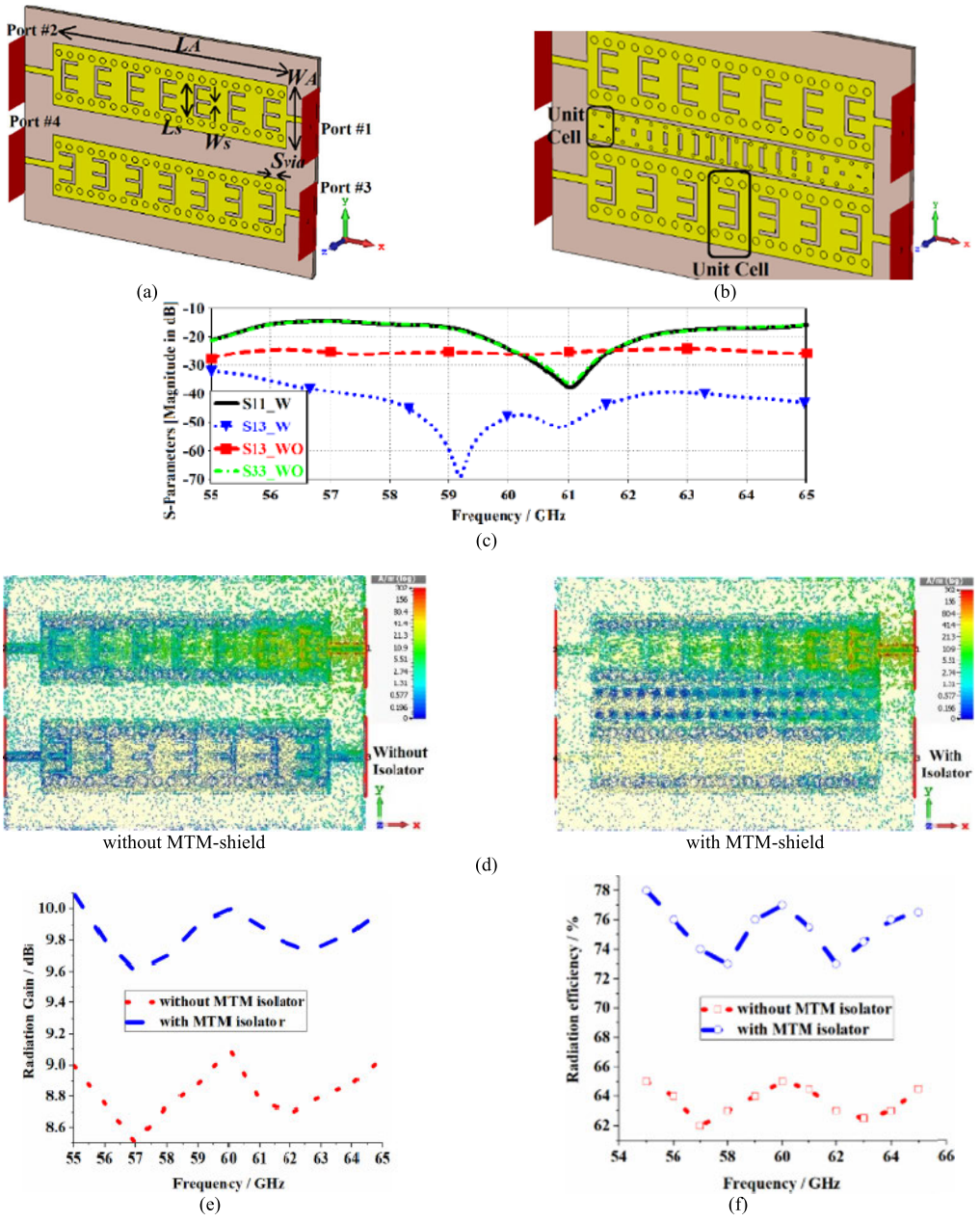

FIGURE 15. (a) Reference array antenna, (b) proposed antenna array with MTM-shield, (c) S-parameters, (d) surface current density distributions without and with MTM-shield at 60 GHz, (e) gain, and (f) efficiency [125].

surface current distributions curves entire the antenna array. With the adoption of the MTM decoupling slab, powerful currents are induced on the patches that obviously investigates the effects of the MTM decoupling slab in reducing surface current wave interaction between the elements. At 9.95 and 10.63 GHz the gain value is 4.52 dBi and 5.40 dBi, respectively. Additionally, this way omits poor front-to-back ratio occurred in other isolating approaches, and it is comparatively easy to realize. Supposing sufficient distance is existing between the neighbor elements, the MTM decoupling slab can be embedded with available antenna arrays, which makes this technique versatile.

D. ISOLATION IMPROVEMENT UTILIZING INTEGRATED MTM EBG DECOUPLING SLAB FOR DENSELY PACKED ARRAY ANTENNAS

In [124], the work presented in [123] is further developed and extended from 1 × 2 linear array antennas, which consist of two radiation elements, to 2 × 2 matrix array antenna configurations, which consist of four radiation antennas. An innovative method to suppress the mutual coupling in adjacent antennas array by incorporating an MTM EBG frame in the distance between the patches to reduce surface currents that would otherwise participate in interferences between the array antennas is developed and investigated. This MTM EBG decoupling frame is a cross-formed microstrip

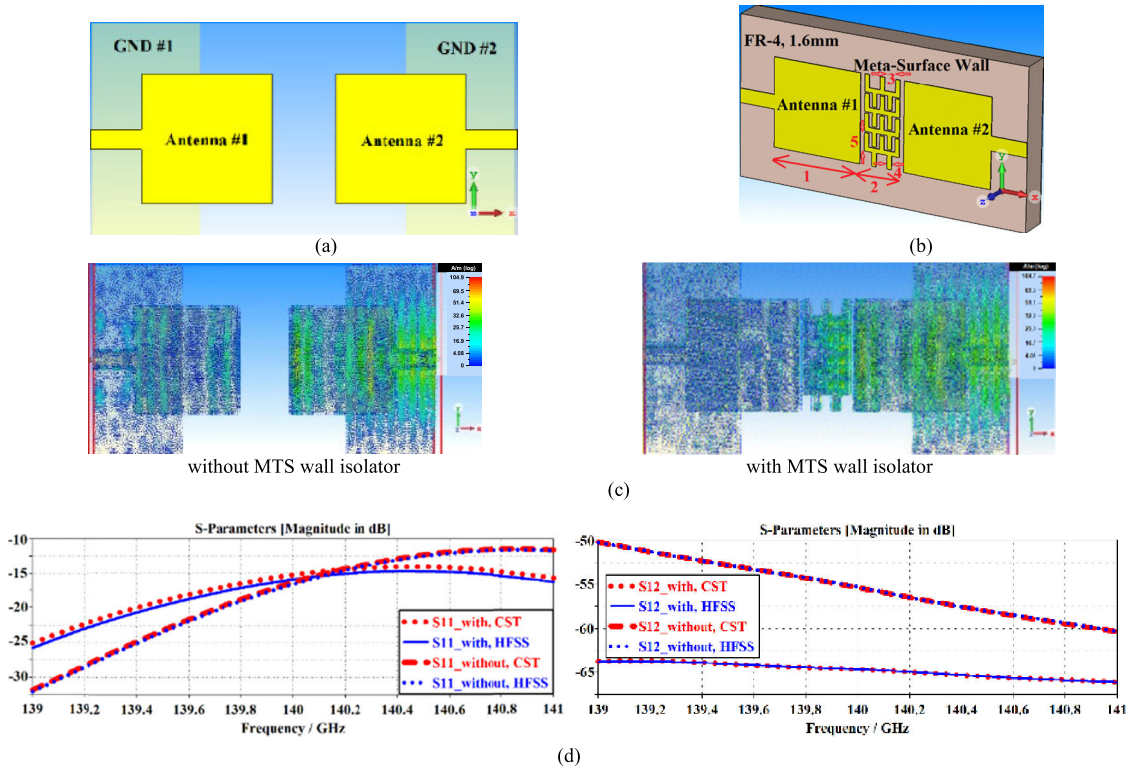

FIGURE 16. Antenna array (a) without and (b) with MTS wall isolator, (c) surface current distributions without and with MTS wall isolator at 140 GHz, and (d) S-parameters [126].

transmission line on which two outward facing E-formed slots are imprinted as shown in Fig.14. Inverse other MTM prototypes, it is via free. The highest experimental decoupling obtained between the four-element array antennas is 60dB at 9.18 GHz. Throughout the empirical working band of 9.12 - 9.96 GHz, the lowest experimental coupling between each element is −34.2dB at 9.48 GHz, and without any decay in radiation patterns. The average experimental mutual coupling across the bandwidth is −47dB. Current density distributions explain that the MTM EBG decoupling frame soaks up the fringing fields that would otherwise couple with the neighbor radiating patches. The results shown in Fig.14 affirm this method is proper for applications in MIMO and SAR systems.

E. CRLH MTM-BASED LEAKY-WAVE ARRAY ANTENNA WITH LOW MUTUAL COUPLING REALIZED ON SIW WITH ±30° FREQUENCY BEAM-SCATTERING ABILITY

A practical investigation to implement a novel MTM leaky-wave antenna (LWA) applied in the making of a 1 × 2 array that is built utilizing SIW methodology for millimeter-wave beam-scanning applications is discussed in [125]. As shown in Fig.15, the array structure is composed of two LWAs with MTM unit-cells printed on the top surface of the SIW. The MTM unit-cell that is an E-formed transverse slit, leads leakage loss and disconnects the current flow across the SIW to increase the performance parameters of the array. The physical dimension of the LWA is 40 mm × 10 mm × 0.75 mm. The isolation level between the array antennas is boosted through integrating an MTM sheet between the elements. The LWA works throughout the bandwidth of 55 - 65 GHz that corresponds to 16.66% feasible bandwidth. The structure is depicted to display beam-scanning of ±30° across the bandwidth. Backward (−30°), broadside (0°), and forward (+30°) gain are 8.5, 10.1, and 9.5 dBi, respectively. The isolator shield is exhibited to have a minimized influence on the impedance bandwidth and radiation properties. After applying the MTM-sheet an average improvement of ∼25 dB, ∼1 dBi, and ∼13% have been achieved on the isolation, gain, and efficiency, respectively. The surface current density distributions illustrate that the MTM-sheet is an efficient electromagnetic band-gap frame that significantly obstacles surface currents from electromagnetic waves interacting with the closely radiation antennas in the array structure. The ruinous effects of surface currents in the array are remarkably repressed from affecting the array antenna's far-field.

F. ISOLATION IMPROVEMENT BETWEEN ANTENNA ARRAYS BASED ON MTS-WALL FOR TERAHERTZ BAND

A new two-dimensional MTS wall to suppress the interference between in antennas in array working at terahertz band of 139 to 141 GHz applicable for security screening, medical and communications systems have been proposed in [126]. The MTS unit-cell contains connected twin

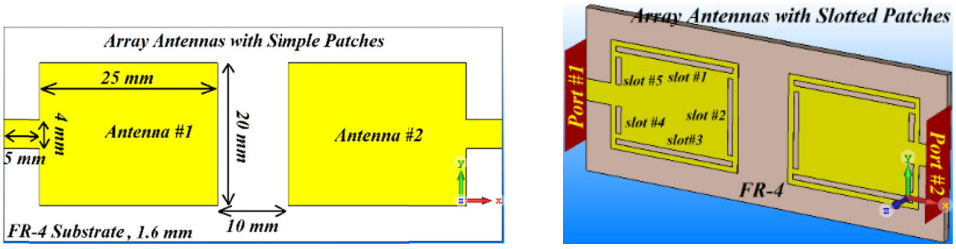

(a) (b)

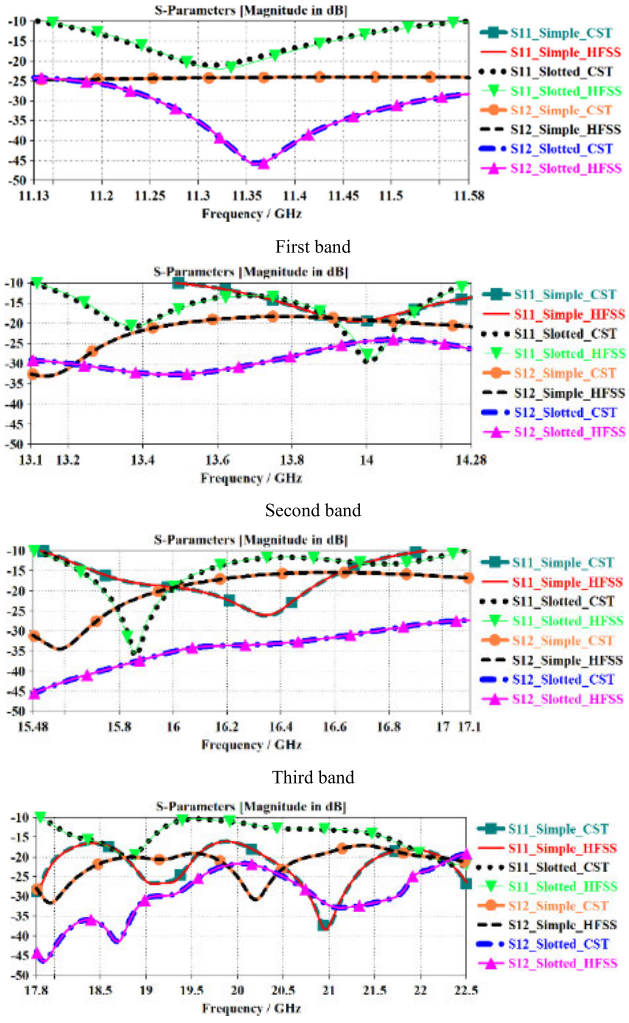

(c)

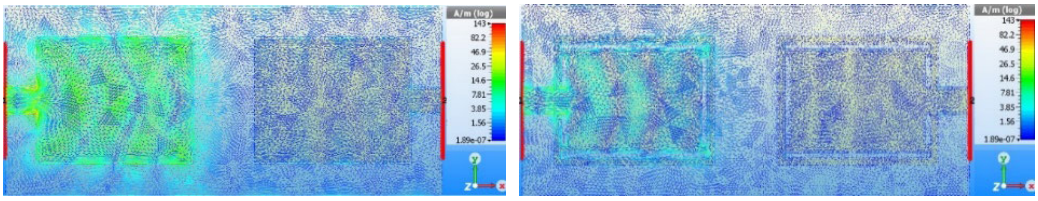

(d)

FIGURE 17. (a) Reference array, (b) proposed slotted array, (c) S-parameters, and (d) surface current distributions without and with slotted-patches at 11.37GHz [127].

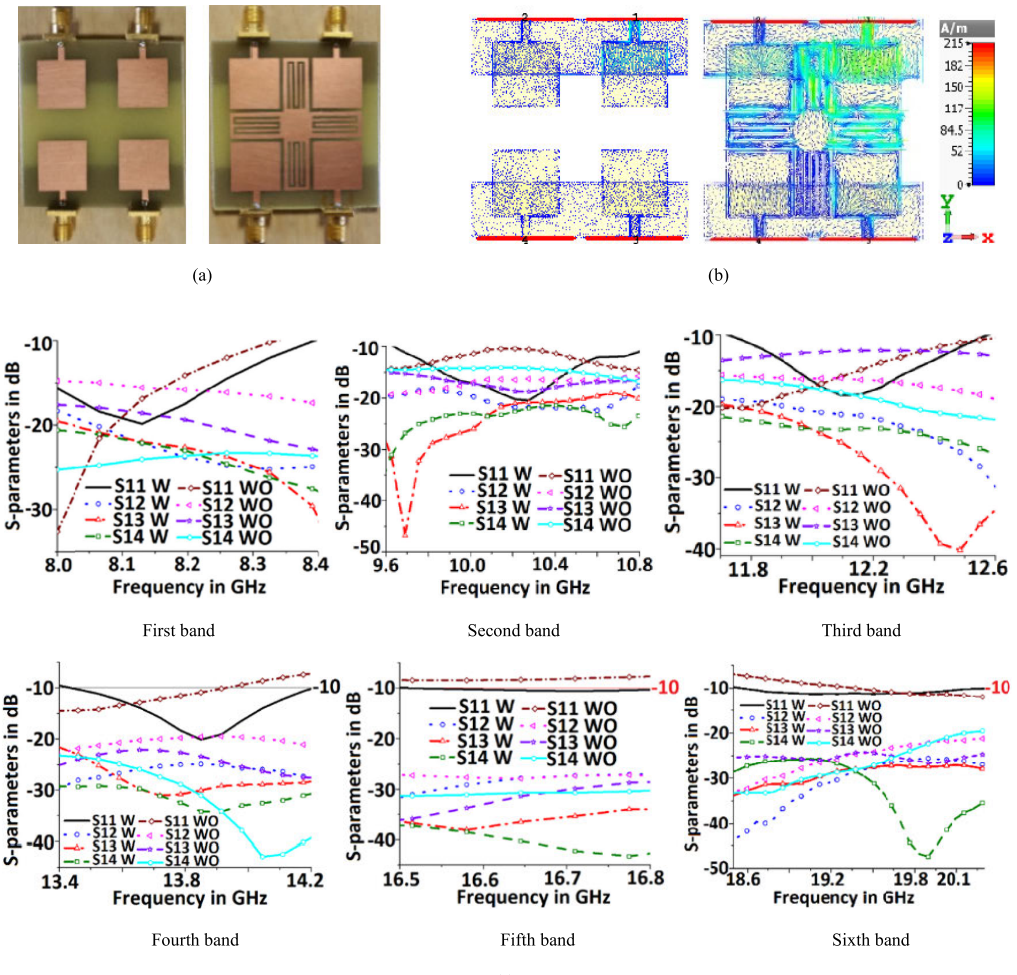

FIGURE 18. (a) Manufactured prototypes of the reference and proposed structures before (WO) and after (W) apply MTS decoupling shield, (b) surface current distributions without and with the MTS decoupling shield at 8.15 GHz, (c) measured S-parameters, and (d) measured radiation patterns [130].

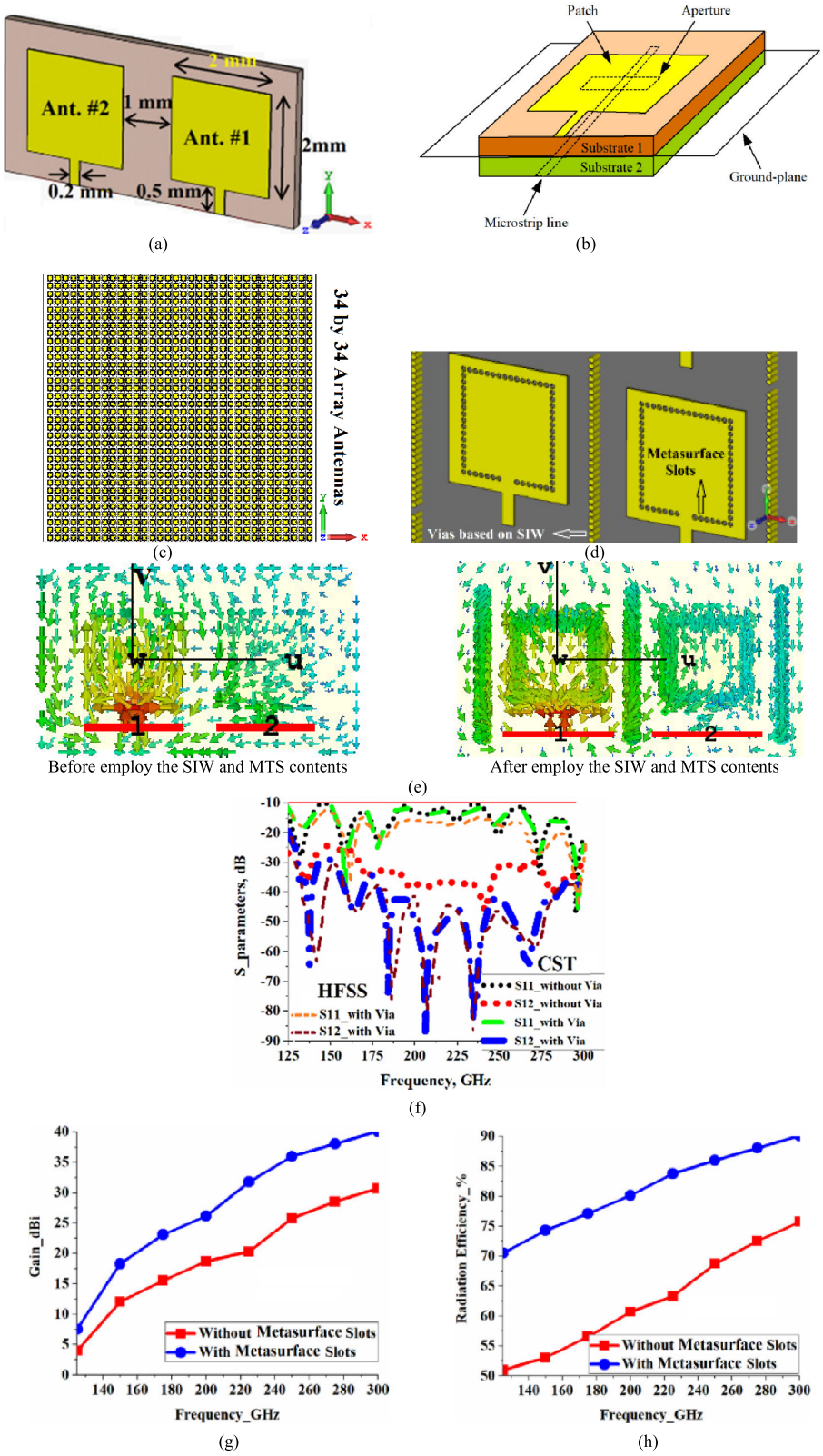

FIGURE 19. (a) Reference 1 × 2 array antenna, (b) feeding structure, (c) layout of whole 34 × 34 array antennas inspired SIW and MTS concepts, (d) zoomed view to depict two central antennas after apply the SIW and MTS principles, (e) surface current density distribution before and after applying the SIW and MTS properties at 250 GHz for two central antennas, (f) S-parameter responses, (g) gain curve, (h) efficiency curve, (i) 3-D radiation diagrams, and (j) co- and cross-polarized radiation gain patterns [131].

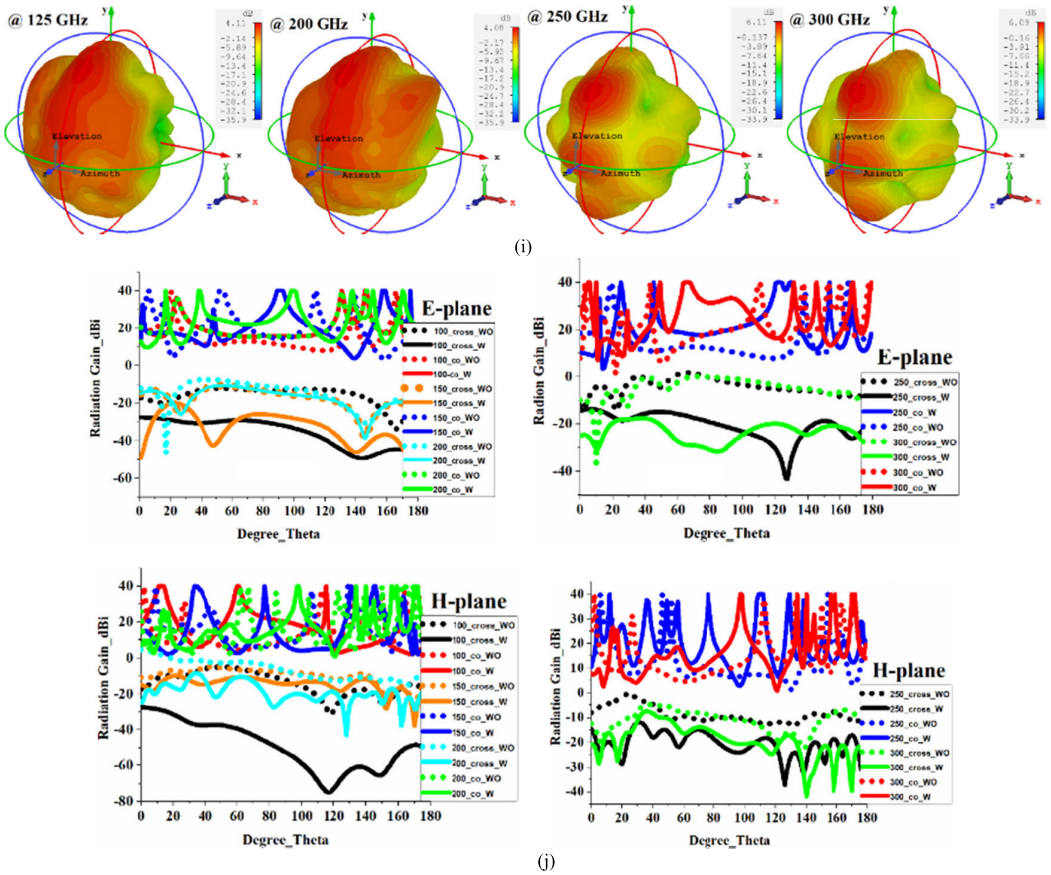

FIGURE 19. *(Continued.)* **(a) Reference 1 × 2 array antenna, (b) feeding structure, (c) layout of whole 34 × 34 array antennas inspired SIW and MTS concepts, (d) zoomed view to depict two central antennas after apply the SIW and MTS principles, (e) surface current density distribution before and after applying the SIW and MTS properties at 250 GHz for two central antennas, (f) S-parameter responses, (g) gain curve, (h) efficiency curve, (i) 3-D radiation diagrams, and (j) co- and cross-polarized radiation gain patterns [131].**

'Y-formed' microstrip structures that are inter-digitally incorporated with each other to generate the MTS wall. The MTS wall does not have via holes, and it includes a shorten ground plane to simplifying the manufacturing process. As shown in Fig.16, the MTS wall is located firmly between the elements to increase the decoupling and suppress the surface-waves. To achieve the lowest coupling, the wall is implemented upright to the antennas. Over the terahertz frequency bandwidth, the gain and isolation of the array antennas are 9.0 dBi and less than −63 dB, respectively. This method obtains isolation improvement of higher than 10dB across a large frequency band (2 GHz) than obtained to date. The decoupling effects are remarked through imagining the surface current curves throughout the array structure. The surface current density distribution shows that without MTS wall and when element #1 is stimulated, the electromagnetic signal is transferred to element #2, and contrariwise. However, when the MTS wall is located between the elements, it remarkably obstructs the electromagnetic signal from element #1 being transferred to element #2. By applying this approach, the edge-to-edge space between the radiation patch has decreased to 2.5mm. The size of the antennas and GND are 5 mm × 5 mm and 9 mm × 4.25 mm when realized on a 1.6 mm thick traditional layer.

G. ISOLATION IMPROVEMENT ACROSS BROAD FREQUENCY BAND APPLYING INTEGRATED PERIPHERY SLOT FOR ANTENNA ARRAYS

A new mechanism to increase the isolation between closely spaced radiating patches has been proposed and modeled in [127]. This method enabled the implementation of low-profile construction of extremely compact antenna geometries needful in MIMO and SAR communication devices. Contrary to other traditional approaches of reduction interferences where an isolator sheet is placed between the antennas, this method is easier and just needs integrating linear slits close the periphery of the radiating element, as shown in Fig.17. The main properties of this way are (i) substantial suppression in the minimum coupling between the neighbor patches by −26.7dB in X-band and >−15dB in Ku and K-bands; (ii) decrement in the center-to-center distance between the elements up to 10 mm (0.37λ); and (iii) more than 40% gain increment across specified angular directions that changes between 4.5 and 8.2 dBi. The investigation of the

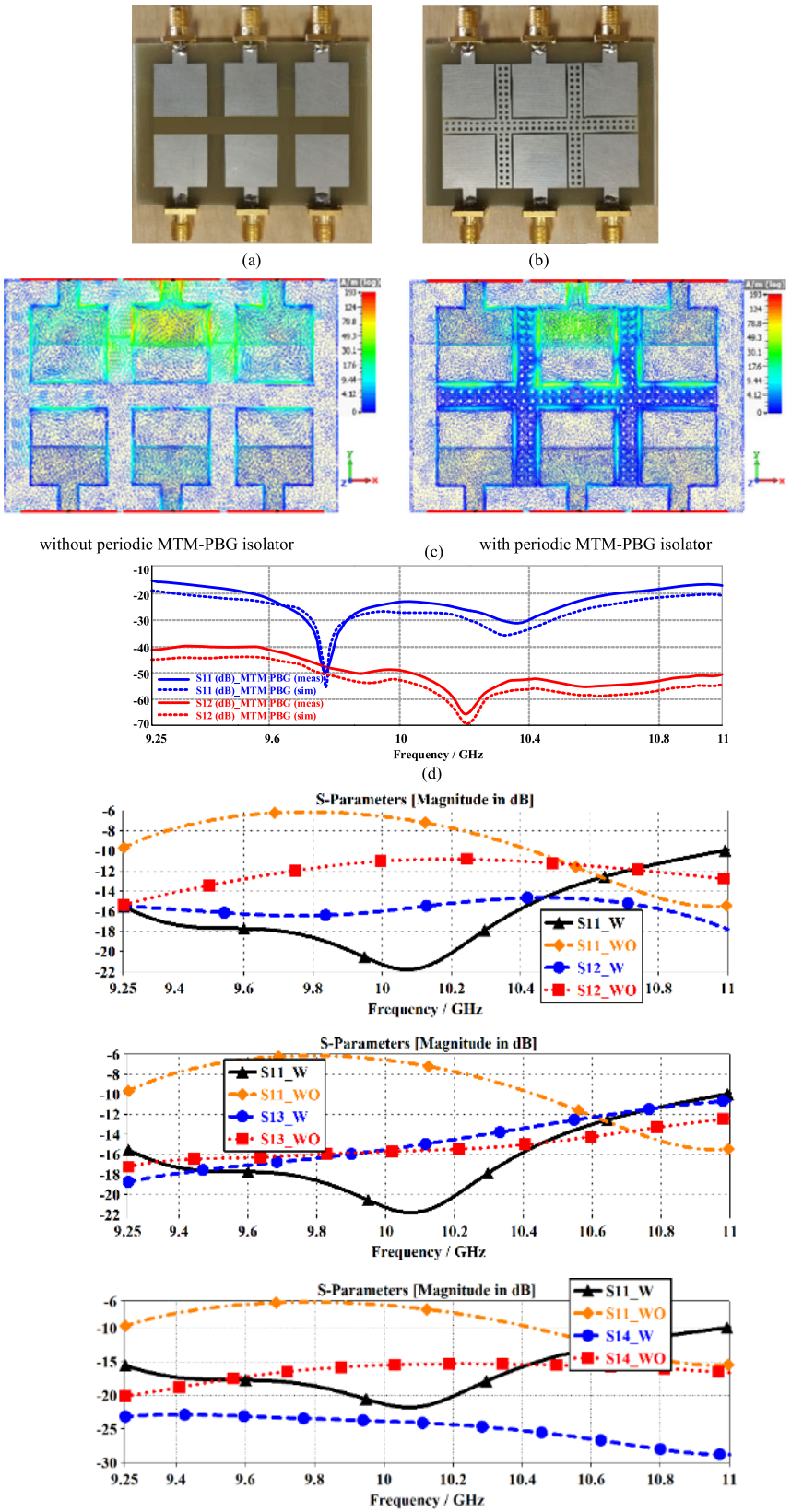

FIGURE 20. (a) 2 × 3 reference antenna array, (b) 2 × 3 proposed antenna array structure with periodic MTM-PBG isolator, (c) surface current distributions without and with periodic MTM-PBG isolator at 9.25 GHz, (d) S-parameters of the MTM PBG isolator, (e) empirical S-parameters of the arrays without (WO) and with (W) proposed isolator, (f) input impedances (Ω) after apply the periodic MTM-PBG isolator, (g) circuit model including MTM-PBG isolator sheet, (h) gain curve, (i) radiation efficiency curve, and (j) experimental radiation patterns before and after the periodic MTM-PBG isolator [132].

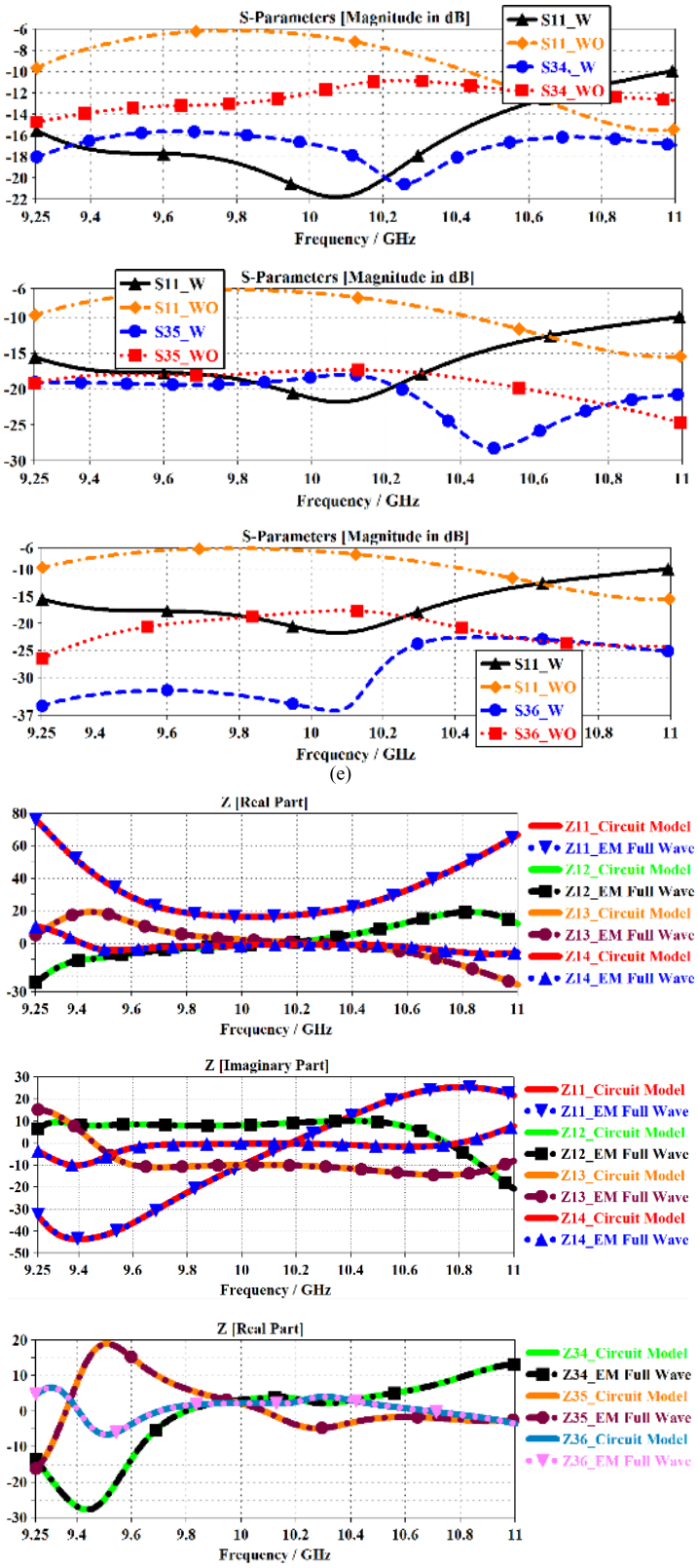

FIGURE 20. *(Continued.)* **(a) 2 × 3 reference antenna array, (b) 2 × 3 proposed antenna array structure with periodic MTM-PBG isolator, (c) surface current distributions without and with periodic MTM-PBG isolator at 9.25 GHz, (d) S-parameters of the MTM PBG isolator, (e) empirical S-parameters of the arrays without (WO) and with (W) proposed isolator, (f) input impedances (Ω) after apply the periodic MTM-PBG isolator, (g) circuit model including MTM-PBG isolator sheet, (h) gain curve, (i) radiation efficiency curve, and (j) experimental radiation patterns before and after the periodic MTM-PBG isolator [132].**

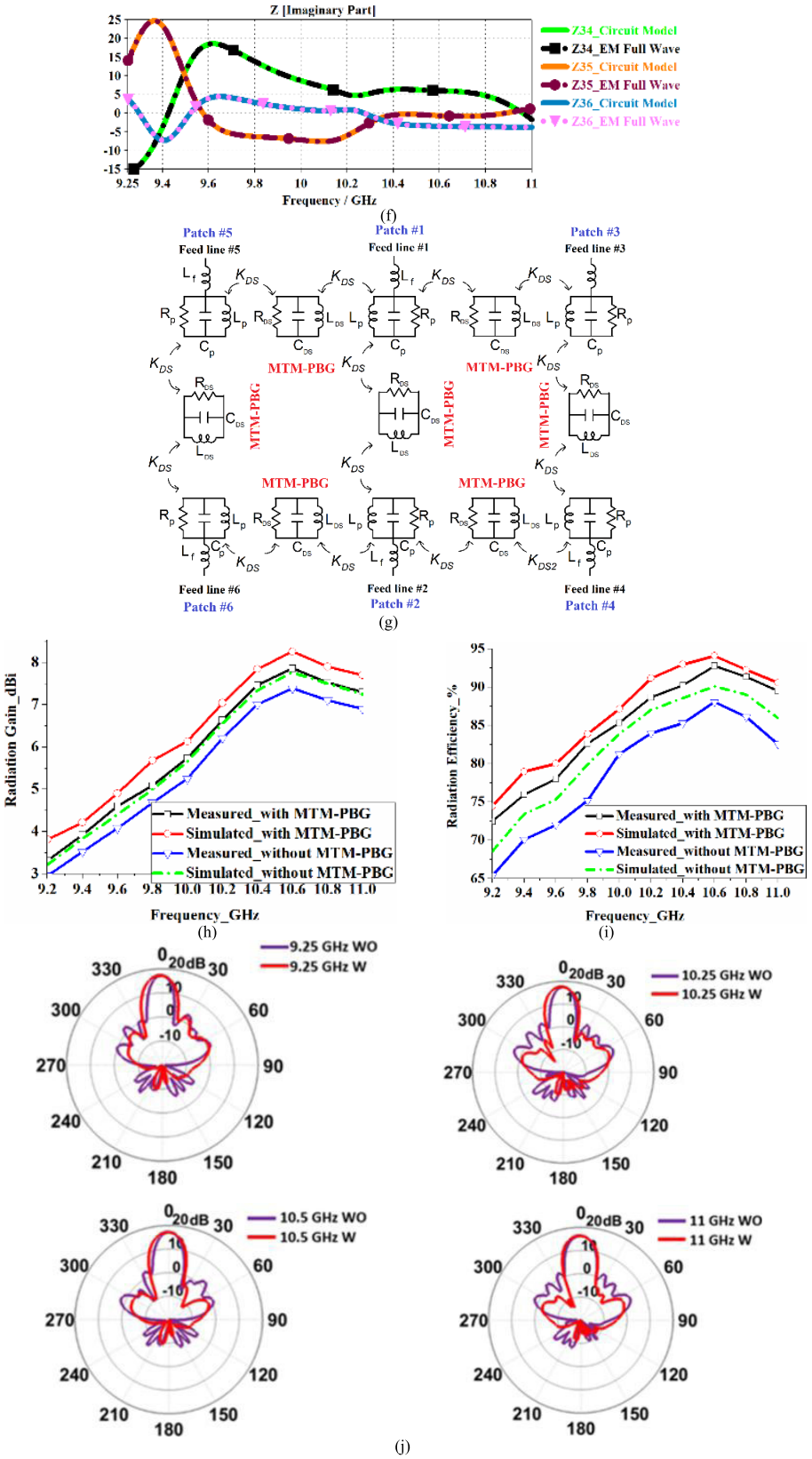

FIGURE 20. *(Continued.)* **(a) 2 × 3 reference antenna array, (b) 2 × 3 proposed antenna array structure with periodic MTM-PBG isolator, (c) surface current distributions without and with periodic MTM-PBG isolator at 9.25 GHz, (d) S-parameters of the MTM PBG isolator, (e) empirical S-parameters of the arrays without (WO) and with (W) proposed isolator, (f) input impedances (Ω) after apply the periodic MTM-PBG isolator, (g) circuit model including MTM-PBG isolator sheet, (h) gain curve, (i) radiation efficiency curve, and (j) experimental radiation patterns before and after the periodic MTM-PBG isolator [132].**

TABLE 10. Isolation Improvement With Metasurface.

Frequency	$\|S_{12}\|$ () Min., Max., Ave.	$\|S_{13}\|$ (dB) Min., Max., Ave.	$\|S_{14}\|$ (dB) Min., Max., Ave.
I: 8 to 8.4 GHz	7.5 , 8.5 , 8 dB	2 , 8.5 , 6 dB	- , 3 , - dB
II: 9.6 to 10.8 GHz	2.5 , 3.5 , 3 dB	5 , 28 , 17 dB	7 , 18 , 12.5 dB
III: 11.7 to 12.6 GHz	3.5 , 13 , 9.5 dB	8 , 27 , 18 dB	5 , 5 , 5 dB
IV: 13.4 to 14.2 GHz	5.5 , 7.5 , 6.5 dB	- , 4 , 2 dB	- , 6.5 , 3.5 dB
V: 16.5 to 16.8 GHz	- , 3.5 , 2 dB	2 , 5.5 , 4 dB	7 , 13 , 10.5 dB
VI: 18.5 to 20.3 GHz	4.5 , 22.5 , 13.5 dB	2.5 , 7.5 , 5.5 dB	5.5 , 20 , 13 dB

surface current distribution shows that the slits act like an isolating frame that soak up the surface-waves that would otherwise couple with the adjacent patches. The proposed technique is easy and inexpensive.

H. SURFACE-WAVE SUPPRESSION IN ARRAY ANTENNAS APPLYING MTS CONTENT FOR SAR AND MIMO APPLICATIONS

An efficient approach for isolation improvement between closely spaced antennas which is based on MTS decoupling for MIMO and SAR applications, is presented in [130]. It has accomplished by constraining the surface current waves induced across the antenna through the insertion of a cross-formed MTS structure between the antennas, as shown in Fig.18. This MTS minimizes the influences of electromagnetic coupling coming from space-wave and the near-field. Each arm of the cross-formed structure establishing the MTS has a meander-line slit (MLS) etching. The MTS's effectiveness is investigated for a 2 × 2 antenna array that works throughout six frequency sub-bands in X, Ku, and K-bands. In the X-band, the antenna's applications are wideband global satellite communication systems (WGS) and military communication. In the Ku-band, the antenna's applications are radar and terrestrial microwave, particularly, in police traffic speed-detectors. In the K-band, the antenna's applications are found in airport surface detection equipment (ASDE). Fig.18 illustrates that with this method, the optimum increment obtained in improving isolation between adjacent radiation patches is: 8.5dB (8 to 8.4 GHz), 28dB (9.6 to 10.8 GHz), 27dB (11.7 to 12.6 GHz), 7.5dB (13.4 to 14.2 GHz), 13dB (16.5 to 16.8 GHz) and 22.5dB (18.5 to 20.3 GHz). The results are provided in Table 10. Also by employing the presented way, minimal edge-to-edge space between the elements is achieved up to $0.26\lambda_0$, where λ_0 is specified at 8.0 GHz, the utilize of defected ground plane becomes inessential, apply of via-holes are refrained, the challenge of poor front-to-back ratio is addressed and integration to existing arrays becomes possible.

I. STUDY ON INTERFERENCES REDUCTION AND RADIATION BEHAVIOURS OF A 34 × 34 SIW AND MTS-BASED ARRAY ANTENNAS FOR APPLICATIONS ACROSS 0.125-0.3 THz

In [131], the possibility of a perceptual model of a 34 × 34 array antenna for working throughout 0.125 to 0.3 THz,

TABLE 11. Radiation performances.

	Gain (dBi)
Min. with no metasurface slits	3.96
Min. with metasurface slits	7.51
Improvement	3.55

	Gain (dBi)
Max. with no metasurface slits	30.71
Max. with metasurface slits	40.08
Improvement	9.37

	Efficiency (%)
Min. with no metasurface slits	50.96
Min. with metasurface slits	70.51
Improvement	19.55

	Efficiency (%)
Max. with no metasurface slits	75.71
Max. with metasurface slits	90.11
Improvement	14.40

which relates to a feasible bandwidth of 82.35% is described. Fig.19 shows that, each of the radiation elements which constitute the array comprises of a square patch having a physical dimension of 2 × 2 mm^2 and stimulated via a matched microstrip line. Each element has separated from each other by via-holes that are realized based on the SIW method. This approach is exhibited to efficiently improve the isolation between closely spaced antennas that can otherwise disturb the radiation properties. The periphery of each patch is integrated with circular dielectric slits that are implemented based on the MTS principle to improve the radiation performances. By employing these methods, the isolation has improved on average by 25dB across the working bandwidth, and the array's effective aperture area has enlarged with keeping constant its dimensions. The array structure shows a variation on gain and radiation efficiency of 7.51 dBi to 40.08 dBi, and 70.51% to 90.11%, respectively. The data are listed in Table 11. It is clear that after implementing the MTS slits, almost 60% and 30% increments in gain and efficiency have been accomplished. The 34 × 34 antennas array is a suitable candidate to apply in wireless telecommunication apparatus at THz region.

J. DECOUPLING IMPROVEMENT OF ADJACENT ARRAY ANTENNAS WITH PERIODIC MTM PBG FOR MIMO AND SAR APPLICATIONS

In [132] an MTM photonic bandgap (PBG) periodic structure is utilized as an isolator slab to repress the mutual coupling

TABLE 12. Decoupling improvement applying the periodic MTM PBG technique.

S_{11}	9.25 – 11 GHz, FBW = 17.28%	Max. increment of matching: ~15 dB
S_{12} (T/R)	Max. reduction: 5dB @ 10.98 GHz	Ave. reduction: 4dB
S_{13} (T/T)	Max. reduction: 6 dB @9.25GHz	Ave. reduction: 3 dB
S_{14} (T/R)	Max. reduction: 14 dB @ 10.97 GHz	Ave. reduction: 10 dB
S_{34} (T/R)	Max. reduction: 10dB @ 10.25 GHz	Ave. reduction: 8dB
S_{35} (T/T)	Max. reduction: 10dB @ 10.5 GHz	Ave. reduction: 5dB
S_{36} (T/R)	Max. reduction: 19 dB @ 10.07 GHz	Ave. reduction: 7 dB

TABLE 13. Performance comparison of decoupling mechanisms based MIMO and SAR antennas.

Refs.	Approaches	Max. decoupling improvement (dB)	Number of elements	Symmetricity	Impact on the size after applying the technique	Altering and developing (DGS)	Complexity
[133]	UC-EBG	10	2 (1×2)	NO	Yes	Yes	Yes
[134]	Slot in Ground plane	40	2 (1×2)	NO	Yes	Yes	Yes
[135]	EBG	4	2 (1×2)	NO	Yes	Yes	Yes
[136]	Compact EBG	17	2 (1×2)	NO	Yes	Yes	Yes
[137]	DGS	17.43	2 (1×2)	NO	Yes	Yes	Yes
[138]	U-shaped resonator	10	2 (1×2)	NO	Yes	Yes	Yes
[139]	Slotted Meander Line Resonator	16	2 (1×2)	NO	Yes	Yes	Yes
[140]	I-shaped resonator	30	2 (1×2)	NO	Yes	Yes	Yes
[141]	SCSRR	10	2 (1×2)	NO	Yes	Yes	Yes
[142]	SCSSRR	14.6	2 (1×2)	NO	Yes	Yes	Yes
[143]	Waveguide MTM	20	2 (1×2)	NO	Yes	Yes	Yes
[144]	Waveguide MTM	18	2 (1×2)	NO	Yes	Yes	Yes
[145]	Meander line resonator	10	2 (1×2)	NO	Yes	Yes	Yes
[146]	Fractal load with DGS	16	2 (1×2)	NO	Yes	Yes	Yes
[147]	Antenna Interference Cancellation Chip (AICC)	15	2 (1×2)	Yes	No	No	Yes
[148]	3-D Metamaterial Structure (3DMMS)	18	2 (1×2)	Yes	Yes	No	No
[121]	Metamaterial fractal load	37	2 (1×2)	Yes	NO	NO	NO
[122]	Fractal metamaterial electromagnetic bandgap	17 for S_{12} 37 for S_{13} 17 for S_{14}	4 (2×2)	Yes	NO	NO	NO
[123]	Metamaterial	57	2 (1×2)	Yes	NO	NO	NO
[124]	Metamaterial	40 for S_{12} ~7 for S_{13} 11 for S_{14}	4 (2×2)	Yes	NO	NO	NO
[125]	Metamaterials and Substrate Integrated Waveguide	42.5	2 (2×1)	Yes	NO	NO	NO
[126]	Metasurface wall isolator	13.5	2 (1×2)	Yes	NO	NO	NO
[127]	Slots	>26	2 (1×2)	Yes	NO	NO	NO
[130]	Metasurface	32 (X-band) 27 (Ku-band) 26 (K-band)	4 (2×2)	Yes	NO	NO	NO
[131]	SIW & Metasurface	50	1156 (34×34)	Yes	NO	NO	NO
[132]	MTM-PBG	10 for S_{34} 14 for S_{14} 19 for S_{36}	6 (3×2)	Yes	NO	NO	NO

in densely packed array antenna for SAR and MIMO applications as displayed in Fig.20. By this method, the MTM PBG layout is exhibited to efficiently reduce surface-wave distributions between the patch arrays by an average of 12dB, see Table 12. MTM PBG layer contains a periodic organization of dielectric circles printed in the cross-formed microstrip sheet that is incorporated between the antennas. It obstacles the distribution of surface-waves on the patches to increment decoupling between the elements. Surface current distribution depicted in Fig.20 provides deeper discernment of how the surface currents are decreased. It is clear that the cross-formed MTM PBG isolator shield dramatically interacts with the surface currents to obstacle them from affecting neighbor antennas in the array configuration. Ruinous influences of surface currents in the antenna are considerably repressed from effecting the antenna array's far-field. The equivalent circuit diagram of the proposed array structure is presented in Fig.20. Contrary to the existing techniques in the literature, the attributes of this method are: (i) easiness; (ii) inexpensive; and (iii) can be retrofitted in available array structures. This structure has fabricated to work across a wide bandwidth of 9.25 to 11 GHz with a feasible bandwidth of 17.28%. By this mechanism (i) the side-lobes have decreased; (ii) there is a negligible influence on the radiation performances; and (iii) the shortest center-to-center distance between neighbor antennas has decreased to 0.15λ at 9.25 GHz. Input impedance calculated utilizing CST software and circuit diagram has been presented in Fig.20. Since the circuit model parameters have extracted applying optimization approach in CST throughout a specific bandwidth, a perfect match between the results achieved by the circuit model and CST has occurred. The gain and efficiency plots have displayed in Fig.20. There is an excellent agreement between the simulated and experimented curves. After apply MTM PBG, a maximum empirical gain and efficiency of 7.85 dBi and 92.78% have obtained at 10.6 GHz. So, before applying the proposed method, the highest magnitude of these parameters was 7.38 dBi and 88.05% at the same frequency. This explains that the radiation specifications are not intensely influenced by realizing the MTM PBG decoupling frame.

Table 13 shows comparisons in the performance parameters of the abovementioned techniques relative to the studied literature in terms of the mutual coupling reduction techniques, maximum isolation improvement, number of applied elements in the array structure, design complexity and simplicity, impact on the size after applying the technique, and augmentation and development of the array after applying the technique. Results show that the papers discussed in this section, which are based on combined isolation techniques such as metamaterials, metasurfaces, and EM bandgaps, showcase higher performance parameters with simpler design structures.

VI. CONCLUSION

Antenna arrays plays an important role in improving various radiation characteristics of antennas. The mutual coupling between radiation elements in the array is an undesirable effect which degrades the performance of array. Over the years many compensation techniques have been proposed to overcome such harmful effects. The effectiveness of various methods mainly depends on the applications in which arrays are to be implemented. The survey presented here provides a comprehensive study on the investigations on various isolation improvement approaches based on metamaterial and metasurface inspired techniques for antenna arrays. It is well known that strong mutual coupling tends to occur between antenna elements that are closely spaced to each other as in the case of antenna arrays where the average element spacing is smaller than about half a wavelength. The consequence of strong mutual coupling is distortion in the array's performance, and it constrains the array's miniaturization. Therefore, in the multiple-input multiple-output (MIMO) and synthetic aperture radar (SAR) systems, high isolation is very important. In SAR systems the coupling effect is also known to influence the resolution capability, interference rejection, and direction-of-arrival (DOA) estimation.

Mutual coupling reduction is an important area of research which has direct impact on the development of the next generation wireless communication systems, such as 5G, 6G and massive MIMO. Although several isolation improvement approaches are reported in the literature to date, most of these studies are confined to two-port antenna arrays. This review discusses diverse and promising decoupling methods based on metamaterial/metasurface inspired techniques for applications such as MIMO and SAR systems. Comprehensive comparisons are given of the various techniques and how they affect the radiation performance of the arrays. The main aim of researchers is to mitigate or suppress the mutual coupling as much as possible with negligible effect on the array's performance and, if possible, without increasing the array's physical footprint. To achieve this aim researchers have employed various techniques including the use of complementary split-ring resonators (CSRR) and defected ground structures (DGS). This review should serve as a reference for researchers to advance the art.

REFERENCES

[1] M. Sánchez-Fernández, E. Rajo-Iglesias, O. Quevedo-Teruel, and M. L. Pablo-Gonzalez, "Spectral efficiency in MIMO systems using space and pattern diversities under compactness constraints," *IEEE Trans. Veh. Technol.*, vol. 57, no. 3, pp. 1637–1645, May 2008.

[2] L. Wang, G. Wang, and Q. Zhao, "Suppressing mutual coupling of MIMO antennas with parasitic fragment-type elements," in *Proc. 46th Eur. Microw. Conf. (EuMC)*, Oct. 2016, pp. 1303–1306.

[3] X. Wang, Z. Feng, and K.-M. Luk, "Pattern and polarization diversity antenna with high isolation for portable wireless devices," *IEEE Antennas Wireless Propag. Lett.*, vol. 8, pp. 209–211, 2009.

[4] A. J. Paulraj, D. A. Gore, R. U. Nabar, and H. Bolcskei, "An overview of MIMO commusnications—A key to gigabit wireless," *Proc. IEEE*, vol. 92, no. 2, pp. 198–218, Feb. 2004.

[5] K. Wei, J.-Y. Li, L. Wang, and R. Xu, "Microstrip antenna array mutual coupling suppression using coupled polarisation transformer," *IET Microw., Antennas Propag.*, vol. 11, no. 13, pp. 1836–1840, Oct. 2017.

[6] L. H. Trinh, F. Ferrero, L. Lizzi, J.-M. Ribero, and R. Staraj, "4×4 MIMO multiband antenna system for mobile handsets," *Int. J. Antennas Propag.*, vol. 2015, Nov. 2015, Art. no. 857876.

[7] Z. Ying, "Antennas in cellular phones for mobile communications," *Proc. IEEE*, vol. 100, no. 7, pp. 2286–2296, Jul. 2012.
[8] P.-Y. Qin, Y. J. Guo, and C.-H. Liang, "Effect of antenna polarization diversity on MIMO system capacity," *IEEE Antennas Wireless Propag. Lett.*, vol. 9, pp. 1092–1095, Nov. 2010.
[9] H. S. Lui and H. T. Hui, "Mutual coupling compensation for direction-of arrival estimations using the receiving-mutual-impedance method," *Int. J. Antennas Propag.*, vol. 2010, Jan. 2010, Art. no. 373061.
[10] Y. Wu, J. W. M. Bergmans, and S. Attallah, "Effects of antenna correlation and mutual coupling on the carrier frequency offset estimation in MIMO systems," in *Proc. Int. Conf. Comput. Intell. Softw. Eng.*, Sep. 2010, pp. 1–4.
[11] B. Wang, Y. Chang, and Y. Sun, "Performance of the large-scale adaptive array antennas in the presence of mutual coupling," *IEEE Trans. Antennas Propag.*, vol. 64, no. 6, pp. 2236–2245, Jun. 2016.
[12] D. M. Pozar, "A relation between the active input impedance and the active element pattern of a phased array," *IEEE Trans. Antennas Propag.*, vol. 51, no. 9, pp. 2486–2489, Sep. 2003.
[13] I. Nadeem and D.-Y. Choi, "Study on mutual coupling reduction technique for MIMO antennas," *IEEE Access*, vol. 7, pp. 563–586, 2019.
[14] X. Chen, S. Zhang, and Q. Li, "A review of mutual coupling in MIMO systems," *IEEE Access*, vol. 6, pp. 24706–24719, 2018.
[15] H. Singh, H. L. Sneha, and R. M. Jha, "Mutual coupling in phased arrays: A review," *Int. J. Antennas Propag.*, vol. 2013, Mar. 2013, Art. no. 348123.
[16] C. Craeye and D. González-Ovejero, "A review on array mutual coupling analysis," *Radio Sci.*, vol. 46, no. 2, pp. 1–25, 2011.
[17] X. Zhu, X. Yang, Q. Song, and B. Lui, "Compact UWB-MIMO antenna with metamaterial FSS decoupling structure," *EURASIP J. Wireless Commun. Netw.*, vol. 2017, no. 1, p. 115, Dec. 2017.
[18] Y. Ou, X. Cai, and K. Qian, "Two-element compact antennas decoupled with a simple neutralization line," *Prog. Electromagn. Res. Lett.*, vol. 65, pp. 63–68, Jan. 2017.
[19] C. H. See, R. A. Abd-Alhameed, Z. Z. Abidin, N. J. McEwan, and P. S. Excell, "Wideband printed MIMO/diversity monopole antenna for WiFi/WiMAX applications," *IEEE Trans. Antennas Propag.*, vol. 60, no. 4, pp. 2028–2035, Apr. 2012.
[20] C. H. See, H. I. Hraga, R. A. Abd-Alhameed, N. J. McEwan, and J. M. Noras, "Compact multiple input and multiple output/diversity antenna for portable and mobile ultra-wideband applications," *IET Microw., Antennas Propag.*, vol. 7, no. 6, pp. 444–451, Apr. 2013.
[21] M. Bilal, R. Saleem, H. H. Abbasi, M. F. Shafique, and A. K. Brown, "An FSS-based nonplanar quad-element UWB-MIMO antenna system," *IEEE Antennas Wireless Propag. Lett.*, vol. 16, pp. 987–990, 2017.
[22] M. S. Khan, A.-D. Capobianco, S. M. Asif, D. E. Anagnostou, R. M. Shubair, and B. D. Braaten, "A compact CSRR-enabled UWB diversity antenna," *IEEE Antennas Wireless Propag. Lett.*, vol. 16, pp. 808–812, 2017.
[23] M. A. Abdalla and A. A. Ibrahim, "Design and performance evaluation of metamaterial inspired MIMO antennas for wireless applications," *Wireless Pers. Commun.*, vol. 95, no. 2, pp. 1001–1017, Jul. 2017.
[24] Y.-S. Chen and C.-P. Chang, "Design of a four-element multiple-input–multiple-output antenna for compact long-term evolution small-cell base stations," *IET Microw., Antennas Propag.*, vol. 10, no. 4, pp. 385–392, Mar. 2016.
[25] C. H. See, R. A. Abd-Alhameed, N. J. McEwan, S. M. R. Jones, R. Asif, and P. S. Excell, "Design of a printed MIMO/diversity monopole antenna for future generation handheld devices," *Int. J. RF Microw. Comput.-Aided Eng.*, vol. 24, no. 3, pp. 348–359, May 2014.
[26] Z. Wang, L. Zhao, Y. Cai, S. Zheng, and Y. Yin, "A meta-surface antenna array decoupling (MAAD) method for mutual coupling reduction in a MIMO antenna system," *Sci. Rep.*, vol. 8, Feb. 2018, Art. no. 3152, doi: 10.1038/s41598-018-21619-z.
[27] J. Tang, F. Faraz, X. Chen, Q. Zhang, Q. Li, Y. Li, and S. Zhang, "A metasurface superstrate for mutual coupling reduction of large antenna arrays," *IEEE Access*, vol. 8, pp. 126859–126867, 2020, doi: 10.1109/ACCESS.2020.3008162.
[28] K.-L. Wu, C. Wei, X. Mei, and Z.-Y. Zhang, "Array-antenna decoupling surface," *IEEE Trans. Antennas Propag.*, vol. 65, no. 12, pp. 6728–6738, Dec. 2017, doi: 10.1109/TAP.2017.2712818.
[29] M. Li, X. Chen, A. Zhang, W. Fan, and A. A. Kishk, "Split-ring resonator-loaded baffles for decoupling of dual-polarized base station array," *IEEE Antennas Wireless Propag. Lett.*, vol. 19, no. 10, pp. 1828–1832, Oct. 2020.
[30] S. Chouhan, D. K. Panda, M. Gupta, and S. Singhal, "Multiport MIMO antennas with mutual coupling reduction techniques for modern wireless transreceive operations: A review," *Int. J. RF Microw. Comput.-Aided Eng.*, vol. 28, no. 2, pp. 1–13, Feb. 2018.
[31] A. Dadgarpour, B. Zarghooni, B. S. Virdee, T. A. Denidni, and A. A. Kishk, "Mutual coupling reduction in dielectric resonator antennas using metasurface shield for 60-GHz MIMO systems," *IEEE Antennas Wireless Propag. Lett.*, vol. 16, pp. 477–480, 2017.
[32] G. Zhai, Z. N. Chen, and X. Qing, "Enhanced isolation of a closely spaced four-element MIMO antenna system using metamaterial mushroom," *IEEE Trans. Antennas Propag.*, vol. 63, no. 8, pp. 3362–3370, Aug. 2015.
[33] M. Akbari, H. A. Ghalyon, M. Farahani, A.-R. Sebak, and T. A. Denidni, "Spatially decoupling of CP antennas based on FSS for 30-GHz MIMO systems," *IEEE Access*, vol. 5, pp. 6527–6537, 2017.
[34] R. Karimian, A. Kesavan, M. Nedil, and T. A. Denidni, "Low-mutual-coupling 60-GHz MIMO antenna system with frequency selective surface wall," *IEEE Antennas Wireless Propag. Lett.*, vol. 16, pp. 373–376, 2017.
[35] S. Shrestha, S.-K. Noh, and D.-Y. Choi, "Comparative study of antenna designs for RF energy harvesting," *Int. J. Antennas Propag.*, vol. 2013, Jan. 2013, Art. no. 385260.
[36] M. S. Sharawi, A. T. Hassan, and M. U. Khan, "Correlation coefficient calculations for MIMO antenna systems: A comparative study," *Int. J. Microw. Wireless Technol.*, vol. 9, no. 10, pp. 1991–2004, Dec. 2017.
[37] L. Malviya, R. K. Panigrahi, and M. V. Kartikeyan, "MIMO antennas with diversity and mutual coupling reduction techniques: A review," *Int. J. Microw. Wireless Technol.*, vol. 9, no. 8, pp. 1763–1780, Oct. 2017.
[38] L. Savy and M. Lesturgie, "Coupling effects in MIMO phased array," in *Proc. IEEE Radar Conf.*, Philadelphia, PA, USA, May 2016, pp. 1–6.
[39] L. K. Yeung and Y. E. Wang, "Mode-based beamforming arrays for miniaturized platforms," *IEEE Trans. Microw. Theory Techn.*, vol. 57, no. 1, pp. 45–52, Jan. 2009.
[40] J. Andersen and H. Rasmussen, "Decoupling and descattering networks for antennas," *IEEE Trans. Antennas Propag.*, vol. 24, no. 6, pp. 841–846, Nov. 1976.
[41] L. Zhao, L. K. Yeung, and K.-L. Wu, "A novel second-order decoupling network for two-element compact antenna arrays," in *Proc. Asia–Pacific Microw. Conf.*, 2012, pp. 1172–1174.
[42] K.-L. Wong, C.-Y. Tsai, and J.-Y. Lu, "Two asymmetrically mirrored gap-coupled loop antennas as a compact building block for eight-antenna MIMO array in the future smartphone," *IEEE Trans. Antennas Propag.*, vol. 65, no. 4, pp. 1765–1778, Apr. 2017.
[43] B. K. Lau, J. B. Andersen, G. Kristensson, and A. F. Molisch, "Impact of matching network on bandwidth of compact antenna arrays," *IEEE Trans. Antennas Propag.*, vol. 54, no. 11, pp. 3225–3238, Nov. 2006.
[44] L. Zhao, L. K. Yeung, and K.-L. Wu, "A coupled resonator decoupling network for two-element compact antenna arrays in mobile terminals," *IEEE Trans. Antennas Propag.*, vol. 62, no. 5, pp. 2767–2776, May 2014.
[45] A. C. K. Mak, C. R. Rowell, and R. D. Murch, "Isolation enhancement between two closely packed antennas," *IEEE Trans. Antennas Propag.*, vol. 56, no. 11, pp. 3411–3419, Nov. 2008.
[46] S.-C. Chen, Y.-S. Wang, and S.-J. Chung, "A decoupling technique for increasing the port isolation between two strongly coupled antennas," *IEEE Trans. Antennas Propag.*, vol. 56, no. 12, pp. 3650–3658, Dec. 2008.
[47] J. Baek and J. Choi, "The design of a LTE/MIMO antenna with high isolation using a decoupling network," *Microw. Opt. Technol. Lett.*, vol. 56, pp. 2187–2190, Sep. 2014.
[48] Y. K. Choukiker, S. K. Sharma, and S. K. Behera, "Hybrid fractal shape planar monopole antenna covering multiband wireless communications with MIMO implementation for handheld mobile devices," *IEEE Trans. Antennas Propag.*, vol. 62, no. 3, pp. 1483–1488, Mar. 2014.
[49] Q. Kewei and G. Decheng, "Compact tunable network for closely spaced antennas with high isolation," *Microw. Opt. Technol. Lett.*, vol. 58, no. 1, pp. 65–69, Jan. 2016.
[50] Z. Li, M. Han, and J. Choi, "Compact dual-band MIMO antenna for 4G USB dongle applications," *Microw. Opt. Technol. Lett.*, vol. 54, no. 3, pp. 744–748, Mar. 2012.
[51] W. Lee and B. Jang, "A small 4 by 4 MIMO antenna system for LTE smart phones," *Microw. Opt. Technol. Lett.*, vol. 58, pp. 2668–2672, Nov. 2016.
[52] Y. Liu, L. Yang, Y. Liu, J. Ren, J. Wang, and X. Li, "Dual-band planar MIMO antenna for WLAN application," *Microw. Opt. Technol. Lett.*, vol. 57, no. 10, pp. 2257–2262, Oct. 2015.

[53] Y. Yu, J. Ji, W. Seong, and J. Choi, "A compact MIMO antenna with improved isolation bandwidth for mobile applications," *Microw. Opt. Technol. Lett.*, vol. 53, no. 10, pp. 2314–2317, Oct. 2011.
[54] B.-Y. Park, J.-H. Choi, S.-O. Park, T.-S. Yang, and J.-H. Byun, "Design of a decoupled MIMO antenna for LTE applications," *Microw. Opt. Technol. Lett.*, vol. 53, no. 3, pp. 582–586, Mar. 2011.
[55] M. Bilal, R. Saleem, M. F. Shafique, and H. A. Khan, "MIMO application UWB antenna doublet incorporating a sinusoidal decoupling structure," *Microw. Opt. Technol. Lett.*, vol. 56, no. 7, pp. 1547–1553, Jul. 2014.
[56] D. Wu, S. W. Cheung, Q. L. Li, and T. I. Yuk, "Decoupling using diamond-shaped patterned ground resonator for small MIMO antennas," *IET Microw., Antennas Propag.*, vol. 11, no. 2, pp. 177–183, Jan. 2017.
[57] L. Zhao and K.-L. Wu, "A decoupling technique for four-element symmetric arrays with reactively loaded dummy elements," *IEEE Trans. Antennas Propag.*, vol. 62, no. 8, pp. 4416–4421, Aug. 2014.
[58] L. Zhao and K.-L. Wu, "A dual-band coupled resonator decoupling network for two coupled antennas," *IEEE Trans. Antennas Propag.*, vol. 63, no. 7, pp. 2843–2850, Jul. 2015.
[59] C. F. Ding, X. Y. Zhang, C.-D. Xue, and C.-Y.-D. Sim, "Novel pattern-diversity-based decoupling method and its application to multielement MIMO antenna," *IEEE Trans. Antennas Propag.*, vol. 66, no. 10, pp. 4976–4985, Oct. 2018.
[60] C.-X. Mao and Q.-X. Chu, "Compact coradiator UWB-MIMO antenna with dual polarization," *IEEE Trans. Antennas Propag.*, vol. 62, no. 9, pp. 4474–4480, Sep. 2014.
[61] S. T. Fan, Y. Z. Yin, B. Lee, W. Hu, and X. Yang, "Bandwidth enhancement of a printed slot antenna with a pair of parasitic patches," *IEEE Antennas Wireless Propag. Lett.*, vol. 11, pp. 1230–1233, 2012.
[62] J.-S. Row and S.-W. Wu, "Circularly-polarized wide slot antenna loaded with a parasitic patch," *IEEE Trans. Antennas Propag.*, vol. 56, no. 9, pp. 2826–2832, Sep. 2008.
[63] Z. Li, Z. Du, M. Takahashi, K. Saito, and K. Ito, "Reducing mutual coupling of MIMO antennas with parasitic elements for mobile terminals," *IEEE Trans. Antennas Propag.*, vol. 60, no. 2, pp. 473–481, Feb. 2012.
[64] M. Ayatollahi, Q. Rao, and D. Wang, "A compact, high isolation and wide bandwidth antenna array for long term evolution wireless devices," *IEEE Trans. Antennas Propag.*, vol. 60, no. 10, pp. 4960–4963, Oct. 2012.
[65] S. Soltani and R. D. Murch, "A compact planar printed MIMO antenna design," *IEEE Trans. Antennas Propag.*, vol. 63, no. 3, pp. 1140–1149, Mar. 2015.
[66] R. V. S. R. Krishna and R. Kumar, "Microstrip fed square ring slot antenna for ultra-wideband dual polarisation with good isolation," *IET Microw., Antennas Propag.*, vol. 10, no. 7, pp. 791–796, May 2016.
[67] T. K. Roshna, U. Deepak, V. R. Sajitha, K. Vasudevan, and P. Mohanan, "A compact UWB MIMO antenna with reflector to enhance isolation," *IEEE Trans. Antennas Propag.*, vol. 63, no. 4, pp. 1873–1877, Apr. 2015, doi: 10.1109/TAP.2015.2398455.
[68] S. Zhang, Z. Ying, J. Xiong, and S. He, "Ultrawideband MIMO/diversity antennas with a tree-like structure to enhance wideband isolation," *IEEE Antennas Wireless Propag. Lett.*, vol. 8, pp. 1279–1282, 2009.
[69] G. Srivastava and A. Mohan, "Compact MIMO slot antenna for UWB applications," *IEEE Antennas Wireless Propag. Lett.*, vol. 15, pp. 1057–1060, 2016.
[70] M. S. Khan, A.-D. Capobianco, A. Iftikhar, R. M. Shubair, D. E. Anagnostou, and B. D. Braaten, "Ultra-compact dual-polarised UWB MIMO antenna with meandered feeding lines," *IET Microw., Antennas Propag.*, vol. 11, no. 7, pp. 997–1002, Jun. 2017.
[71] M. K. Khandelwal, B. K. Kanaujia, and S. Kumar, "Defected ground structure: Fundamentals, analysis, and applications in modern wireless trends," *Int. J. Antennas Propag.*, vol. 2017, Feb. 2017, Art. no. 2018527.
[72] A. K. Arya, M. V. Kartikeyan, and A. Patnaik, "Defected ground structure in the perspective of microstrip antennas: A review," *Frequenz*, vol. 64, nos. 5–6, pp. 79–84, Jan. 2010.
[73] P. Lindberg, L. Morton, A. Kaikkonen, S. Cheng, and P. Hallbjorner, "Technique of ground size tuning for isolation between monopoles in compact wireless terminals," *IEEE Trans. Antennas Propag.*, vol. 60, no. 11, pp. 5488–5491, Nov. 2012.
[74] J. Lu, Z. Kuai, X. Zhu, and N. Zhang, "A high-isolation dual-polarization microstrip patch antenna with quasi-cross-shaped coupling slot," *IEEE Trans. Antennas Propag.*, vol. 59, no. 7, pp. 2713–2717, Jul. 2011.
[75] R. Hussain and M. S. Sharawi, "Planar meandered-F-shaped 4-element reconfigurable multiple-input–multiple-output antenna system with isolation enhancement for cognitive radio platforms," *IET Microw., Antennas Propag.*, vol. 10, no. 1, pp. 45–52, Jan. 2016.
[76] K. Wei, L. Wang, Z. Xing, R. Xu, and J. Li, "S-shaped periodic defected ground structures to reduce microstrip antenna array mutual coupling," *Electron. Lett.*, vol. 52, no. 15, pp. 1288–1290, Jul. 2016.
[77] R. Anitha, V. P. Sarin, K. Vasudevan, and P. Mohanan, "Enhanced isolation with defected ground structure in MIMO antenna," *Electron. Lett.*, vol. 50, no. 24, pp. 1784–1786, Nov. 2014.
[78] C. R. Jetti and V. R. Nandanavanam, "Trident-shape strip loaded dual band-notched UWB MIMO antenna for portable device applications," *AEU-Int. J. Electron. Commun.*, vol. 83, pp. 11–21, Jan. 2018.
[79] F.-G. Zhu, J.-D. Xu, and Q. Xu, "Reduction of mutual coupling between closely-packed antenna elements using defected ground structure," *Electron. Lett.*, vol. 45, no. 12, pp. 601–602, Jun. 2009.
[80] A. Ramachandran, S. V. Pushpakaran, M. Pezholil, and V. Kesavath, "A four-port MIMO antenna using concentric square-ring patches loaded with CSRR for high isolation," *IEEE Antennas Wireless Propag. Lett.*, vol. 15, pp. 1196–1199, 2016.
[81] M. S. Sharawi, M. U. Khan, A. B. Numan, and D. N. Aloi, "A CSRR loaded MIMO antenna system for ISM band operation," *IEEE Trans. Antennas Propag.*, vol. 61, no. 8, pp. 4265–4274, Aug. 2013.
[82] D.-G. Yang, D. O. Kim, and C.-Y. Kim, "Design of dual-band MIMO monopole antenna with high isolation using slotted CSRR for WLAN," *Microw. Opt. Technol. Lett.*, vol. 56, no. 10, pp. 2252–2257, Oct. 2014.
[83] P. R. Prajapati, "Application of defected ground structure to suppress out of-band harmonics for WLAN microstrip antenna," *Int. J. Microw. Sci. Technol.*, vol. 2015, Nov. 2015, Art. no. 210608.
[84] Y. Wang and Z. Du, "A wideband printed dual-antenna with three neutralization lines for mobile terminals," *IEEE Trans. Antennas Propag.*, vol. 62, no. 3, pp. 1495–1500, Mar. 2014.
[85] S.-W. Su, C.-T. Lee, and F.-S. Chang, "Printed MIMO-antenna system using neutralization-line technique for wireless USB-dongle applications," *IEEE Trans. Antennas Propag.*, vol. 60, no. 2, pp. 456–463, Feb. 2012.
[86] Y. Wang and Z. Du, "A wideband printed dual-antenna system with a novel neutralization line for mobile terminals," *IEEE Antennas Wireless Propag. Lett.*, vol. 12, pp. 1428–1431, 2013.
[87] S.-W. Su, C.-T. Lee, and F.-S. Chang, "Printed MIMO-antenna system using neutralization-line technique for wireless USB-dongle applications," *IEEE Trans. Antennas Propag.*, vol. 60, no. 2, pp. 456–463, Feb. 2012.
[88] S. Wang and Z. Du, "Decoupled dual-antenna system using crossed neutralization lines for LTE/WWAN smartphone applications," *IEEE Antennas Wireless Propag. Lett.*, vol. 14, pp. 523–526, 2015.
[89] W. A. E. Ali and A. A. Ibrahim, "A compact double-sided MIMO antenna with an improved isolation for UWB applications," *AEU-Int. J. Electron. Commun.*, vol. 82, pp. 7–13, Dec. 2017.
[90] J.-H. Lim, Z.-J. Jin, C.-W. Song, and T.-Y. Yun, "Simultaneous frequency and isolation reconfigurable MIMO PIFA using PIN diodes," *IEEE Trans. Antennas Propag.*, vol. 60, no. 13, pp. 5939–5946, Dec. 2012.
[91] D. Piazza, N. J. Kirsch, A. Forenza, R. W. Heath, Jr., and K. R. Dandekar, "Design and evaluation of a reconfigurable antenna array for MIMO systems," *IEEE Trans. Antennas Propag.*, vol. 56, no. 3, pp. 869–880, Mar. 2008.
[92] D. E. Anagnostou, M. T. Chryssomallis, B. D. Braaten, J. L. Ebel, and N. Sepulveda, "Reconfigurable UWB antenna with RF-MEMS for on-demand WLAN rejection," *IEEE Trans. Antennas Propag.*, vol. 62, no. 2, pp. 602–608, Feb. 2014.
[93] S. Soltani, P. Lotfi, and R. D. Murch, "A port and frequency reconfigurable MIMO slot antenna for WLAN applications," *IEEE Trans. Antennas Propag.*, vol. 64, no. 4, pp. 1209–1217, Apr. 2016.
[94] R. Hussain, M. S. Sharawi, and A. Shamim, "An integrated four-element slot-based MIMO and a UWB sensing antenna system for CR platforms," *IEEE Trans. Antennas Propag.*, vol. 66, no. 2, pp. 978–983, Feb. 2018.
[95] R. Hussain, M. S. Sharawi, and A. Shamim, "4-element concentric pentagonal slot-line-based ultra-wide tuning frequency reconfigurable MIMO antenna system," *IEEE Trans. Antennas Propag.*, vol. 66, no. 8, pp. 4282–4287, Aug. 2018.
[96] J.-H. Lim, Z.-J. Jin, C.-W. Song, and T.-Y. Yun, "Simultaneous frequency and isolation reconfigurable MIMO PIFA using PIN diodes," *IEEE Trans. Antennas Propag.*, vol. 60, no. 12, pp. 5939–5946, Dec. 2012.
[97] A. N. Kulkarni and S. K. Sharma, "Frequency reconfigurable microstrip loop antenna covering LTE bands with MIMO implementation and wideband microstrip slot antenna all for portable wireless DTV media player," *IEEE Trans. Antennas Propag.*, vol. 61, no. 2, pp. 964–968, Feb. 2013.

[98] *Hitachi's Research & Development. EBG Structure*. Accessed: Aug. 13, 2018. [Online]. Available: http://www.hitachi.com/rd/portal/glossary/e/ebg_structure.html

[99] Y. Rahmat-Samii, "Electromagnetic band gap (EBG) structures in antenna engineering: From fundamentals to recent advances," in *Proc. Asia–Pacific Microw. Conf.*, Dec. 2008, pp. 1–2.

[100] M. S. Alam, N. Misran, B. Yatim, and M. T. Islam, "Development of electromagnetic band gap structures in the perspective of microstrip antenna design," *Int. J. Antennas Propag.*, vol. 2013, pp. 1–22, Mar. 2013.

[101] A. Suntives and R. Abhari, "Miniaturization and isolation improvement of a multiple-patch antenna system using electromagnetic bandgap structures," *Microw. Opt. Technol. Lett.*, vol. 55, no. 7, pp. 1609–1612, Jul. 2013.

[102] S. Ghosh, T.-N. Tran, and T. Le-Ngoc, "Dual-layer EBG-based miniaturized multi-element antenna for MIMO systems," *IEEE Trans. Antennas Propag.*, vol. 62, no. 8, pp. 3985–3997, Aug. 2014.

[103] B. Mohamadzade and M. Afsahi, "Mutual coupling reduction and gain enhancement in patch array antenna using a planar compact electromagnetic bandgap structure," *IET Microw., Antennas Propag.*, vol. 11, no. 12, pp. 1719–1725, Sep. 2017.

[104] J.-Y. Lee, S.-H. Kim, and J.-H. Jang, "Reduction of mutual coupling in planar multiple antenna by using 1-D EBG and SRR structures," *IEEE Trans. Antennas Propag.*, vol. 63, no. 9, pp. 4194–4198, Sep. 2015.

[105] M. S. Khan, A.-D. Capobianco, M. F. Shafique, B. Ijaz, A. Naqvi, and B. D. Braaten, "Isolation enhancement of a wideband MIMO antenna using floating parasitic elements," *Microw. Opt. Technol. Lett.*, vol. 57, no. 7, pp. 1677–1682, Jul. 2015.

[106] H. Huang, Y. Liu, and S.-X. Gong, "Broadband omnidirectional dual-polarized antenna with high isolation," *Microw. Opt. Technol. Lett.*, vol. 57, no. 8, pp. 1848–1852, Aug. 2015.

[107] K.-L. Wong, C.-H. Chang, B. Chen, and S. Yang, "Three-antenna MIMO system for WLAN operation in a PDA phone," *Microw. Opt. Technol. Lett.*, vol. 48, no. 7, pp. 1238–1242, Jul. 2006.

[108] L. Malviya, R. K. Panigrahi, and M. V. Kartikeyan, "A multi-standard, wide-band 2×2 compact MIMO antenna with ground modification techniques," *Int. J. Microw. Opt. Technol.*, vol. 11, no. 4, pp. 259–267, 2016.

[109] H. Bae, F. J. Harackiewicz, M.-J. Park, T. Kim, N. Kim, D. Kim, and B. Lee, "Compact mobile handset MIMO antenna for LTE 700 applications," *Microw. Opt. Technol. Lett.*, vol. 52, no. 11, pp. 2419–2422, 2010.

[110] S. R. Rengarajan, M. S. Zawadzki, and R. E. Hodges, "Design, analysis, and development of a large Ka-band slot array for digital beamforming application," *IEEE Trans. Antennas Propag.*, vol. 57, no. 10, pp. 3103–3109, Oct. 2009.

[111] J. R. Costa, E. B. Lima, C. R. Medeiros, and C. A. Fernandes, "Evaluation of a new wideband slot array for MIMO performance enhancement in indoor WLANs," *IEEE Trans. Antennas Propag.*, vol. 59, no. 4, pp. 1200–1206, Apr. 2011.

[112] M. Alibakhshikenari, B. S. Virdee, M. Khalily, C. H. See, R. Abd-Alharueed, F. Falcone, and E. Limiti, "A new study to suppress mutual-coupling between waveguide slot array antennas based on metasurface bulkhead for MIMO systems," in *Proc. Asia–Pacific Microw. Conf. (APMC)*, Kyoto, Japan, Nov. 2018, pp. 500–502.

[113] M. Alibakhshikenari, B. S. Virdee, M. Khalily, C. H. See, R. Abd-Alhameed, F. Falcone, and E. Limiti, "New approach to suppress mutual coupling between longitudinal-slotted arrays based on SIW antenna loaded with metal-fences working on VHF/UHF frequency-bands: Study, investigation, and principle," in *Proc. Asia–Pacific Microw. Conf. (APMC)*, Kyoto, Japan, Nov. 2018, pp. 1564–1566.

[114] M. Alibakhshikenari, B. S. Virdee, C. H. See, R. Abd-Alhameed, F. Falcone, A. Andujar, J. Anguera, and E. Limiti, "Study on antenna mutual coupling suppression using integrated metasurface isolator for SAR and MIMO applications," in *Proc. 15th Eur. Radar Conf. (EuRAD)*, Sep. 2018, pp. 1425–1428.

[115] M. Alibakhshikenari, B. S. Virdee, C. H. See, R. Abd-Alhameed, F. Falcone, and E. Limiti, "A new waveguide slot array antenna with high isolation and high antenna bandwidth operation on Ku- and K-bands for radar and MIMO systems," in *Proc. 15th Eur. Radar Conf. (EuRAD)*, Sep. 2018, pp. 1421–1424.

[116] M. Alibakhshikenari, M. Vittori, S. Colangeli, B. S. Virdee, A. Andujar, J. Anguera, and E. Limiti, "EM isolation enhancement based on metamaterial concept in antenna array system to support full-duplex application," in *Proc. IEEE Asia–Pacific Microw. Conf. (APMC)*, Kuala Lumpur, Malaysia, Nov. 2017, pp. 740–742.

[117] M. Alibakhshikenari, B. S. Virdee, C. H. See, R. Abd-Alhameed, F. Falcone, and E. Limiti, "Mutual-coupling reduction in metamaterial substrate integrated waveguide slotted antenna arrays using metal fence isolators for SAR and MIMO applications," in *Proc. 12th Int. Congr. Artif. Mater. Novel Wave Phenomena (Metamaterials)*, Espoo, Finland, Aug./Sep. 2018, pp. 13–15.

[118] M. Alibakhshikenari, A. Salvucci, G. Polli, B. S. Virdee, C. H. See, R. Abd-Alhameed, F. Falcone, A. Andújar, J. Anguera, and E. Limiti, "Mutual coupling reduction using metamaterial supersubstrate for high performance & densely packed planar phased arrays," in *Proc. 22nd Int. Microw. Radar Conf. (MIKON)*. Poznań, Poland: Warsaw Univ. Technology, May 2018, pp. 675–678.

[119] M. Alibakhshikenari, B. S. Virdee, C. H. See, R. Abd-Alhameed, F. Falcone, and E. Limiti, "Array antenna for synthetic aperture radar operating in X and Ku-bands: A study to enhance isolation between radiation elements," in *Proc. 12th Eur. Conf. Synth. Aperture Radar (EUSAR)*, Aachen, Germany, Jun. 2018, pp. 1083–1087.

[120] M. Alibakhshikenari, B. S. Virdee, and E. Limiti, "A technique to suppress mutual coupling in densely packed antenna arrays using metamaterial supersubstrate," in *Proc. 12th Eur. Conf. Antennas Propag. (EuCAP)*, London, U.K., Apr. 2018, pp. 9–13.

[121] M. Alibakhshikenari, M. Khalily, B. S. Virdee, C. H. See, R. A. Abd-Alhameed, and E. Limiti, "Mutual coupling suppression between two closely placed microstrip patches using EM-bandgap metamaterial fractal loading," *IEEE Access*, vol. 7, pp. 23606–23614, 2019.

[122] M. Alibakhshikenari, B. S. Virdee, C. H. See, R. Abd-Alhameed, A. H. Ali, F. Falcone, and E. Limiti, "Study on isolation improvement between closely-packed patch antenna arrays based on fractal metamaterial electromagnetic bandgap structures," *IET Microw., Antennas Propag.*, vol. 12, no. 14, pp. 2241–2247, Nov. 2018.

[123] M. Alibakhshikenari, B. S. Virdee, P. Shukla, C. H. See, R. Abd-Alhameed, M. Khalily, F. Falcone, and E. Limiti, "Interaction between closely packed array antenna elements using meta-surface for applications such as MIMO systems and synthetic aperture radars," *Radio Sci.*, vol. 53, no. 11, pp. 1368–1381, Nov. 2018.

[124] M. Alibakhshikenari, M. Khalily, B. S. Virdee, C. H. See, R. A. Abd-Alhameed, and E. Limiti, "Mutual-coupling isolation using embedded metamaterial EM bandgap decoupling slab for densely packed array antennas," *IEEE Access*, vol. 7, pp. 5182–51840, 2019.

[125] M. Alibakhshikenari, B. S. Virdee, C. H. See, R. A. Abd-Alhameed, F. Falcone, and E. Limiti, "High-isolation leaky-wave array antenna based on CRLH metamaterial implemented on SIW with ±30° frequency beam-scanning capability at millimeter-waves," *Electronics*, vol. 8, vol. 6, pp. 1–15, 2019.

[126] M. Alibakhshikenari, B. S. Virdee, P. Shukla, C. H. See, R. A. Abd-Alhameed, F. J. Falcone, and E. Limiti, "Meta-surface wall suppression of mutual coupling between microstrip patch antenna arrays for THZ-band applications," *Prog. Electromagn. Res. Lett.*, vol. 75, pp. 105–111, Jan. 2018.

[127] M. Alibakhshikenari, B. S. Virdee, P. Shukla, C. H. See, R. Abd-Alhameed, M. Khalily, F. Falcone, and E. Limiti, "Antenna mutual coupling suppression over wideband using embedded periphery slot for antenna arrays," *Electronics*, vol. 7, no. 9, pp. 1–11, 2018.

[128] H. Qi, L. Liu, X. Yin, H. Zhao, and W. J. Kulesza, "Mutual coupling suppression between two closely spaced microstrip antennas with an asymmetrical coplanar strip wall," *IEEE Antennas Wireless Propag. Lett.*, vol. 15, pp. 191–194, 2016.

[129] S. Gupta, Z. Briqech, A. R. Sebak, and T. A. Denidni, "Mutual-coupling reduction using metasurface corrugations for 28 GHz MIMO applications," *IEEE Antennas Wireless Propag. Lett.*, vol. 16, pp. 2763–2766, 2017.

[130] M. Alibakhshikenari, B. S. Virdee, C. H. See, R. A. Abd-Alhameed, F. Falcone, and E. Limiti, "Surface wave reduction in antenna arrays using metasurface inclusion for MIMO and SAR systems," *Radio Sci.*, vol. 54, no. 11, pp. 1067–1075, Nov. 2019.

[131] M. Alibakhshikenari, B. S. Virdee, and E. Limiti, "Study on isolation and radiation behaviours of a 34×34 array-antennas based on SIW and metasurface properties for applications in terahertz band over 125–300 GHz," *Optik*, vol. 206, Mar. 2020, Art. no. 163222.

[132] M. Alibakhshikenari, B. S. Virdee, P. Shukla, C. H. See, R. A. Abd-Alhameed, F. Falcone, K. Quazzane, and E. Limiti, "Isolation enhancement of densely packed array antennas with periodic MTM-photonic bandgap for SAR and MIMO systems," *IET Microw., Antennas Propag.*, vol. 14, no. 3, pp. 183–188, Feb. 2020.

[133] H. S. Farahani, M. Veysi, M. Kamyab, and A. Tadjalli, "Mutual coupling reduction in patch antenna arrays using a UC-EBG superstrate," *IEEE Antennas Wireless Propag. Lett.*, vol. 9, pp. 57–59, 2010.
[134] J. OuYang, F. Yang, and Z. M. Wang, "Reduction of mutual coupling of closely spaced microstrip MIMO antennas for WLAN application," *IEEE Antennas Wireless Propag. Lett.*, vol. 10, pp. 310–312, 2011.
[135] A. Yu and X. Zhang, "A novel method to improve the performance of microstrip antenna arrays using a dumbbell EBG structure," *IEEE Antennas Wireless Propag. Lett.*, vol. 2, pp. 170–172, 2003.
[136] M. T. Islam and M. S. Alam, "Compact EBG structure for alleviating mutual coupling between patch antenna array elements," *Prog. Electromagn. Res.*, vol. 137, pp. 425–438, Feb. 2013.
[137] F. G. Zhu, J.-D. Xu, and Q. Xu, "Reduction of mutual coupling between closely packed antenna elements using defected ground structure," *Electron. Lett.*, vol. 45, no. 12, pp. 601–602, 2012.
[138] S. Farsi, H. Aliakbarian, D. Schreurs, B. Nauwelaers, and G. A. E. Vandenbosch, "Mutual coupling reduction between planar antennas by using a simple microstrip U-section," *IEEE Antennas Wireless Propag. Lett.*, vol. 11, pp. 1501–1503, 2012.
[139] M. G. N. Alsath, M. Kanagasabai, and B. Balasubramanian, "Implementation of slotted meander-line resonators for isolation enhancement in microstrip patch antenna arrays," *IEEE Antennas Wireless Propag. Lett.*, vol. 12, pp. 15–18, 2013.
[140] C. K. Ghosh and S. K. Parui, "Reduction of mutual coupling between E-shaped microstrip antennas by using a simple microstrip I-section," *Microw. Opt. Technol. Lett.*, vol. 55, no. 11, pp. 2544–2549, Nov. 2013.
[141] M. M. Bait-Suwailam, O. F. Siddiqui, and O. M. Ramahi, "Mutual coupling reduction between microstrip patch antennas using slotted-complementary split-ring resonators," *IEEE Antennas Wireless Propag. Lett.*, vol. 9, pp. 876–878, 2010.
[142] M. F. Shafique, Z. Qamar, L. Riaz, R. Saleem, and S. A. Khan, "Coupling suppression in densely packed microstrip arrays using metamaterial structure," *Microw. Opt. Technol. Lett.*, vol. 57, no. 3, pp. 759–763, Mar. 2015.
[143] X. M. Yang, X. G. Liu, X. Y. Zhou, and T. J. Cui, "Reduction of mutual coupling between closely packed patch antennas using waveguided metamaterials," *IEEE Antennas Wireless Propag. Lett.*, vol. 11, pp. 389–391, 2012.
[144] Z. Qamar and H. C. Park, "Compact waveguided metamaterials for suppression of mutual coupling in microstrip array," *Prog. Electromagn. Res.*, vol. 149, pp. 183–192, Jan. 2014.
[145] J. Ghosh, S. Ghosal, D. Mitra, and S. R. B. Chaudhuri, "Mutual coupling reduction between closely placed microstrip patch antenna using meander line resonator," *Prog. Electromagn. Res. Lett.*, vol. 59, pp. 115–122, Jan. 2016.
[146] X. Yang, Y. Liu, Y.-X. Xu, and S.-X. Gong, "Isolation enhancement in patch antenna array with fractal UC-EBG structure and cross slot," *IEEE Antennas Wireless Propag. Lett.*, vol. 16, pp. 2175–2178, 2017.
[147] L. Zhao, F. Liu, X. Shen, G. Jing, Y.-M. Cai, and Y. Li, "A high-pass antenna interference cancellation chip for mutual coupling reduction of antennas in contiguous frequency bands," *IEEE Access*, vol. 6, pp. 38097–38105, 2018.
[148] K. Yu, Y. Li, and X. Liu, "Mutual coupling reduction of a MIMO antenna array using 3-D novel meta-material structures," *Appl. Comput. Electromagn. Soc. J.*, vol. 33, no. 7, pp. 758–763, 2018.

MOHAMMAD ALIBAKHSHIKENARI (Member, IEEE) was born in Mazandaran, Iran, in 1988. He received the Ph.D. degree (Hons.) in electronic engineering from the University of Rome "Tor Vergata," Italy, in February 2020.

In 2018 for eight months, he has worked as a Ph.D. Visiting Researcher with the Antenna System Division, Department of Electrical Engineering, Chalmers University of Technology, Gothenburg, Sweden. His training during the Ph.D. included a research stage in the Swedish company Gap Waves AB that is developing components in a technology. He is currently working as a Postdoctoral Grant Holder Researcher with the University of Rome "Tor Vergata." During his Ph.D. research period, he has participated in 14 international IEEE conferences over the world, where he has presented 20 articles mostly in oral presentations. He acts as a referee in several high-reputed journals and IEEE international conferences. His research interests include antennas and wave-propagations, phased antenna arrays, metamaterials and metasurfaces, synthetic aperture radars (SAR), multiple-input multiple-output (MIMO) systems, waveguide slotted antenna arrays, substrate integrated waveguides (SIWs), impedance matching circuits, on-chip antennas, microwave components, millimeter-waves and terahertz integrated circuits, and electromagnetic systems. The above research lines have produced more than 90 publications on refereed-international journals, presentations within international-conferences, and book chapters with a total number of the citations more than 1150, H-index of 23, and I10-index of 42 reported by the Google Scholar Citation. During his Ph.D. degree, he was winner of 13 grants for participating in the European Doctoral and Postdoctoral Schools on Antennas and Metamaterials organized by several European Universities and European School of Antennas (ESoA). He was a recipient of two years postdoctoral research grant awarded by the Electronic Engineering Department of the University of Rome "Tor Vergata," in 2019. He was also a recipient of the International Postgraduate Research (Ph.D.) Scholarship (IPRS) by Italian Government started in 2016 for three years. He was two recipients of the 47th and 48th European Microwave Conference (EuMC) Young Engineer Prize, Nuremberg, Germany, in 2017, and Madrid, Spain, in 2018, where he has presented his articles. In April 2020, his article titled "High-Gain Metasurface in Polyimide On-Chip Antenna Based on CRLH-TL for Sub Terahertz Integrated Circuits" published in *Scientific Reports* was awarded as the Best Month Paper at the University of Bradford, U.K. He gave an invited lecture titled "Metamaterial Applications to Antenna Systems" at the Department of Information and Telecommunication Engineering, Incheon National University, Incheon, South Korea, in August 2019, which was in conjunction with the 8th Asia-Pacific Conference on Antennas and Propagation (APCAP 2019), where he was the Chair of the metamaterial session. He has been serving as an Editorial Board Member for *HighTech and Innovation Journal* and *International Journal of Electrical and Computer Engineering (IJECE)* and a Guest Editor for a Special Issue titled "Millimeter-Wave and Terahertz Applications of Metamaterials" of *Applied Sciences*.

FATEMEH BABAEIAN (Member, IEEE) received the B.Sc. degree in electrical engineering from Shiraz University, Shiraz, Iran, in 2010, the M.Sc. degree in electrical engineering (telecommunication) from the Amirkabir University of Technology, Tehran, Iran, in 2013, and the Ph.D. degree from the Department of Electrical and Computer Systems Engineering (ECSE), Monash University, Melbourne, VIC, Australia. She has more than three years of industrial job experience as an RF Engineer. Her research interests include chipless RFID, RF, microwave, antenna array synthesis, and signal processing.

BAL S. VIRDEE (Senior Member, IEEE) received the B.Sc. and M.Phil. degrees in communications-engineering from the University of Leeds, U.K., and the Ph.D. degree in electronic-engineering from the University of London, U.K. He has worked in industry for various companies, including Philips, U.K., as a Research and Development Engineer, and Filtronic-Components Ltd., as a Future Products Developer in the area of RF/microwave communications. He has taught at several academic institutions before joining London Metropolitan University, where he is currently a Professor of microwave-communications with the Faculty of Life Sciences and Computing, where he also Heads the Center for Communications-Technology and is the Director of London Metropolitan-Microwaves. His research, in collaboration with industry and academia, interest includes microwave wireless communications encompassing mobile-phones to satellite-technology. He has chaired technical sessions at IEEE international conferences and has published numerous research papers. He is an Executive Member of IET's Technical and Professional Network Committee on RF/Microwave-Technology. He is also a Fellow of IET.

SONIA AÏSSA (Fellow, IEEE) received the Ph.D. degree in electrical and computer engineering from McGill University, Montreal, QC, Canada, in 1998. Since then, she has been with the Institut National de la Recherche Scientifique-Energy, Materials, and Telecommunications Center (INRS-EMT), University of Quebec, Montreal, where she is currently a Full Professor. From 1996 to 1997, she was a Researcher with the Department of Electronics and Communications, Kyoto University, and the Wireless Systems Laboratories of NTT, Japan. From 1998 to 2000, she was a Research Associate with INRS-EMT. From 2000 to 2002, while she was an Assistant Professor, she was a Principal Investigator in the major program of personal and mobile communications of the Canadian Institute for Telecommunications Research, leading research in radio resource management for wireless networks. From 2004 to 2007, she was an Adjunct Professor with Concordia University, Canada. She was a Visiting Invited Professor with Kyoto University, Japan, in 2006, and Universiti Sains Malaysia, in 2015. Her research interest includes the modeling, design, and performance analysis of wireless communication systems and networks. She is a Fellow of the Canadian Academy of Engineering. Awards to her credit include the NSERC University Faculty Award in 1999; the Quebec Government FRQNT Strategic Faculty Fellowship from 2001 to 2006; the INRS-EMT Performance Award multiple times since 2004, for outstanding achievements in research, teaching and service; and the Technical Community Service Award from the FRQNT Centre for Advanced Systems and Technologies in Communications, in 2007. She was a co-recipient of five IEEE Best Paper Awards and the 2012 IEICE Best Paper Award; and a recipient of the NSERC Discovery Accelerator Supplement Award. She is the Founding Chair of the IEEE Women in Engineering Affinity Group in Montreal, from 2004 to 2007; acted as the TPC Symposium Chair or Co-Chair at IEEE ICC 2006, 2009, 2011, and 2012; the Program Co-Chair at IEEE WCNC 2007; the TPC Co-Chair of IEEE VTC-Spring 2013; the TPC Symposia Chair of IEEE Globecom 2014; the TPC Vice-Chair of IEEE Globecom 2018; and serves as the TPC Chair for IEEE ICC 2021. Her main editorial activities include as an Editor of IEEE TRANSACTIONS ON WIRELESS COMMUNICATIONS from 2004 to 2012; an Associate Editor and a Technical Editor of *IEEE Communications Magazine* from 2004 to 2015; a Technical Editor of *IEEE Wireless Communications Magazine* from 2006 to 2010; and an Associate Editor of *Security and Communication Networks* journal (Wiley) from 2007 to 2012. She currently serves as an Area Editor for the IEEE TRANSACTIONS ON WIRELESS COMMUNICATIONS. She has served as a Distinguished Lecturer for the IEEE Communications Society and a member of its Board of Governors from 2013 to 2016 and 2014 to 2016, respectively.

LEYRE AZPILICUETA (Senior Member, IEEE) received the degree in telecommunications engineering, the master's degree in communications, and the Ph.D. degree in telecommunication technologies from the Public University of Navarre (UPNa), Spain, in 2009, 2011, and 2015, respectively. In 2010, she was a Radio Engineer with the Research and Development Department, RFID Osés. She is currently an Associate Professor and a Researcher with the Tecnologico de Monterrey, Monterrey, Mexico. She has over 150 contributions in relevant journals and conference publications. Her research interests include radio propagation, mobile radio systems, ray tracing, and channel modeling. She was a recipient of the IEEE Antennas and Propagation Society Doctoral Research Award in 2014, the Young Professors and Researchers Santander Universities 2014 Mobility Award, the ECSA 2014 Best Paper Award, the IISA 2015 Best Paper Award, the ISSI 2019 Best Paper Award, the Best Ph.D. from the Colegio Oficial de Ingenieros de Telecomunicación in 2016, and the N2Women Rising Stars in Computer Networking and Communications 2018 Award.

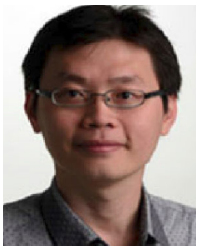

CHAN HWANG SEE (Senior Member, IEEE) received the B.Eng. degree (Hons.) in electronic, telecommunication, and computer engineering and the Ph.D. degree from the University of Bradford, U.K., in 2002 and 2007, respectively. He was a Senior Lecturer (Programme Leader) in electrical and electronic engineering with the School of Engineering, University of Bolton, U.K. He is currently an Associate Professor and the Head of electrical engineering and mathematics with the School of Engineering and the Built Environment, Edinburgh Napier University, U.K. He is also a Visiting Research Fellow with the School of Engineering and Informatics, University of Bradford. Prior to this, he was a Senior Research Fellow with the Antennas and Applied Electromagnetics Research Group, University of Bradford. His research interests include wireless sensor network system design, computational electromagnetism, antennas, and acoustic sensor design. He has published over 200 peer-reviewed journal articles and conference papers in the areas of antennas, computational electromagnetics, microwave circuits, acoustic sensors, and wireless sensor system designs. He is a coauthor for one book and three book chapters. He is a Fellow of the Institution of Engineering and Technology and the Higher Education Academy. He was a recipient of two Young Scientist Awards from the International Union of Radio Science (URSI) and Asia-Pacific Radio Science Conference (AP-RASC) in 2008 and 2010, respectively. He was awarded the Certificate of Excellence for his successful Knowledge Transfer Partnership (KTP) with Yorkshire Water on the design and implementation of a wireless sensor system for sewerage infrastructure monitoring in 2009. He is a Chartered Engineer. He is also an Associate Editor of IEEE ACCESS.

AYMAN ABDULHADI ALTHUWAYB (Member, IEEE) received the B.Sc. degree (Hons.) in electrical engineering (electronics and communications) from Jouf University, Saudi Arabia, in 2011, the M.Sc. degree in electrical engineering from California State University, Fullerton, CA, USA, in 2015, and the Ph.D. degree in electrical engineering from Southern Methodist University, Dallas, TX, USA, in 2018. He is currently an Assistant Professor with the Department of Electrical Engineering, Jouf University. His current research interests include antenna design and propagation, microwaves and millimeter-waves, wireless power transfer, ultrawideband and multiband antennas, filters, and other.

ISABELLE HUYNEN (Senior Member, IEEE) received the Ph.D. degree in applied sciences from the Université Catholique de Louvain (UCLouvain), Louvain-la-Neuve, Belgium, in 1994. Since 1999, she has been with FRS-FRNS, Bruxelles, Belgium. She is currently the Research Director and a part-time Professor with UCLouvain. Her current research interests include nanotechnology, nanodevices, and nanomaterials for microwave and millimeter wave applications, including metamaterials, antennas, and absorbers.

RAED A. ABD-ALHAMEED (Senior Member, IEEE) received the B.Sc. and M.Sc. degrees from Basrah University, Basrah, Iraq, in 1982 and 1985, respectively, and the Ph.D. degree from the University of Bradford, Bradford, U.K., in 1997, all in electrical engineering. He is currently a Professor of electromagnetic and radio frequency engineering with the University of Bradford. He has long years' research experience in the areas of radio frequency, signal processing, propagations, antennas, and electromagnetic computational techniques, and has published more than 500 academic journal and conference papers. He is a coauthor of three books and several book chapters. He is currently the Leader of radio frequency, propagation, sensor design, and signal processing; in addition to leading the Communications Research Group for years within the School of Engineering and Informatics, Bradford University. He is also a Principal Investigator for several funded applications to EPSRCs and the Leader of several successful Knowledge Transfer Programmes (KTPs), such as with Arris (previously known as Pace plc), Yorkshire Water plc, Harvard Engineering plc, IETG Ltd., Seven Technologies Group, Emkay Ltd., and Two World Ltd. He has also been a Co-Investigator in several funded research projects, including H2020 MARIE Sklodowska-CURIE ACTIONS: Innovative Training Networks "Secure Network Coding for Next Generation Mobile Small Cells 5G-US," nonlinear and demodulation mechanisms in biological tissue [Department of Health, Mobile Telecommunications and Health Research Programme, and Assessment of the Potential Direct Effects of Cellular Phones on the Nervous System (EU: collaboration with six other major research organizations across Europe)]. He has been a Research Visitor at Glyndwr University, Wrexham, U.K., since September 2009, covering the wireless and communications research areas. His research interests include computational methods and optimizations, wireless and mobile communications, sensor design, EMC, beam steering antennas, energy-efficient PAs, and RF predistorter design applications. He is a Fellow of the Institution of Engineering and Technology, U.K., and the Higher Education Academy. He received the Business Innovation Award for his successful KTP with Pace and Datong companies on the design and implementation of MIMO sensor systems and antenna array design for service localizations. He is the Chair of several successful workshops on Energy Efficient and Reconfigurable Transceivers: Approach Towards Energy Conservation and CO2 Reduction that addresses the biggest challenges for future wireless systems. He was also appointed as a Guest Editor of *IET Science, Measurement and Technology* in 2009 and 2012. He is a Chartered Engineer in U.K.

FRANCISCO FALCONE (Senior Member, IEEE) received the degree in telecommunication engineering and the Ph.D. degree in communication engineering from the Universidad Pública de Navarra (UPNA), Spain, in 1999 and 2005, respectively. From February 1999 to April 2000, he was the Microwave Commissioning Engineer with Siemens-Italtel, deploying microwave access systems. From May 2000 to December 2008, he was a Radio Access Engineer with Telefónica Móviles, performing radio network planning and optimization tasks in mobile network deployment. As a co-founding member in January 2009, he has been the Director of Tafco Metawireless, a spin-off company from UPNA, until May 2009. He was an Assistant Lecturer with the Electrical and Electronic Engineering Department, UPNA, from February 2003 to May 2009. In June 2009, he becomes an Associate Professor with the EE Department, being the Department Head, from January 2012 to July 2018. From January 2018 to May 2018, he was a Visiting Professor with the Kuwait College of Science and Technology, Kuwait. He is also affiliated with the Institute for Smart Cities (ISC), UPNA, which hosts around 140 researchers. He is currently acting as the Head of the ICT Section. His research interests include computational electromagnetics applied to the analysis of complex electromagnetic scenarios, with a focus on the analysis, design, and implementation of heterogeneous wireless networks to enable context-aware environments. He has over 500 contributions in indexed international journals, book chapters, and conference contributions. He has been awarded the CST 2003 and CST 2005 Best Paper Award, the Ph.D. Award from the Colegio Oficial de Ingenieros de Telecomunicación (COIT), in 2006, the Doctoral Award UPNA, in 2010, the 1st Juan Gomez Peñalver Research Award from the Royal Academy of Engineering of Spain, in 2010, the XII Talgo Innovation Award in 2012, the IEEE 2014 Best Paper Award in 2014, the ECSA-3 Best Paper Award in 2016, and the ECSA-4 Best Paper Award in 2017.

ERNESTO LIMITI (Senior Member, IEEE) is currently a Full Professor of electronics with the Engineering Faculty, University of Roma Tor Vergata, since 2002, after being a Research and Teaching Assistant, since 1991, and an Associate Professor, since 1998, with University of Roma Tor Vergata. He represents the University of Roma Tor Vergata in the governing body of the Microwave Engineering Center for Space Applications (MECSA), an inter-universitary center among several Italian Universities. He has been elected to represent the Industrial Engineering sector in the Academic Senate of the University for the period 2007–2010 and 2010–2013. He is actually the President of the Consortium "Advanced Research and Engineering for Space", ARES, formed between the University and two companies. He is actually the President of the Laurea and Laurea Magistrale degrees in electronic engineering of the University of Roma Tor Vergata. His research interests include three main lines, all of them belonging to the microwave and millimetre-wave electronics research area. The first one is related to characterization and modeling for active and passive microwave and millimetre-wave devices. Regarding active devices, the research line is oriented to the small-signal, noise and large signal modeling. Regarding passive devices, equivalent-circuit models have been developed for interacting discontinuities in microstrip, for typical MMIC passive components (MIM capacitors) and to waveguide/coplanar waveguide transitions analysis and design. For active devices, new methodologies have been developed for the noise characterization and the subsequent modeling, and equivalent-circuit modeling strategies have been implemented both for small and large-signal operating regimes for GaAs, GaN, SiC, Si, InP, and MESFET/HEMT devices. The second line is related to design methodologies and characterization methods for low-noise circuits. The main focus is on cryogenic amplifiers and devices. Collaborations are currently ongoing with the major radioastronomy institutes all around Europe within the frame of FP6 and FP7 programmes (RadioNet). The third line is in the analysis methods for nonlinear microwave circuits. In this line, novel analysis methods (Spectral Balance) are developed, together with the stability analysis of the solutions making use of traditional (harmonic balance) approaches. The above research lines have produced more than 250 publications on refereed international journals and presentations within international conferences. He acts as a referee of international journals of the microwave and millimetre wave electronics sector. He is on the steering committee of international conferences and workshops. He is actively involved in research activities with many research groups, both European and Italian, and he is in tight collaborations with high-tech italian (Selex–SI, Thales Alenia Space, Rheinmetall, Elettronica S. p. A., and Space Engineering) and foreign (OMMIC, Siemens, and UMS) companies. He contributed, as a Researcher and/or as unit responsible, to several National (PRIN MIUR, Madess CNR, and Agenzia Spaziale Italiana) and international (ESPRIT COSMIC, Manpower, Edge, Special Action MEPI, ESA, EUROPA, Korrigan, and RadioNet FP6 and FP7) projects. Regarding teaching activities, he teaches, over his institutional duties in the frame of the Corso di Laurea Magistrale in Ingegneria Elettronica, "Elettronica per lo Spazio" within the Master Course in Sistemi Avanzati di Comunicazione e Navigazione Satellitare. He is a member of the committee of the Ph.D. program in telecommunications and microelectronics at the University of Roma Tor Vergata, tutoring an average of four Ph.D. candidates per year.